

CALCULATION OF THE SECOND ORDER MEAN FORCE  
ON A SHIP IN OBLIQUE SEAS

by

PAUL ROSS ERB

S.B., Massachusetts Institute of Technology  
(1976)

SUBMITTED IN PARTIAL FULFILLMENT OF THE REQUIREMENTS  
FOR THE DEGREES OF

MASTER OF SCIENCE

IN NAVAL ARCHITECTURE AND MARINE ENGINEERING

AND

MASTER OF SCIENCE

IN MECHANICAL ENGINEERING

at the

MASSACHUSETTS INSTITUTE OF TECHNOLOGY

June, 1977

Signature of Author . . . . .  
Department of Ocean Engineering  
May 12, 1977

Certified by . / / Thesis Supervisor  
Department of Ocean Engineering

Certified by . . . . .  
Department Reader  
Department of Mechanical Engineering

Accepted by . . . . .  
Chairman,  
Departmental Committee on Graduate Students



CALCULATION OF THE SECOND ORDER MEAN FORCE  
ON A SHIP IN OBLIQUE SEAS

by

PAUL ROSS ERB

Submitted to the Department of Ocean Engineering and the Department of Mechanical Engineering on May 12, 1977 in partial fulfillment of the requirements for the Degree of Master of Science in Naval Architecture and Marine Engineering and the Degree of Master of Science in Mechanical Engineering.

ABSTRACT

A design tool is developed for use by engineers for the calculation of the mean added resistance or drift force on an elongated body such as a ship in a seaway. Only forces arising from wave-ship motion interaction or wave reflection are considered and developed in a form suitable for a computer program. This procedure allows computation of the mean second order force from first order quantities already known in strip theory of ship motions. Regular wave computer results generated by the MIT 5-D motions program for the Mariner cargo vessel are presented and compared with experiment, including a set of new beam seas experiments. Comparison is also made with published results from two other programs. The extension of the regular wave theory to an irregular long-crested seaway and then to a short-crested seaway is outlined. Finally, six representative sea spectra are used in a brief design analysis for the Mariner at service speed.

Thesis Supervisor: Chryssostomos Chryssostomidis

Title: Associate Professor of Naval Architecture

ACKNOWLEDGEMENTS

The author wishes to extend his sincere appreciation for the help and guidance given to him by his advisor, Professor C. Chryssostomidis, not just on this thesis, but throughout his undergraduate and graduate years at M.I.T.

This work would have been very difficult to complete if not for the efforts of several individuals. The experimental work was done with the help of Ysabel Meija. Professors Owen Oakley and Martin Abkowitz generously offered advice and opinions at various stages. Fraternity brothers, Stephen K. Gourley and David B. S. Smith gave invaluable assistance by producing many of the final graphs and figures. Barbara Belt read portions of the draft and offered valuable suggestions. Special thanks are also extended to Elaine Govoni, who prepared the final manuscript.

All computations were performed at the M.I.T. Information Processing Center with a grant from the National Science Foundation. In closing, the author wishes to express his gratitude to the Society of Naval Architects and Marine Engineers for their generous graduate scholarship and to his family for their unfailing support.

TABLE OF CONTENTS

Title Page . . . . .	1
Abstract . . . . .	2
Acknowledgements . . . . .	3
Table of Contents . . . . .	4
List of Figures and Tables . . . . .	5
List of Symbols . . . . .	7
CHAPTER I Introduction . . . . .	12
CHAPTER II Historical Background . . . . .	16
CHAPTER III Theoretical Development . . . . .	24
CHAPTER IV Verification of Theory . . . . .	60
A. Comparison with Experimental Results.	64
B. Comparison with Other Theoretical Results . . . . .	75
CHAPTER V Design Analysis . . . . .	93
CHAPTER VI Conclusion and Recommendations. . . . .	110
References . . . . .	114
Appendices: A. Changes to M.I.T. 5-D Seakeeping Program User's Manual . . . . .	117
B. Sample Output . . . . .	119
C. Subroutines Modified . . . . .	128
D. Listing of <u>Mariner</u> Example Data . . .	169

LIST OF FIGURES AND TABLES

Figures

<u>No.</u>	<u>Title</u>	<u>Page</u>
1	Coordinate System . . . . .	25
2	Mariner Added Resistance Components (Terms in Eq. (86)) . . . . .	62
3	Added Resistance/Head Waves . . . . .	66
4	<u>Mariner</u> Model; $U=0$ ; $\beta=90^\circ$ . . . . .	71
5	<u>Mariner</u> Model; $U=0$ ; $\beta=105^\circ$ . . . . .	72
6	<u>Mariner</u> Model; $U=0$ ; $\beta=75^\circ$ . . . . .	73
7	<u>Mariner</u> - Added Resistance Head Waves ( $\beta=180^\circ$ ) Various Speeds . . . . .	77
8	<u>Mariner</u> - Added Resistance (Speed - 15 knots) Various Headings . . . . .	79
9	<u>Mariner</u> - Added Resistance (Speed - 15 knots) Various Headings . . . . .	80
10	<u>Mariner</u> - Drift Force ( $\beta=120^\circ$ ) Various Speeds . . . . .	82
11	<u>Mariner</u> - Drift Force (Speed - 15 knots) Various Headings . . . . .	84
12	<u>Mariner</u> - Drift Force (Speed - 15 knots) Various Headings . . . . .	85
13	<u>Mariner</u> - Negative Added Resistance (Speed - 15 knots) Various Headings . . . . .	87
14	<u>Mariner</u> - Drift Force (Speed - 15 knots) Various Headings . . . . .	88
15	Sea Spectra . . . . .	98
16	<u>Mariner</u> Irregular Seas Results . . . . . (Mean Added Resistance; Pierson-Moskowitz)	100

Figures (Continued)

<u>No.</u>	<u>Title</u>	<u>Page</u>
17	<u>Mariner</u> Irregular Seas Results (Mean Drift Force; Pierson-Moskowitz) . . .	101
18	<u>Mariner</u> Irregular Seas Results (Mean Added Resistance; Bretschneider) . .	104
19	<u>Mariner</u> Irregular Seas Results (Mean Drift Force; Bretschneider) . . . . .	105

Tables

1	Added Resistance/Drift Force in Pounds for Various Sea States . . . . .	107
---	--	-----

LIST OF SYMBOLS

$a(x)$ or $a_{jk}(x)$	- Sectional added mass coefficient
$A_x$	- Sectional area
$A_{jk}$	- Added mass matrix of the ship
$b$	- Sectional beam
$b(x)$ or $b_{jk}(x)$	- Sectional damping coefficient
$b^*(x)$	- Gerritsma and Beukelman sectional quantity (3a)
$B$	- Ship beam
$B_{jk}$	- Damping matrix of the ship
$C_A$	- After cross-section
$C_{jk}$	- Hydrostatic restoring force matrix of the ship
$d$	- Sectional draft
$E$	- Radiated energy from ship
$E(\omega)$	- Energy spectrum of the sea based on full wave amplitude
$f$	- Functional relation
$f_j(x)$	- Sectional Froude-Kriloff force
$\bar{F}(\beta)$	- Mean second order force in long-crested irregular seas
$\bar{F}(\theta)$	- Mean second order force in short-crested irregular seas
$F_j$	- Complex exciting force vector
$F_j^D$	- Diffraction portion of exciting force

$F_j^I$	- Froude-Kriloff portion of exciting force
$\vec{F}$	- Unsteady hydrodynamic force vector
$\bar{F}$	- Mean value of $\vec{F}$
$F$	- Magnitude of $\vec{F}$
$F_D$	- Component of $F$ related to the diffraction potential
$F_x$	- Added resistance component of second order force
$F_y$	- Drift force component of second order force
$F_j^I$	- Component of $F$ related to the Froude-Kriloff excitation
$F_j^D$	- Component of $F$ analogous to the diffraction excitation
$g$	- Gravitational acceleration
$G_j$	- Added mass and damping part of $H_j$
$h_D(x)$	- Sectional quantity, integrand of $F_D$ (81)
$\hat{h}_j(x)$	- Sectional diffraction force
$\bar{h}_{1/3}$	- Significant wave height
$h_j(x)$	- Sectional quantity, integrand of $F_j^D$ (78d)
$H_j$	- Total hydrodynamic force vector
$i$	- $\sqrt{-1}$
$I_D$	- Integral used to develop $F_D$ expression (82)
$I_{jk}$	- Moment or product of inertia
$j$	- Subscript (1...6; surge, sway, heave, roll, pitch, yaw)
$k$	- similar to $j$



$K$	- Wave number
$L$	- Ship length (L.B.P.)
$m_k$	- Related to ship normal, $n_k$
$M_{jk}$	- Mass matrix of the ship
$n_k$	- Ship hull normal (generalized)
$N_j$	- Two-dimensional normal
$p$	- Pressure in fluid
$Q$	- Represents either A or B
$S$	- Ship surface
$S_F$	- Free surface
$S_\infty$	- Control surface at infinity
$t_{jk}$	- Sectional integrand of $T_{jk}$
$T_{jk}$	- Complex quantity giving the $A_{jk}$ and $B_{jk}$ elements
$U$	- Forward velocity of ship
$V$	- Volume within $S, S_F, S_\infty$
$V_{Za}(x)$	- Relative sectional velocity
$x$	- Longitudinal axis of the ship
$x_b$	- Distance from center of gravity to center of buoyancy
$y$	- Transverse axis of the ship
$z$	- Vertical axis of the ship
$Z_C$	- Coordinate of the center of gravity
$\alpha$	- Wave amplitude (1/2 height)
$\beta$	- Heading angle of the ship

$\epsilon_k$	- Phase angle between motion and excitation
$\zeta$	- Free surface position
$\mathcal{J}_k$	- Complex amplitude of ship motion
$\dot{\eta}^*$	- Corrected free surface velocity
$\theta$	- Principal wind direction for short-crested seas
$\lambda$	- Wave length
$\mu$	- Difference between heading angle $\beta$ and wind direction $\theta$
$\rho$	- Water density
$\sigma$	- Sectional area coefficient ( $A_x/bd$ )
$\phi_B$	- Full body potential amplitude
$\phi_D$	- Diffraction potential amplitude
$\phi_{DC}$	- Non-zero mean higher order potential
$\phi_I$	- Incident wave potential amplitude
$\phi_k$	- Motion potential amplitude
$\phi_k^o$	- Speed independent motion potential
$\phi_k^U$	- Speed dependent motion potential
$\phi_S$	- Steady state potential
$\phi_T$	- Time dependent potential amplitude
$\bar{\Phi}$	- Overall velocity potential
$\bar{\Phi}_B$	- Full body potential
$\bar{\Phi}_I$	- Full incident wave potential
$\bar{\Phi}_{33}^+(\omega)$	- Sea spectrum based on half the wave amplitude

- $\Psi_k$  - Two-dimensional (sectional potential
- $\omega$  - Encounter frequency (rad/sec)
- $\omega_0$  - Incident wave frequency (rad/sec)
- $\omega_p$  - Spectral peak frequency (rad/sec)
- $\omega_s$  - Spectral frequency ordinate (rad/sec)

## I. INTRODUCTION

The forces that act on a ship in a seaway vary widely both in their nature and their relative importance. In general, they represent random processes which can only be quantified meaningfully through statistical analysis. Because of this complexity, naval architects have traditionally been forced to make many design decisions by combining judgement and experience with the results of comparatively simple, idealized analysis or experiments. One example of this process is the use of the ship-beam analogy and the quasistatic trochoidal wave profile for ship structural design. Another illustration can be found in the procedure used to determine ship power requirements. Common practice has been to obtain the results of calm water resistance and self-propulsion model tests, then, to account for the actual operating conditions by applying a power increase of fifteen to thirty percent. This service margin must be appropriate if the ship is to fulfill her owner's requirements consistently, efficiently, and economically in the real ocean environment.

Recently, great progress has been made in the effort to include rigorously in the design process some of the factors that influence a ship at sea. The first order

strip theory of ship motions, due originally to Korvin-Kroukovsky and Jacobs<sup>[13]</sup>, has been extended to the point where motions can be calculated acceptably for a wide variety of ship types, sea states, and heading angles. This makes possible the calculation of dynamic loadings imposed on the ship by a seaway (Salvesen, et. al<sup>[27]</sup>, and others). Statistical methods developed for systems subject to random excitation now provide useful probabilistic statements concerning significant design events (e.g., the chance of slamming or the highest likely bending moment).

Due in part to these advances, the problem of environmental influence on ship power requirements and the related problem of the sideways drift of a ship in a seaway can now be much more fully addressed. The forces involved can be traced to a wide variety of sources, for example:

1. The motions of the ship interact with the ocean waves to produce a net drift or added resistance.
2. The ocean waves reflect off the ship hull causing a net force.
3. Wind present at sea acts on the superstructure to cause a drift force and/or an extra resistance.
4. Marine fouling causes an increase in resistance due to surface roughness.
5. Involved interactions will also be present (e.g., the propeller may operate less efficiently due to

the ship motion, rudder motions necessary for coursekeeping might cause induced drag and side force, or the side slip of the whole vessel might similarly cause drag).

The complexity of the problem outlined still precludes complete analysis. However, it can be appreciated that even a partial solution, which reduces the significance of purely judgemental factors like the service margin, will greatly increase the confidence and capability of the naval architect. This is particularly true for design decisions that break new ground for the profession such as powering for ultra-large tankers, vessels on new trade routes, or even dynamically positioned drilling ships.

In order to develop a useful, flexible design tool of this nature, the following report addresses the portion of the drift force/added resistance problem included in the first two points above, namely the ship motion-wave interaction and the reflection. From this point, 'drift force' and 'added resistance' refer strictly to mean forces averaged during one wave period of encounter and caused by wave-ship hull interaction. 'Added resistance' will be the term for the mean force component parallel to the longitudinal, ship axis, positive toward the stern. 'Drift force' will signify the mean force component perpendicular to the longitudinal ship axis, positive when directed toward the same half-

plane as the wave propagation.

To place the method to be presented in a historical perspective, the paper begins with a discussion of past analytical efforts on the problem. Then a brief description of first order strip theory of ship motions is presented, and the method of calculation of second order mean wave force developed by Salvesen<sup>[28]</sup> is detailed. As will be seen, it is the mean second order wave force which is the drift force/added resistance referred to above. After an investigation of the characteristics of the final Salvesen formulation, an outline of past experimental work done on the problem is given, and an experimental effort devised to test certain areas of applicability is described. Following presentation of the experimental results, some numerical predictions for regular waves are compared with the results shown by Salvesen<sup>[28]</sup> and Loukakis<sup>[16]</sup>. The theoretical basis for a probabilistic extension of the regular wave theory to irregular ocean conditions is described, and a brief design analysis for several sea states is given. Finally, some general conclusions and recommendations are offered. The appendices contain documentation for the computer program developed in the analysis.

## II. HISTORICAL BACKGROUND

Kreitner<sup>[14]</sup> was one of the earliest researchers (1939) to investigate the problem of wave forces on a ship hull. He concluded that the force was caused primarily by the reflection of the incident waves from the hull. However, the real pioneer in the second order force problem was Havelock<sup>[9]</sup> who proposed a theory in 1942 for a ship with no forward speed in regular head seas that was allowed to pitch and heave. He found that Kreitner's reflection force was unrealistic for a pitching and heaving ship in waves of reasonable length. Instead it became clear that the phase difference between the ship motion and wave excitation was the primary source of added resistance. Following this line of thought, Havelock proposed the following:

$$\mathcal{F}_x = \frac{1}{2} K \left\{ |F_3^I| |J_3| \sin \epsilon_3 + |F_5^I| |J_5| \sin \epsilon_5 \right\} \quad (1)$$

where  $F_j^I$  is the exciting force or moment due to the wave (assuming that the ship does not affect the wave flow field); this force (moment) is referred to as the Froude-Kriloff excitation force (moment). Subscript 3 refers to heave, 5 to pitch.  $J_j$  is the motion amplitude,  $\epsilon_j$  is the phase



angle between the motion and the excitation, and  $K$  is the wave number ( $\omega_0^2/g$ ).

Hanaoka<sup>[6]</sup> examined the case of a moving ship in calm water that was externally forced to heave and pitch. He gave an expression for the wave resistance of the ship which predicted a considerable increase over the unforced case. This increase was related to the damping in the radiated waves produced by the moving hull. The damping could, in turn, be associated with the phase lag of Havelock, so the two theories were definitely supportive.

During the time when Hanaoka was working on his formulation (1953), Haskind<sup>[8]</sup> employed a potential flow method to combine the efforts of Havelock and Kreitner. He proposed that the net wave force was the sum of two parts, one wave reflection and the other wave-ship motion interaction. The integral equation that resulted was complicated, involving Kochin H-functions (surface integrals dependent on frequency and form).

The next big step in the field came with Maruo's<sup>[17]</sup> potential flow solution, which was presented in 1957. He divided the velocity potential into three parts: the incident waves, the steady-state body potential, and the time-dependent (oscillatory) body motion potentials. For practical purposes, the body potential was evaluated for

each section of the ship separately in the conventional strip formulation. The end result was a solution for the added resistance consisting of a sum of six terms, one each for heave, pitch, and reflection and one each for their interactions. Maruo's work was very important in that it combined and refined the ideas of Kreitner and Havelock, added a consideration of forward velocity and considered interactions between the motion related and reflection related resistance that had been earlier ignored. Further information on Maruo's theory for head seas can be found in Ref. 7. The extension of Maruo's work to seas approaching the ship from any angle (oblique seas) was accomplished recently by Hosoda<sup>[10]</sup>, but it is extremely complex since it involves twenty-five components for all five degrees of freedom.

Joosen<sup>[11]</sup> offered a new result for the case of head seas in 1966. Joosen's equation resembled Havelock's original work, but included heave and pitch interaction. Newman presented an oblique seas theory in 1967<sup>[20]</sup> which was abstract in that it utilized pure slender body theory and a long wave approximation. Boese<sup>[29]</sup> derived a method for head seas similar to Havelock's in 1970. It was based on the determination of the pressure distribution around the hull in the wave.

Before describing the most recent work done on the

second order wave force problem, some conclusions regarding the nature of the drift force/added resistance can be drawn. These general principles can be inferred from and are supported by the theoretical and experimental work that has been done on the problem.

1. The source of most of the drift force/added resistance (except for very short waves) is the phase lag between ship motions and wave excitations. [9, 17, 29]

A phase lag exists only in the presence of damping and, for ship motions, damping is almost exclusively by radiated waves. Furthermore, the energy loss through damping is directly related to the work necessary to maintain constant phasing. Therefore, the following can be concluded:

2. The drift force/added resistance problem can be formulated in terms of the waves radiated from the hull<sup>[5]</sup>.
3. The second order force is a wave energy phenomenon which must be proportional in magnitude to the incident wave amplitude squared<sup>[17, 29]</sup>

The case for the last point above is particularly strong in that experimental data supports it well (See, for example, Ref. 29). This assertion is also crucial for the application of statistical methods. Two more statements of

importance can also be made:

4. Since the source of the second order force is the seaway, and the associated ship motions, added resistance will be independent of calm water resistance. If some variation affects both, then it will do so through two distinct mechanisms. [17, 29]
5. Being totally a surface wave phenomenon, the drift force/added resistance can be measured in experiments using Froude scaling and fairly small models. (Ref. 29).

Gerritsma and Beukelman presented a theory in 1972<sup>[5]</sup> based on the idea that the added resistance in head waves could be calculated from the radiated energy contained in the outgoing damping and reflection waves around the ship. Their result continues to be extremely useful, due to its reliability and the fact that it is much easier to combine with a strip theory ship motions computer program than many of the other methods mentioned. In their development, they postulate that the energy radiated during one wave encounter period is,

$$E = \frac{\pi}{\omega} \int_0^L b^*(x) V_{za}^2(x) dx \quad (2)$$

where  $\omega$  is the encounter frequency and  $b^*(x)$  and  $V_{za}(x)$  are a sectional coefficient and a relative sectional velocity defined as follows:

$$b^*(x) = b(x) - U \left[ \frac{da(x)}{dx} \right] \quad (3a)$$

$$V_{za} = \dot{\eta}_3 - x_b \dot{\eta}_5 + U \dot{\eta}_5 - \dot{\eta}^* \quad (3b)$$

where  $b(x)$  is the sectional damping coefficient for an oscillating two-dimensional cylinder shaped like the section and  $a(x)$  is the sectional added mass for the same problem.  $U$  is the forward velocity of the ship,  $x_b$  is measured from the center of gravity and  $\dot{\eta}^*$  represents the velocity of the free surface. Referring to the work of Hanaoka et al. [7], it can be shown that the proportionality constant relating radiated energy and added resistance is the wave length,  $\lambda (E = \lambda \mathcal{F}_x)$ . Applying this fact together with (3) in Equation (2) gives:

$$\mathcal{F}_x = \frac{\pi}{\omega} \int_0^L \left\{ b_{33}(x) - U \frac{da_{33}(x)}{dx} \right\} |V_{za}|^2 dx \quad (4)$$

where  $b_{33}(x)$  and  $a_{33}(x)$  are now strictly interpreted as the sectional heave damping and added mass coefficients.

Through the use of energy flux consideration, Loukakis and Sclavounos<sup>[16]</sup> 1977, have succeeded in extending Gerritsmas's theory to computation of drift force and added resistance (and yaw moment) in oblique seas. This represents one of the three newest general methods for computation of second order mean force in oblique seas that seem well suited to inclusion in modern ship motions calculation schemes (the current goal being to obtain good second order mean force estimations from quantities known in the first order motion calculation, thereby minimizing computer time).

The second method that seems to hold promise in this sense is a potential flow theory due to Ankudinov<sup>[1]</sup>. It gives the second order force in a form similar to Havelock except that the total first order exciting force appears instead of just the Froude-Kriloff portion. It would be very easy to incorporate in a motions program, but it neglects wave reflection. Furthermore, there is some question about the validity of the final results presented (Salvesen<sup>[28]</sup>).

J. N. Newman was the originator of the third theory which will be derived and employed in this paper. He has worked on various aspects of the second order force problem

(Ref. 18, 19, 20, 22) but the particular paper that is most relevant to this report is Ref. 21. The method presented there can best be described as a potential flow formulation which determines a net pressure on the hull of the vessel due to higher order wave effects. Newman's equation was in surface integral form, and strict validity was assumed only for a submerged body beneath waves. Salvesen (Ref. 28) extended the analysis to surface vessels and applied the methods of strip theory to make numerical solution for a given ship within the context of a first order ship motions program possible.

### III. THEORETICAL DEVELOPMENT

In order to generate a formula for the prediction of the mean second order force on a ship in oblique waves, it will first be necessary to develop the general potential flow problem that applies. Consider, then, a ship moving at speed  $U$  oriented arbitrarily to regular sinusoidal waves, as shown in Figure 1. The oscillatory motions that result will be assumed to be linear and harmonic. The coordinate system is illustrated in Figure 1. It is a right-handed orthogonal  $(x,y,z)$  system with the  $x$ - $y$  plane coinciding with the plane of the undisturbed free surface,  $x$  along the longitudinal centerline, positive in the direction of forward motion,  $y$  positive to port and  $z$  positive upward through the ship center of gravity.<sup>\*\*</sup> The waves are shown to have their direction of propagation at an angle,  $\beta$ , to the ship  $x$ -axis ( $\beta = 180^\circ$ , head waves).

It is presumed that the ship oscillates as a rigid body in six degrees of freedom with complex motion amplitudes,  $\mathcal{J}_k$ ,  $k=1..6$ , which refer to surge, sway, heave, roll, pitch, and yaw, respectively, as shown in Figure 1. Disregarding

---

<sup>\*\*</sup>The computer program has been generalized so the user can choose the longitudinal position of the origin arbitrarily. The choice of origin at the center of gravity is for the simplicity of this derivation only.



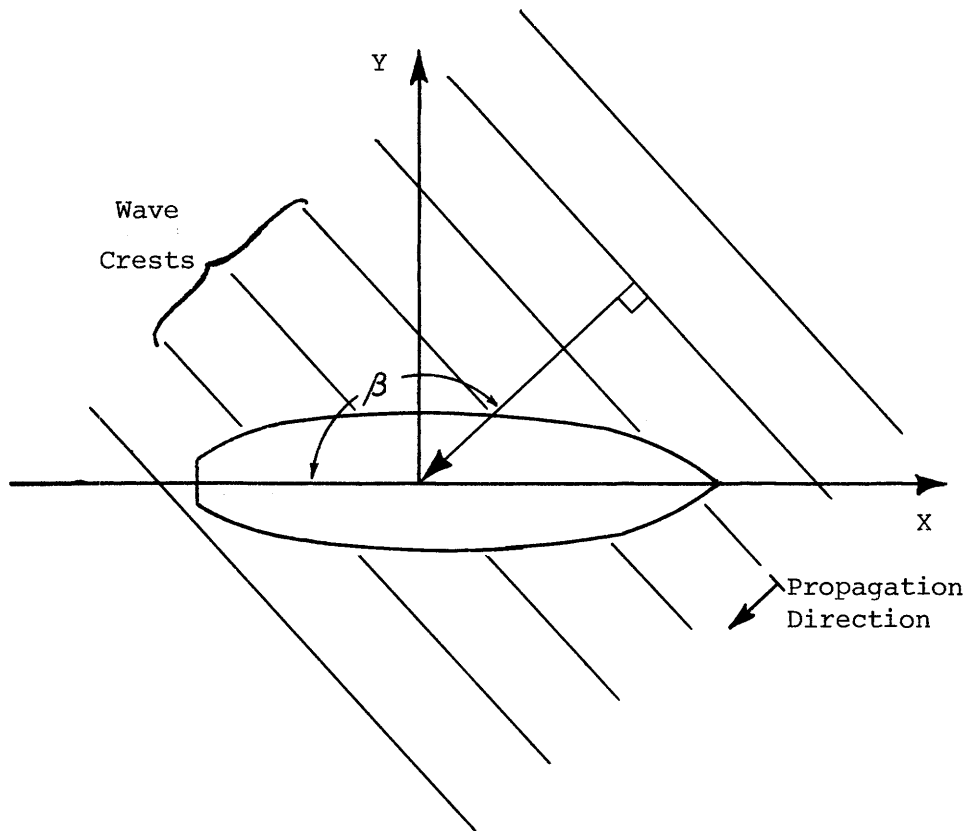
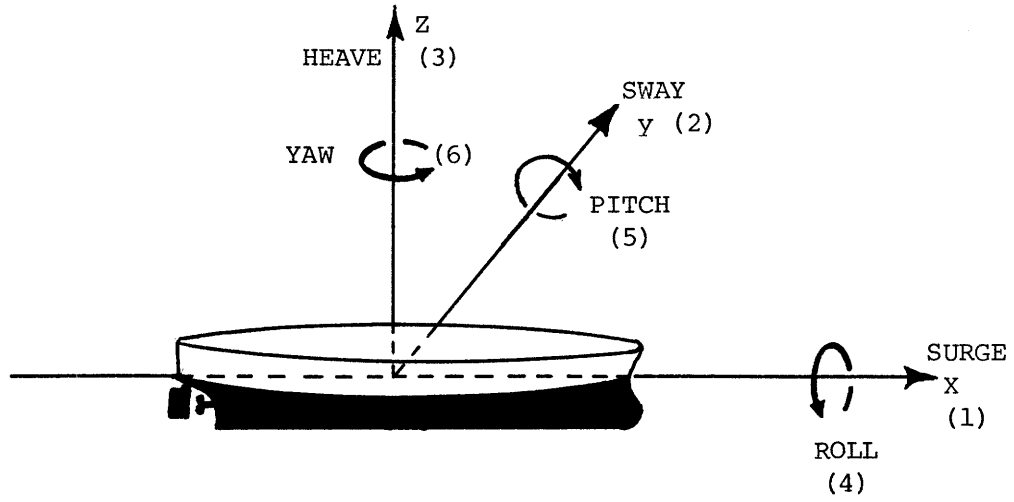


FIGURE 1: COORDINATE SYSTEM

viscosity and assuming irrotationality, potential flow theory can be applied. Thus, there is an overall velocity potential for the problem,  $\Phi(x, y, z, t)$ . This potential must satisfy Laplace's equation and the following exact boundary conditions:

On the ship surface ( $\zeta(x, y, z)=0$ ):

$$\frac{\partial f}{\partial t} + \nabla \Phi \cdot \nabla f = \frac{Df}{Dt} = 0 \quad (5)$$

Equation (5) expresses the condition that there must be zero flow velocity normal to the hull at the hull position.

On the free surface ( $\zeta=\zeta(x, y, t)$ ) the following condition must apply:

$$-\rho \frac{D}{Dt} \left( \frac{\partial \Phi}{\partial t} + \frac{1}{2} |\nabla \Phi|^2 + g\zeta \right) = 0 \quad (6)$$

which expresses a pressure and gravitational force equilibrium at the boundary. Also, a radiation condition must be applied at  $z = -\infty$  guaranteeing that the motion will be zero ( $\nabla \Phi \rightarrow 0$ ).

The first step toward a solution is to separate the velocity potential into its time independent part due to the steady forward motion of the ship and its time dependent part associated with the incident waves and the harmonic

motions,

$$\Phi(x, y, z, t) = [-Ux + \phi_s(x, y, z)] + \phi_T(x, y, z) e^{i\omega t} \quad (7)$$

where  $\omega$  is the frequency of encounter, related to the incident wave frequency,  $\omega_0$ , by.

$$\omega = \omega_0 \left( 1 - \frac{\omega_0}{g} U \cos \beta \right) \quad (8)$$

It should be understood that only the real part is to be taken in expressions involving  $e^{i\omega t}$  that appear in this derivation.

At this point it is necessary to linearize the problem by assuming that  $\phi_s$ , the steady perturbation associated with wavemaking in calm water, is small and so are its derivatives. The potential  $\phi_T$  and its derivatives must also be assumed small. In this way, higher order terms and cross products of the potential components can be neglected. Decomposing the complex amplitude of the time dependent potential gives,

$$\phi_T = \phi_I + \phi_D + \sum_{k=1}^6 \mathcal{J}_k \phi_k \quad (9)$$

where  $\phi_I$  is the incident wave potential,  $\phi_D$  is the diffraction potential, and  $\phi_k$  is the potential contribution from the  $k$ th mode of motion. It can be seen that the problem has

been transformed into the solution and superposition of several simpler potentials.  $\phi_I$  is the well-known potential for an infinite free surface of plane progressive gravity waves.  $\phi_D$  and the  $\phi_k$ 's must be solved, since the first deals with the wave reflecting properties of the motionless ship and the rest, of course, represent the properties of the motion.

An application of a Taylor series expansion about the mean ship position in connection with the above simplifications will show that the boundary conditions can now be linearized as follows:

$$\frac{\partial}{\partial n} (-Ux + \phi_s) = 0 \quad \text{on the 'hull'} \quad (10)$$

which represents the time independent portion of the body boundary condition applied at the mean hull position

$$U^2 \frac{\partial^2 \phi_s}{\partial x^2} + g \frac{\partial \phi_s}{\partial z} = 0 \quad \text{on } \zeta = 0 \quad (11)$$

which represents the time independent part of the free surface boundary condition applied at the undisturbed free surface.

$$\frac{\partial \phi_I}{\partial n} + \frac{\partial \phi_0}{\partial n} = 0 \quad \text{on the 'hull'} \quad (12)$$

which represents the incident and diffraction portion of the

time dependent part of the body boundary condition on the mean hull location.

$$\left[ (i\omega - U \frac{\partial}{\partial x})^2 + g \frac{\partial}{\partial z} \right] (\phi_I, \phi_D) = 0 \quad \text{on } \zeta = 0 \quad (13)$$

which gives the free-surface condition on  $\phi_I$  and  $\phi_D$ . In the above equations,  $n$  is the outward normal to the hull.

The oscillatory motion potentials must satisfy:

$$\frac{\partial \phi_k}{\partial n} = i\omega n_k + U m_k \quad \text{on the 'hull'} \quad (14)$$

and

$$(i\omega - U \frac{\partial}{\partial x})^2 \phi_k + g \frac{\partial \phi_k}{\partial z} = 0 \quad \text{on } \zeta = 0 \quad (15)$$

In these equations,  $n_k$  is a generalized normal defined by,

$$(n_1, n_2, n_3) = \vec{n} \quad \text{and} \quad (n_4, n_5, n_6) = \vec{r} \times \vec{n} \quad (16)$$

where  $\vec{n}$  is the ship hull normal and  $\vec{r}$  is a position vector.

Also,  $m_k$  is defined as follows,

$$m_k = 0 \quad \text{for } k = 1, 2, 3, 4; \quad m_5 = n_3; \quad m_6 = -n_2 \quad (17)$$

Further simplification of the hull boundary condition on the body motion potentials can be achieved by separating the potentials into two parts,

$$\phi_k = \phi_k^{\circ} + \frac{U}{i\omega} \phi_k^{\nu} \quad (18)$$

where  $\phi_k^{\circ}$  will be assumed speed-independent. Substituting (18) into (14) gives two hull conditions,

$$\frac{\partial \phi_k^{\circ}}{\partial n} = i\omega n_k \quad \text{and} \quad \frac{\partial \phi_k^{\nu}}{\partial n} = i\omega m_k \quad (19)$$

Since  $\phi_k^{\nu}$  and  $\phi_k^{\circ}$  must satisfy all the same conditions and the Laplace equation, it follows from the relations (17) and (19) that:

$$\phi_k^{\nu} = 0 \quad \text{for } k=1\dots4 \quad ; \quad \phi_5^{\nu} = \phi_3^{\circ} \quad ; \quad \phi_6^{\nu} = -\phi_2^{\circ} \quad (20)$$

Thus, the oscillatory motion potential components can be given from (18) in a form which includes speed only as a simple factor. (This 'speed-independence' is an involved assumption which will be clarified later.)

$$\phi_k = \phi_k^{\circ} \quad \text{for } k=1\dots4 \quad (21a)$$

$$\phi_5 = \phi_5^{\circ} + \frac{U}{i\omega} \phi_3^{\circ} \quad (21b)$$

$$\phi_6 = \phi_6^0 - \frac{U}{i\omega} \phi_2^0 \quad (21c)$$

with the body boundary condition from (19) being

$$\frac{\partial \phi_k^0}{\partial n} = i\omega n_k \quad (22)$$

and the free surface condition becoming from (15)

$$(i\omega - U \frac{\partial}{\partial x})^2 \phi_k^0 + g \frac{\partial \phi_k^0}{\partial z} = 0 \quad \text{on } \zeta = 0 \quad (23)$$

This completes the synthesis of the relevant conditions governing this problem. To summarize, the general potential is separated into several terms as per Equations (7) and (9). These linearized potentials must satisfy Laplace's equation, the linearized boundary conditions on the calm water surface. (11), (13) and (23), and the body boundary conditions (10), (12), and (22) at the hull position as well as the radiation conditions at infinity.

Having formulated the potential flow problem for a ship moving on an arbitrary heading in regular waves, the equations of motion of the vessel will now be developed. In this way specific quantities that must be extracted from the potential flow solution can be identified.

The ship is considered as a rigid body with six degrees

of freedom. Under the assumption of linear harmonic motions already stated, the governing equations can be written in matrix form in the frequency domain,

$$\sum_{k=1}^6 [-\omega^2(M_{jk} + A_{jk}) + i\omega B_{jk} + C_{jk}] J_k = F_j \quad (24)$$

$j = 1 \dots 6$

where  $M_{jk}$  is the generalized mass matrix of the ship (25),  $A_{jk}$  and  $B_{jk}$  are the added-mass and damping coefficients (26), the  $C_{jk}$ 's are the hydrostatic restoring coefficients, and the  $F_j$ 's are the complex exciting forces and moments. Note that the ship is idealized as a coupled spring-mass-dashpot system with harmonic forcing functions. Assuming that the ship possesses lateral symmetry, then the matrices above can be given as follows:

$$M_{jk} = \begin{bmatrix} M & 0 & 0 & 0 & Mz_c & 0 \\ 0 & M & 0 & -Mz_c & 0 & 0 \\ 0 & 0 & M & 0 & 0 & 0 \\ 0 & -Mz_c & 0 & I_{44} & 0 & -I_{46} \\ Mz_c & 0 & 0 & 0 & I_{55} & 0 \\ 0 & 0 & 0 & -I_{46} & 0 & I_{66} \end{bmatrix} \quad (25)$$

where the center of gravity is located at  $(0, 0, z_c)$ ,  $M$  is the



ship mass, and the  $I_{jk}$ 's are mass moments of inertia, when  $j=k$  and products of inertia for  $j \neq k$ .

$$A_{jk} \text{ or } B_{jk} = \begin{bmatrix} Q_{11} & 0 & Q_{13} & 0 & Q_{15} & 0 \\ 0 & Q_{22} & 0 & Q_{24} & 0 & Q_{26} \\ Q_{31} & 0 & Q_{33} & 0 & Q_{35} & 0 \\ 0 & Q_{42} & 0 & Q_{44} & 0 & Q_{46} \\ Q_{51} & 0 & Q_{53} & 0 & Q_{55} & 0 \\ 0 & Q_{62} & 0 & Q_{64} & 0 & Q_{66} \end{bmatrix} \quad (26)$$

where  $Q$  stands for  $A$  or  $B$ .

These terms (26) are hydrodynamic in nature and must be developed from the potential flow problem outlined. For the hydrostatic coefficients the only nonzero terms are  $C_{33}$ ,  $C_{44}$ ,  $C_{55}$ , and  $C_{35}$ . All these are quantities well known to the naval architect from hydrostatics.

An examination of the matrices in Equations (25), (26), and the  $C$ -matrix will reveal that for the laterally symmetric ship there are two sets of three equations, one for surge, heave, and pitch, and another for sway, roll, and yaw. These two sets are decoupled. Furthermore, under the assumption that the hull form is slender, it has been shown that the forces associated with surge are small, and

this mode can be disregarded leaving five degrees of freedom.

To solve these equations, it will be necessary to develop the added mass and damping matrix elements and the five exciting forces from the potential flow solution already outlined. These are all obtainable from the pressure in the fluid on the hull. By Bernoulli's equation,

$$p = -\rho \left( \frac{\partial \Phi}{\partial t} + \frac{1}{2} |\nabla \Phi|^2 + gz \right) \quad (27)$$

If this pressure is expanded in a Taylor series about the mean hull position and linearized consistently, it follows that the unsteady pressure is

$$p = -\rho \left( i\omega - U \frac{\partial}{\partial x} \right) \phi_T e^{i\omega t} - \rho g (\eta_3 + \eta_4 y - \eta_5 x) e^{i\omega t} \quad (28)$$

The last term is just the hydrostatic restoring force which was already separately included in the equations of motion (see above). Thus, the hydrodynamic force and moment acting on the ship will be given by

$$H_j = -\rho \iint_{S_1} n_j \left( i\omega - U \frac{\partial}{\partial x} \right) \phi_T ds \quad (29)$$

$j = 2, \dots, 6$

where  $\mathcal{S}$  is the hull surface at its mean position. The use of Equation (9) will allow the division of (29) into two parts, the exciting force and moment due to the wave (including the diffracting effects of the hull):

$$F_j = -\rho \iint_{\mathcal{S}} n_j (i\omega - U \frac{\partial}{\partial x}) (\phi_I + \phi_D) ds \quad (30)$$

and the force and moment due to the body motions (which physically represent both the added mass and damping).

$$G_j = -\rho \iint_{\mathcal{S}} n_j (i\omega - U \frac{\partial}{\partial x}) \sum_{k=2}^6 \mathcal{F}_k \phi_k ds \quad (31)$$

$$= \sum_{j=2}^6 T_{jk} \mathcal{F}_k \quad (32)$$

where

$$T_{jk} = -\rho \iint_{\mathcal{S}} n_j (i\omega - U \frac{\partial}{\partial x}) \phi_k ds \quad (33)$$

Equation (24) shows that the real part of (33) will be the added mass while the imaginary part will be the damping.

Therefore,

$$T_{jk} = \omega^2 A_{jk} - i\omega \quad (34)$$

The evaluation of Equation (33) is not currently possible because the motion potentials involved are three-dimensional in nature and associated with an arbitrary hull shape. Strip theory allows the solution of the problem through a simple lengthwise integration of two-dimensional potentials associated with each section. This is developed using a variant of Stokes Theorem derived in Ref. 27.

$$\iint_S n_j U \frac{\partial \phi}{\partial x} ds = U \iint_S m_j \phi ds - U \int_{C_A} n_j \phi dl \quad (35)$$

Applying this to (33), and assuming that the ship has zero after cross-section ( $C_A$ )\*\* yields

$$T_{jk} = -\rho i\omega \iint_S n_j \phi_k ds + U\rho \iint_S m_j \phi_k ds \quad (36)$$

---

\*\* In the original MIT motions program, this after section term was included in the calculation. For consistency with the second order force subroutine to follow, either all these terms must be removed from the motions calculation or a "zero" after section must be included in the input.

Using (36), the  $T_{jk}$ 's can be written for any desired  $jk$  combination by substituting from (21). Next, conventional strip theory approximations can be applied by assuming that the ship hull is long and slender. This allows the following transformation of the surface integral of (36) for the speed-independent potentials

$$T_{jk}^{\circ} = -\rho i \omega \int_L \int_{C_x} n_j \phi_k^{\circ} d\ell dx \equiv \int_L t_{jk} dx \quad (37)$$

As a consequence of the slender-hull assumption, it can be seen that, along the hull,  $\partial/\partial x \ll \partial/\partial y$  or  $\partial/\partial z$  and  $n_1 \ll n_2$  or  $n_3$ . The last of these allows substitution of a two-dimensional normal,  $N_j$ , (noting that now  $n_5 = -xN_3$  and  $n_6 = xN_2$ ).

In view of the above assumptions, it is possible to quantify the limitations inherent in making the motion potentials 'speed independent' (See (21)). The free surface condition (15) gives, upon reduction, that  $w \gg U^2/2x$  for the speed-independence to be workable. This is equivalent to a wave-length on the order of the ship beam. Fortunately, this theoretical restriction on strip theory does not preclude very reasonable answers for fairly long waves, since the hydrostatic terms grow in importance for the

smaller frequencies.

The above observations can now be used to infer that the speed-independent, three-dimensional motion potentials,  $\phi_k^o$ , can be replaced as follows with sectional potentials

$$\phi_k^o = \Psi_k \text{ for } k=2,3,4 \quad (38a)$$

$$\phi_5^o = -x \Psi_3 \quad (38b)$$

$$\phi_6^o = x \Psi_2 \quad (38c)$$

where the  $\Psi_k$ 's are the potentials for the two-dimensional problems of an infinite cylinder with the shape of the section oscillating in sway, heave, or roll. The problem of a cylinder oscillating in any of these modes is a classic one in hydrodynamics, and several techniques exist for mapping the solution to an arbitrary section shape. These methods include the Frank close-fit source-distribution Tsai-Porter close-fit mapping method, the Demanche bulb-form, and the Lewis form. The last two are used by the M.I.T. 5-D program.

In summary, the sectional potentials can be computed by known numerical methods, then combined with Equation (37)

to give

$$t_{jk} = -\rho i \omega \int_{c_x} N_j \Psi_k dl = \omega^2 a_{jk} - i \omega b_{jk} \quad (39)$$

for  $j=k=2,3,4$  and  $j=2, k=4$

where  $a_{jk}$  and  $b_{jk}$  are the sectional added mass and damping inferred from (34). This makes possible the computation of all the speed-independent  $T_{jk}^{\circ}$ 's which can be used in (36) in conjunction with (21) to give the full  $T_{jk}$ 's. The real and imaginary parts of the  $T_{jk}$ 's then correspond (34) to the desired damping and added mass. The process is complicated in an algebraic sense, but further details, including results, are available in Reference 27. The final answers are given in terms of the sectional added mass and damping for the two-dimensional problem, for example,

$$A_{53} = -\int_L x a_{33} dx + \frac{U}{\omega^2} B_{33}^{\circ} \quad (40a)$$

or

$$B_{46} = \int_L x b_{24} dx - U A_{24}^{\circ} \quad (40b)$$

where

$$B_{33}^{\circ} = \int_L b_{33} dx$$

$$\text{and, } A_{24}^{\circ} = \int_L a_{24} dx$$

The  $B_{44}$  damping term developed in this way does not give realistic answers when used in Equation (24). This is due to the fact that ship rolling is governed by viscous effects. The resulting non-linearity can be handled by defining a quasi-linear damping augmentation based on roll velocity and using an iterative scheme (See Ref. [27]).

The development of the exciting force and moment from (30) is also crucial to the understanding of the second-order force theory to be derived. Salvesen, et. al<sup>[27]</sup> show that the forces and moments can be expressed in terms of the sectional potentials discussed above. This method due to Haskin circumvents the solution of the diffraction potential,  $\phi_D$ , a very important simplification.

To proceed, the exciting force (30) is separated into two parts,

$$F_j = F_j^I + F_j^D \quad (41)$$

where

$$F_j^I = -\rho \iint_{S_j} n_j (i\omega - U \frac{\partial}{\partial x}) \phi_I ds \quad (42)$$



and

$$F_j^D = -\rho \iint_S n_j (i\omega - U \frac{\partial}{\partial x}) \phi_D ds \quad (43)$$

The potential for the incident waves is well known from classic linear gravity wave theory:

$$\phi_I = \frac{ig\alpha}{\omega_0} \exp[-iK(x\cos\beta - y\sin\beta) + Kz] \quad (44)$$

(where  $\alpha$  = wave amplitude,  $K = \omega_0^2/g$  = wave number)

This quantity can be substituted into (42), giving,

$$F_j^I = -\rho i \iint_S n_j \omega_0 \phi_I ds \quad (45)$$

where  $\omega_0$  is written as a consequence of (8). Equation (45) is the Froude-Kriloff exciting force which is easily computed without knowledge of the sectional potentials.

Continuing with Equation (43), the diffraction part of the exciting force, application of the special version of Stokes theorem used earlier (35) gives, for a ship with zero after cross-section,

$$F_j^D = -\rho \iint_S (i\omega n_j - U m_j) \phi_D ds \quad (46)$$

Use of the hull boundary condition (19) yields:

$$F_j^D = -\rho \iint_{S'} \frac{\partial}{\partial n} \left( \phi_j^o - \frac{U}{i\omega} \phi_j^v \right) \phi_D ds \quad (47)$$

A theorem of vector calculus known as 'Green's Second Identity' can be used with two functions ( $\phi$  and  $\psi$ ) satisfying the same Laplace equation, free-surface condition, radiation condition, and bottom condition to yield the following identity

$$\iint_{S'} \phi \frac{\partial \psi}{\partial n} ds = \iint_{S'} \psi \frac{\partial \phi}{\partial n} ds \quad (48)$$

Applying this to (47) gives the result

$$F_j^D = -\rho \iint_{S'} \left( \phi_j^o - \frac{U}{i\omega} \phi_j^v \right) \frac{\partial \phi_D}{\partial n} ds \quad (49)$$

Now the use of the hull boundary condition (12) leads to

$$F_j^D = \rho \iint_{S'} \left( \phi_j^o - \frac{U}{i\omega} \phi_j^v \right) \frac{\partial \phi_I}{\partial n} ds \quad (50)$$

It is clear from (50) that the diffraction potential has

been extracted from the problem. The normal derivative of the incident wave potential (44) becomes, after use of strip theory assumptions:

$$\frac{\partial \phi_I}{\partial n} = (in_2 \sin \beta + n_3) K \phi_I \quad (51)$$

Using (51) and the motion potential relations (20) in Equation (50) and invoking the standard strip theory assumptions to transform the surface integral gives,

$$F_j^D = \rho \alpha \int_L e^{-iKx \cos \beta} \int_{C_x} e^{iKY \sin \beta} e^{Kz} \left\{ \omega_0 (in_3 - n_2 \sin \beta) \phi_j^0 \right. \\ \left. \pm \omega_0 \frac{U}{i\omega} [ (in_3 - n_2 \sin \beta) \phi_{3,2}^0 ]_{j=5,6} \right\} dl dx \quad (52)$$

Making use of the two-dimensional sectional normal, and the concept of a sectional force, allows the following simplifications:

From (45):

$$F_j^I = \rho \alpha \int_L f_j(x) dx \quad j=2,3,4 \quad (53a)$$

$$F_s^I = -\rho \alpha \int_L x f_3(x) dx \quad (53b)$$

$$F_c^I = \rho \alpha \int_L x f_2(x) dx \quad (53c)$$

where

$$f_j(x) = g e^{-iKx \cos \beta} \int_{c_x} N_j e^{iKy \sin \beta} e^{Kz} dl \quad (53d)$$

$j = 2, 3, 4$

from (52):

$$F_j^D = \rho \alpha \int_L h_j(x) dx \quad (54a)$$

$$F_5^D = \rho \alpha \int_L \left(x + \frac{U}{i\omega}\right) h_3(x) dx \quad (54b)$$

$$F_c^D = -\rho \alpha \int_L \left(x + \frac{U}{i\omega}\right) h_2(x) dx \quad (54c)$$

where

$$h_j(x) = \omega_0 e^{-iKx \cos \beta} \int_{c_x} (iN_3 - N_2 \sin \beta) e^{iKy \sin \beta} \dots \dots e^{Kz} \Psi_j dl \quad (54d)$$

The strip theory formulation of the linearized ship motions problem has now been completed. Once the sectional, two-dimensional potentials for sway, heave, and roll are determined by one of the methods mentioned (See Ref. [27]), then these can be used in (39) to produce the various sectional damping and added mass coefficients. Equation (40) and other similar relationships detailed in Ref. [27] can then be applied to find the added mass and damping matrices for the whole ship. This means that the left side of (24) is known. The exciting force is then determined from (41), (53), and (54) since the sectional potentials are known. After this (24) is easily solved for the complex motion amplitudes,  $\mathcal{P}_k$ . These complex quantities contain both the real motion amplitudes and the phasing. It should be reemphasized that these motions are, by assumption, linear and harmonic in the frequency of encounter.

In a nonlinear analysis of the problem, higher order terms in the incident wave potential would tend to interact with the other potentials, producing periodic higher order forces with non-zero means. Of course, these forces tend to be small in comparison with the simple harmonic first order excitations. They are, in fact, negligible in the pitch, roll, and heave modes because of the strong hydrostatic restoring forces that are acting. However, they can act to produce large displacements over time in the horizontal

modes. It can be seen, then, that in order to force the ship to perform the assumed motion at constant speed,  $U$ , and constant heading angle,  $\beta$ , in the 'real' ocean, an extra time varying force will have to be applied both longitudinally and transversely (also a moment will be necessary). In the absence of these the ship will drift and its speed will vary from that expected in calm water.

A method by Newman, already mentioned in Section II, makes possible the calculation of the mean of the second order force which produces the speed loss and drift. As will be shown, this can be done using only quantities known from the first order analysis.

The unsteady hydrodynamic force on a body in an inviscid medium with a free surface is given by Equation (29). This can be expressed in a more general form as follows:

$$\vec{F} = \iint_{\mathcal{S}} p \vec{n} ds \quad (55)$$

where  $\mathcal{S}$  is the wetted surface of the body. Applying Gauss' theorem and utilizing the fact that  $p=0$  on the free surface,

$$\vec{F} = \iiint_V \nabla p dv - \iint_{S_\infty} p \vec{n} ds \quad (56)$$

where  $S_\infty$  is a control surface in the far field and  $V$  is the volume enclosed between  $S$ ,  $S_\infty$ , and the free surface. Bernoulli's equation gives the pressure in terms of the total velocity potential:

$$\vec{F} = -\rho \iiint_V \left\{ \nabla \frac{\partial \Phi}{\partial t} + \frac{1}{2} \nabla |\nabla \Phi|^2 \right\} dv + \rho \iint_{S_\infty} \left\{ \frac{\partial \Phi}{\partial t} + \frac{1}{2} |\nabla \Phi|^2 \right\} ds \quad (57)$$

The transport theorem<sup>[23]</sup> shows that

$$\frac{d}{dt} \iiint_V \nabla \Phi dv = \iiint_V \nabla \frac{\partial \Phi}{\partial t} dv + \iint_{S+S_F} \nabla \Phi \frac{\partial \Phi}{\partial n} ds \quad (58)$$

where  $S_F$  is the free surface. The truth of (58) depends on the fact that  $\vec{V} \cdot \vec{n} = 0$  on  $S_\infty$  and  $\vec{V} \cdot \vec{n} = \frac{\partial \Phi}{\partial n}$  on  $S$  and  $S_F$  (where  $\vec{V}$  is the surface velocity). Using (58) in (57) yields

$$\begin{aligned} \vec{F} = & -\rho \frac{d}{dt} \iiint_V \nabla \Phi dv + \rho \iint_{S+S_F} \nabla \Phi \frac{\partial \Phi}{\partial n} ds - \\ & \frac{\rho}{2} \iiint_V \nabla |\nabla \Phi|^2 dv + \rho \iint_{S_\infty} \left\{ \frac{\partial \Phi}{\partial t} + \frac{1}{2} |\nabla \Phi|^2 \right\} \cdot \vec{n} ds \end{aligned} \quad (59)$$

Again, Gauss' theorem can be employed to change the first volume integral to a surface integral, with the result:

$$-\rho \frac{\partial}{\partial t} \iiint_V \nabla \Phi dv = -\rho \frac{\partial}{\partial t} \iint_{S'+S'_F} \Phi \cdot \vec{n} ds - \rho \iint_{S'_\infty} \frac{\partial \Phi}{\partial t} \cdot \vec{n} ds \quad (60)$$

When this is included in (59) the result is

$$\begin{aligned} \vec{F} = & -\rho \frac{\partial}{\partial t} \iint_{S'+S'_F} \Phi \cdot \vec{n} ds + \rho \iint_{S'+S'_F} \nabla \Phi \frac{\partial \Phi}{\partial n} ds - \\ & \frac{1}{2} \rho \iiint_V \nabla |\nabla \Phi|^2 dv + \frac{1}{2} \rho \iint_{S'_\infty} |\nabla \Phi|^2 \vec{n} ds \end{aligned} \quad (61)$$

Once more invoking Gauss' theorem,

$$\frac{1}{2} \iiint_V \nabla |\nabla \Phi|^2 dv = \iint_{S'+S'_F+S'_\infty} \frac{\partial \Phi}{\partial n} \nabla \Phi ds \quad (62)$$

Putting (62) in (61) gives as a final result,



$$\vec{F} = -\rho \frac{\partial}{\partial t} \iint_{S+S_F} \Phi \cdot \vec{n} ds - \rho \iint_{S_\infty} \left\{ \frac{\partial \Phi}{\partial n} \nabla \Phi - \frac{1}{2} |\nabla \Phi|^2 \vec{n} \right\} ds \quad (63)$$

The expression (63) provides the force on a body in a fluid with a free surface exactly (within the limits of the theory of potential flow). Using a first order potential in (63), would yield (after linearization) the oscillatory hydrodynamic force components (30) and (31). The simplest higher order potential that could be used in the problem would be of the form

$$\Phi = (\phi_S^{(1)} + \phi_S^{(2)} + \dots) + (\phi_T^{(1)} e^{i\omega t} + \phi_T^{(2)} e^{2i\omega t} + \phi_{D.C.}^{(2)} + \dots) \quad (64)$$

where the numbers in parentheses indicate the order of the terms and the 'D.C.' is responsible for the non-zero mean of the oscillatory potential. Putting (64) in (63) shows that there will be no net contribution from the first integral because the DC-potential has no time derivative. The second integral will give a steady state contribution

which can be developed by writing  $\Phi = \Phi_I + \Phi_B$ , substituting in (63), and performing the vector calculus,

$$\vec{F} = \rho \iint_{S_\infty} (\Phi_B \frac{\partial}{\partial n} - \frac{\partial \Phi_B}{\partial n}) (\nabla \Phi_I + \frac{1}{2} \nabla \Phi_B) ds \quad (65)$$

Newman applied a 'weak scatterer' assumption at this point ( $\Phi_B \ll \Phi_I$ ). This is easily justified for a body submerged beneath the surface. Salvesen reasoned that this might also be true for a slender body like a ship, an assumption that will be more accurate for head than beam seas. The result is

$$\vec{F} = \rho \iint_{S_\infty} (\Phi_B \frac{\partial}{\partial n} - \frac{\partial \Phi_B}{\partial n}) \nabla \Phi_I ds \quad (66)$$

Writing  $\Phi_B = \phi_S + \phi_B e^{i\omega t}$  and  $\Phi_I = \phi_I e^{i\omega t}$ , taking the mean value of (66), and using Green's theorem to change the integration surface from the far-field to the body, gives the following:

$$\vec{F} = \frac{1}{T} \int_T \vec{F} dt = -\frac{1}{2} \rho \iint_{S'} (\phi_B \frac{\partial}{\partial n} - \frac{\partial \phi_B}{\partial n}) \nabla \phi_I^* ds \quad (67)$$

where ( )<sup>\*</sup> refers to the complex conjugate and  $\vec{\mathcal{F}}$  represents the mean force vector for one regular wave period.

Since only the horizontal component of  $\vec{\mathcal{F}}$  is of interest,  $\nabla\phi_I^*$  can be written,

$$\nabla\phi_I^* = iK(\cos\beta\hat{i} - \sin\beta\hat{j})\phi_I^* \quad (68)$$

Substitution of (68) in (67) allows the magnitude of (67) to be given as,

$$|\vec{\mathcal{F}}| = \mathcal{F} = -\frac{i}{2}\rho K \iint_{S'} (\phi_B \frac{\partial}{\partial n} - \frac{\partial \phi_B}{\partial n}) \phi_I^* ds \quad (69)$$

In the ship coordinate system, the beam and lengthwise components of this mean force will be,

$$\mathcal{F}_x = \mathcal{F}\cos\beta \quad \mathcal{F}_y = \mathcal{F}\sin\beta \quad (70)$$

which follows because  $\vec{\mathcal{F}}$  is in the direction of wave propagation. It should be noted that (69) is a form of the Kochin function, first developed in connection with this problem by Haskind.

As a consequence of the fact that the mean higher order

force contribution has been reexpressed in terms of the full body potential, substitution of the first order body potential of strip theory will not give an approximation of the net force contributed by the higher order DC terms in the full potential (64). The extra mean force necessary to sustain the prescribed body motion in waves is given by substituting  $\phi_B \approx \sum_{j=2}^6 \phi_j \mathcal{F}_j + \phi_D$  in (69).

$$\mathcal{F} = -\frac{i}{2} \rho K \sum_{j=2}^6 \left\{ \mathcal{F}_j \iint_{S'} \left( \phi_j \frac{\partial}{\partial n} - \frac{\partial \phi_j}{\partial n} \right) \phi_I^* ds \right\} - \frac{i}{2} \rho K \iint_{S'} \left( \phi_D \frac{\partial}{\partial n} - \frac{\partial \phi_D}{\partial n} \right) \phi_I^* ds \quad (71)$$

This can be rewritten for computational purposes as

$$\mathcal{F} = \sum_{j=2}^6 \left\{ \mathcal{F}_j^I + \mathcal{F}_j^D \right\} + \mathcal{F}_D \quad (72a)$$

where

$$\mathcal{F}_j^I = \frac{i}{2} \rho K \mathcal{F}_j \iint_{S'} \frac{\partial \phi_j}{\partial n} \phi_I^* ds \quad (72b)$$

$$\mathcal{F}_j^D = -\frac{i}{2} \rho K \mathcal{P}_j \iint_S \phi_j \frac{\partial \phi_I^*}{\partial n} ds \quad (72c)$$

and after application of the body boundary condition (12)

$$\mathcal{F}_D = -\frac{i}{2} \rho K \iint_S \phi_D \frac{\partial \phi_I^*}{\partial n} ds \quad (72d)$$

The next problem is to express Equations (72) in strip theory terms. Examining (72b) first, a substitution of the boundary condition (14) gives

$$\mathcal{F}_j^I = \frac{i}{2} \rho K \mathcal{P}_j \iint_S (i\omega n_j + U m_j) \phi_I^* ds \quad (73)$$

Applying the variant of Stokes theorem (35) and substituting for  $\omega_0$  from (8):

$$\mathcal{F}_j^I = -\frac{1}{2} \rho K \mathcal{P}_j \iint_S \omega_0 n_j \phi_I^* ds \quad (74)$$

Comparing this with (45) reveals that:

$$\mathcal{F}_j^I = \frac{i}{2} K \mathcal{F}_j (F_j^I)^* \quad (75)$$

This can easily be shown by trigonometric identity to be the same as the formula developed by Havelock (1).

Continuing now to (72c), it follows from the strip theory assumption,  $n_1 \ll n_2$  or  $n_3$ , and (44) that

$$\frac{\partial \phi_I^*}{\partial n} = K (-n_3 + i n_2 \sin \beta) \phi_I^* \quad (76)$$

Including (76) in (72c) and replacing  $\phi_j$  using (21)

$$\mathcal{F}_j^D = \frac{i}{2} \rho K^2 \mathcal{F}_j \iint_{S'} \phi_j^o (-n_3 + i n_2 \sin \beta) \phi_I^* ds \quad (77a)$$

$j = 2, 3, 4$

$$\mathcal{F}_{5,6}^D = \frac{i}{2} \rho K^2 \mathcal{F}_{5,6} \iint_{S'} \left( \phi_{5,6}^o \pm \frac{U}{i\omega} \phi_{3,2}^o \right) \dots \dots (-n_3 + i n_2 \sin \beta) \phi_I^* ds \quad (77b)$$

The next step is to replace the unknown 3-D potentials with the sectional potentials according to (38) and transform the surface integral,

$$\mathcal{F}_j^D = \frac{i}{2} K \mathcal{P}_j \int_L \hat{h}_j(x) dx \quad j=2,3,4 \quad (78a)$$

$$\mathcal{F}_{5,6}^D = \mp \frac{i}{2} K \mathcal{P}_{5,6} \int_L \left(x + \frac{iU}{\omega}\right) \hat{h}_{3,2}(x) dx \quad (78b)$$

where a sectional quantity  $\hat{h}_j(x)$  has been defined as

$$\hat{h}_j(x) = \rho K \int_{c_x} \Psi_j (-N_3 + iN_2 \sin\beta) \phi_I^* dl \quad (78c)$$

$j = 2, 3, 4$

$$\hat{h}_j(x) = \rho \alpha \omega_0 e^{iKx \cos\beta} \int_{c_x} (N_2 \sin\beta + iN_3) \dots \dots \dots e^{-iKy \sin\beta} e^{-Kz} \Psi_j dl \quad j = 2, 3, 4 \quad (78d)$$

The similarity between (78) and (54) can be seen; however, the two are not algebraically related and must be computed separately. For simplicity, let:

$$\hat{F}_j^D = \int_L \hat{h}_j(x) dx \quad j=2,3,4 \quad (79a)$$

$$\hat{F}_{5,6}^D = \mp \int_L \left(x + \frac{iU}{\omega}\right) \hat{h}_{3,2}(x) dx \quad (79b)$$

giving

$$\mathcal{F}_j^D = \frac{i}{2} K \mathcal{F}_j \hat{F}_j^D \quad (79c)$$

Finally, consider the third contributor (72d). Substituting (76) and rewriting the expression:

$$\mathcal{F}_D = \frac{1}{2} \int_L h_D(x) dx \quad (80a)$$

$$h_D(x) = i \rho K^2 \int_{c_x} \phi_D (-n_3 + i n_2 \sin \beta) \phi_I^* dl \quad (80b)$$



Including the expression for  $\phi_I^*$ :

$$h_D(x) = \alpha \rho K \omega_0 e^{iKx \cos \beta} \int_{C_x} \phi_D(-n_3 + in_2 \sin \beta) e^{-Kz} e^{iKy \sin \beta} dl \quad (81)$$

In order to simplify computation, it is consistent with the strip theory assumptions already made to replace  $e^{+Kz}$  with  $e^{+Kd\sigma}$  and  $e^{-iKy \sin \beta}$  with  $e^{-iK(\pm \frac{1}{2}b)\sigma \sin \beta}$ , where  $d \equiv$  sectional draft,  $\sigma \equiv$  sectional area coefficient ( $A_x/bd$ ), and  $b \equiv$  sectional beam. The first of these is conventional in strip theory and the second should be legitimate if  $\lambda \gg \frac{1}{2}b$ . All this gives:

$$h_D(x) = \alpha \rho K \omega_0 e^{-Kd\sigma} e^{-iK(\pm \frac{1}{2}b)\sigma \sin \beta} e^{iKx \cos \beta} \dots \dots \int_{C_x} \phi_D(-n_3 + in_2 \sin \beta) dl \quad (82)$$

$\underbrace{\hspace{10em}}_{I_D}$

The integral in (82) can be rewritten by substituting for the hull normal from (22) and using Green's second identity (48) in two dimensions.

$$I_D = -\frac{i}{\omega} \int_{C_x} (-\phi_3^0 + i \sin \beta \phi_2^0) \frac{\partial \phi_D}{\partial n} dl \quad (83)$$

Using the now familiar hull condition (12), writing out the wave potential (44) and applying the same assumptions about  $e^{-Kz}$  and  $e^{iKy} \sin$  outlined above in route to (82) gives:

$$h_D(x) = \alpha^2 \rho K \frac{\omega_0^2}{\omega} e^{-2Kd\sigma} \int_{C_x} \{ \phi_3^0 n_3 + \sin^2 \beta \phi_2^0 n_2 \} dl \quad (84)$$

where the symmetric section assumption has been used to neglect two cross products involving the potentials and hull normals. Examination of (84) will reveal that when the two dimensional normals and sectional potentials are introduced (39) will be directly applicable. This will allow the reexpression of (84) in terms of the sectional added mass and damping already known.

$$h_D(x) = \alpha^2 K \frac{\omega_0^2}{\omega} e^{-2Kd\sigma} \left\{ b_{33}(x) + \sin^2 \beta b_{22}(x) \right\} \quad (85)$$

Where (85) represents just the real part of (84) because the imaginary part is not needed in (72a). (The reader is reminded, "...only the real part is to be taken in expressions involving  $e^{i\omega t}$  that appear in this derivation.")

In summary, the mean second order 'DC' force on a ship in regular waves is available from the real part of the following expression,

$$\mathcal{F} = \sum_{j=2}^6 \frac{i}{2} K \mathcal{F}_j [(F_j^I)^* + \hat{F}_j^D] + \mathcal{F}_D \quad (86)$$

where the motions are available from the first order computation already outlined,  $(F_j^I)^*$  is also available from that process,  $\hat{F}_j^D$  can be developed from (79) using strictly quantities known from strip theory, and  $\mathcal{F}_D$  comes from (80) in combination with (85). Then the added resistance and drift force can be given by simply applying (70). The M.I.T. 5-D motions program has been modified to properly extract and recombine these quantities (See Appendices for details).

#### IV. VERIFICATION OF THEORY

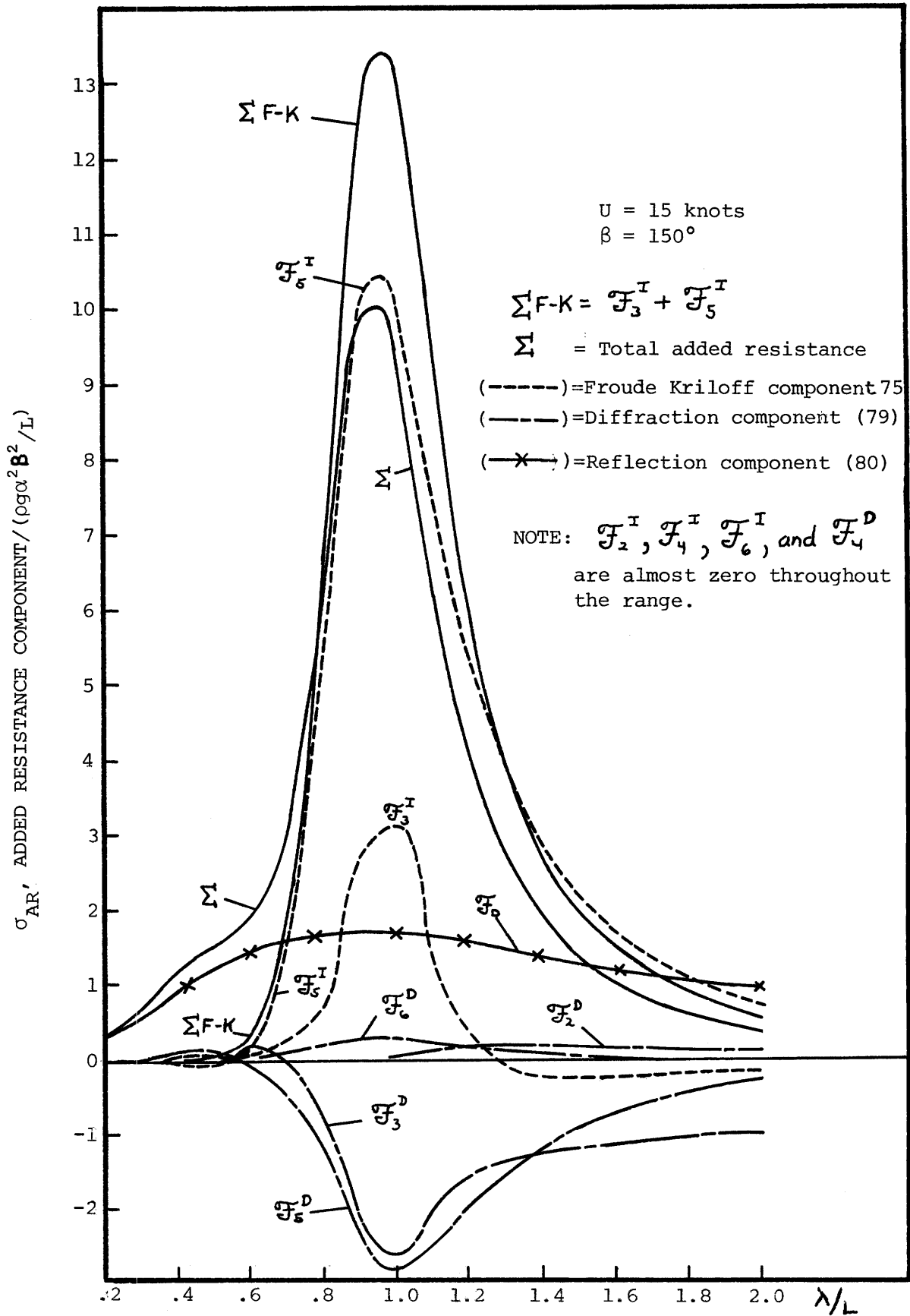
In Chapter III it was shown how the added resistance and drift force could be computed for any ship using Equations (86) and (70). This capability was incorporated in the M.I.T. 5-D motions program in the form of two subroutines (ADDRES and RESIST). The first of these is primarily an output organizer; the second does the actual calculation outlined earlier. As mentioned before, all the input necessary is directly available from the first-order motions calculation except the sectional quantity given by (78d). This quantity is generated from the sectional potentials within subroutine INTRPL. A user's manual for the program, briefly describing these routines, is presented in the appendices, together with input and output samples.

In order to maximize the possibilities for comparison with existing second-order force results, the Mariner-type fast cargo vessel was used in all the examples that follow. The Mariner was designed about 1950 at the Bethlehem Steel yard in Quincy, MA<sup>[25]</sup>. She has a length-between-perpendiculars of 528 feet, a beam of 76 feet, and a service speed of 20 knots. For this study, a full load draft of 29.75 feet was chosen giving a displacement of 21,000 tons. The pitch radius of gyration was set at about 25% of the L.B.P.

Further details on the ship can be obtained from Appendix D which gives a copy of the input used for this study in the M.I.T. 5-D program.

As a first step in a consideration of the theory, Equation (86) will be examined in detail for one particular oblique regular seas case ( $\beta = 150^\circ$ ,  $U = 15$  knots). From the form of the equation, it is clear that the second-order force prediction is generated as the sum of eleven components: Froude-Kriloff and Diffraction terms for each of the five modes of motion and the wave reflection term. These components are all plotted separately in Figure 2. The non-dimensionalized added resistance component (defined by  $\sigma_{AR} = \text{Added Resistance} / \rho g \alpha^2 B^2 / L$ , where  $B$  is the ship beam,  $L$  is the L.B.P., and  $\alpha$  is the wave amplitude) is given as a function of wave-length to ship length ratio. For this case, the Froude-Kriloff pitch term ( $\mathcal{F}_5^I$ , Eq. (75),  $j = 5$ ) makes a large contribution as does the Froude-Kriloff heave term ( $\mathcal{F}_3^I$ , Eq. (75),  $j = 3$ ). The wave reflection term ( $\mathcal{F}_D$  in Eq. (80)) also makes a contribution, particularly for very short waves, where it is totally dominant. The heave and pitch 'wave diffraction' terms ( $\mathcal{F}_3^D$ ,  $\mathcal{F}_5^D$ , Eq. (77),  $j = 3, 5$ ) act to reduce the added resistance considerably, while all the terms involving roll, sway, and yaw are practically insignificant. These relative magnitudes persist

(62) FIGURE 2: MARINER ADDED RESISTANCE COMPONENTS (Terms in Eq. (86))



in general in all near-head sea conditions, but in near beam seas, the pitch terms,  $\mathfrak{F}_5^I$  and  $\mathfrak{F}_5^D$ , play a much less important role while the sway, yaw, and reflection terms, ( $\mathfrak{F}_2^D$ ,  $\mathfrak{F}_2^I$ ,  $\mathfrak{F}_6^D$ ,  $\mathfrak{F}_6^I$ , and  $\mathfrak{F}_D$ ) increase their relative magnitudes. In following waves, the contributions of the various components are heavily dependent on encounter frequency and the associated accuracy of the strip theory, a question which will be discussed later at greater length.

It can be seen that all the significant motion-related second-order force components peak at one place (generally near the heave or pitch resonance, respectively) producing a sharp peak in the total force (marked  $\mathfrak{Z}$ ). This sharp peak is present for all heading angles, although its location varies, depending primarily on the location of the heave and pitch peaks in bow and beam waves. One final observation that can be made is that, for near head seas, the original formula of Havelock ((2), marked  $\mathfrak{Z}_{F-k}$ ) can be applied with some success. Since all the force components peak in the same area, and Havelock's formula contains two of the most significant positive terms, it will predict the peak location for the second-order force. Several investigators have found the magnitude of its predictions to be within a factor of two in most cases [5,28]. This has engineering significance because the Froude-Kriloff

force (See (75) and (45)) can be computed easily without knowledge of the sectional potentials. In fact, the calculations can be done by hand if a first order motions printout giving sectional Froude-Kriloff force is available.

Having generated a working second-order force computational scheme based on (86), the next step is to ascertain its validity. This will be done by comparison with experimental results and analytical predictions generated by other methods.

#### A. Comparison With Experimental Results

Experimental efforts on the second-order force problem are historically very complex and not too repeatable. The main reason for most of the difficulties can be easily identified. The periodic forces involved are extremely small, making measurement very difficult, especially in the presence of friction in the mechanical equipment, vibration in the towing carriage, and electronic noise. Most of the towing tank work that has been done has been directed toward finding the added resistance in regular head seas. There are two methods for carrying out these measurements: constant velocity (where the model is free only to heave and pitch) and constant thrust (where a self-propelled model is attached to a movable sub-carriage and allowed to



surge, as well). All the experimental work presented in this report was obtained using the constant velocity method. This allows a more effective comparison with the computer program, which neglects surge.

As mentioned before, the second-order force is primarily a wave phenomenon and can be scaled by Froude number so that the force on the real ship will be proportional to the model force times the cube of the scale ratio. Pure Froude scaling also implies that the use of small models is justifiable, but this must be tempered with the realization that the forces involved must remain measurable. It is also important that the wave height be kept fairly small to be consistent with the linear strip theory.

The paper by Strom-Tejsten, et. al.<sup>[29]</sup> contains a detailed description of an experimental program carried out at NSRDC to determine the added resistance in head seas of a range of Series 60 models, a destroyer, and a high-speed form. Other extensive head sea experiments have been done by Gerritsma and Beukelman<sup>[5]</sup>, Beck and Wang at M.I.T.<sup>[2,31]</sup>, and the University of Osaka<sup>[10]</sup>. Sibul has also done a great deal of work with Series 60 models at the University of California<sup>[28]</sup>, and some of his results are shown in Figure 3.

It is intended that this figure will be representative

(66)

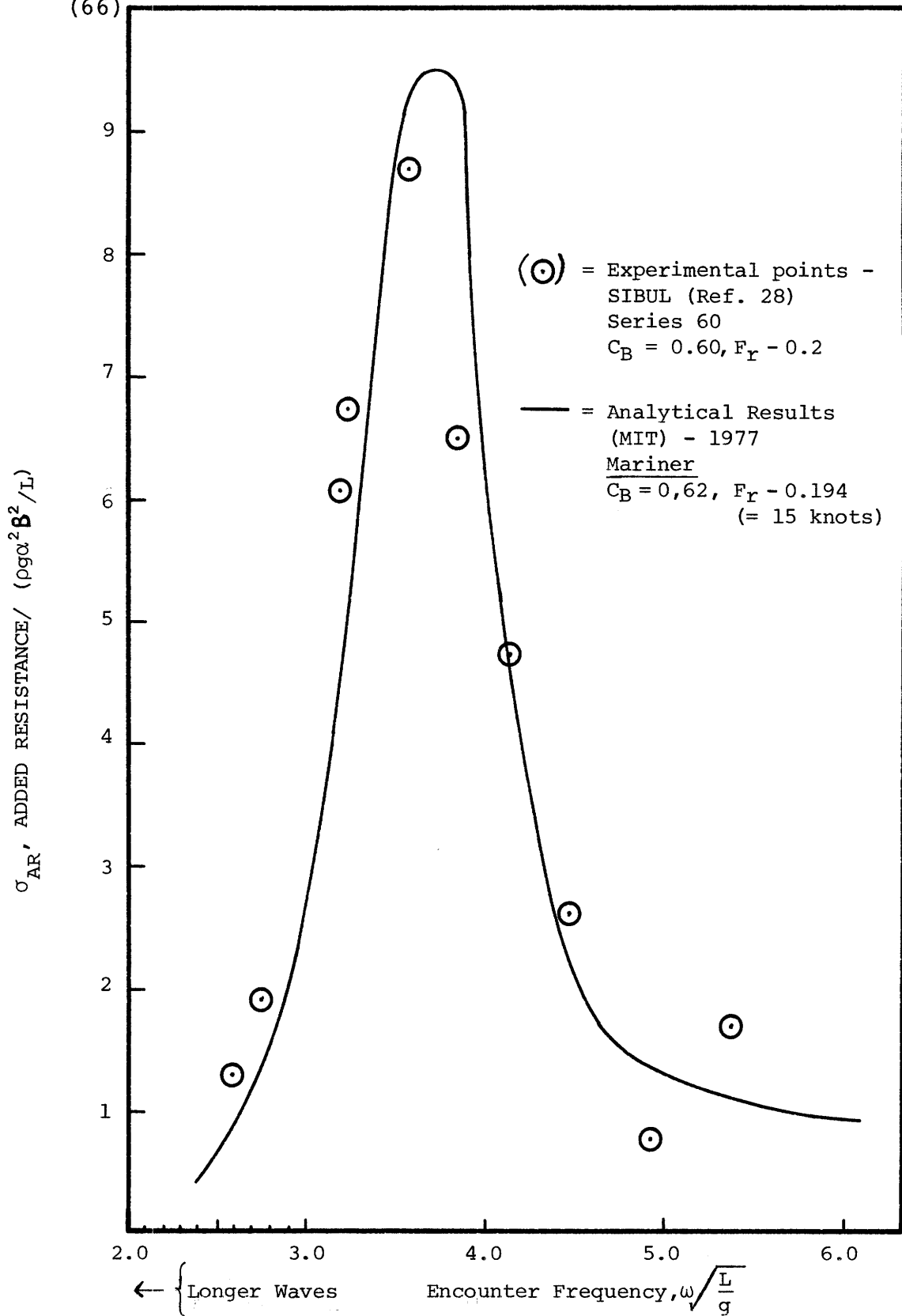


FIGURE 3: ADDED RESISTANCE/HEAD WAVES

of the fact that Equation (86) provides a very good correlation with experiments for the familiar case of head seas. The plot shows experimental results for a Series 60 model very similar to the Mariner at nearly the same Froude number. The agreement with (86) is well within experimental error throughout most of the range of practical wavelengths. However, acceptable theoretical prediction methods for added resistance in head seas have been available for several years, and this report is primarily intended to address the more general problem of second-order force in oblique seas.

As soon as the head seas restriction is lifted, the experimental difficulties involved become almost insurmountable. A large basin must be available to achieve the desired range of heading angles, furthermore the model must now ideally be allowed complete freedom of motion, making measurement very difficult. Many other complexities might be enumerated, but it is perhaps sufficient to say that very little oblique seas second-order force data is presently available. Spens and Lalangas have done some work on a Series 60 model at Stevens, measuring drift force and yawing moment [28]. Also, Hosoda presents a few results for a container ship [10]. Journee [12] did work at Delft with another container ship in following seas.

The work done at Stevens has already been employed by

Salvesen for comparison in his paper [28]. Since comparison with Salvesen's calculations will later be presented, the Stevens results are not reproduced here. Furthermore, ship characteristics were not readily available for the other cases. Consequently, it was decided that an oblique seas experiment should be carried out in order to provide a basis for theoretical comparison in this report. The only work of this nature that could be done in the M.I.T. ship model towing tank involved near beam sea cases at zero speed. The zero speed restriction is obvious since the carriage and the generated waves must run parallel to the long axis of the conventionally shaped tank. The beam seas restriction was intended to minimize interference between the outgoing damping waves of the ship and the tank walls.

An existing fiberglass Mariner model (L.B.P. = 5.42') was employed for the experiment. It was mounted beamwise in the tank and connected to the carriage by a heave staff and a roll bearing. All other modes of motion were thus restrained. The M.I.T. tank is 108' long, 8-1/2' wide, and 4' deep, and the model was positioned at approximately the halfway point. Waves were generated by a pivoted hydraulically driven paddle. Only regular sinusoidal waves of varying length were used.

Instrumentation consisted of a dynamometer-force block

fixed transversely in the model to measure drift force, a transducer on the heave rod, a transducer on the roll bearing, and an electrical resistance wave probe for measuring incident wave height. All the data was taken to a Sanborn multi-channel chart recorder which provided a real-time visualization of the signals. Data was taken at regular wavelengths ranging from about one-half to about four times the ship length. Smaller waves could not be generated, and longer ones were pointless because of the 'deep water wave' assumption inherent to the theory. Newman states<sup>[23]</sup> that if the depth over wavelength ratio becomes less than  $1/2$ , the 'deep water wave' assumption begins to break down. This affects the incident wave potential formulation (44). For a wave in the tank four times the ship length, the ratio is less than  $1/4$ .

Throughout the experiment wave height was kept constant at about 1.25 inches. This represented a compromise between the desires for small wave heights for linearity and large wave heights for measurable forces. At the most, the mean forces measured represented a few tenths of a pound, and the motions were at times unavoidably large. The experimental procedure consisted of sending a regular wave train toward the model and taking data until a steady state was obtained in all the responses. The data record

was stopped when the incident regular wave train became contaminated (e.g. by reflected waves from the towing tank beach.) The mean drift force was obtained by graphical measurement using the output from the chart recorder. The wave amplitude (necessary for nondimensionalization) was similarly estimated. The resulting experimental points are shown as circled-dots on Figures 4, 5, and 6 for the three heading angles investigated ( $\beta = 90^\circ$ ,  $105^\circ$ , and  $75^\circ$ , respectively).

Two drift force computations are also shown on each of the graphs. The solid line corresponds to the full five degrees of freedom prediction, (Eq. (86),  $j=2,..6$ ) while the starred line represents a calculation in which the computer program was artificially restrained\* to represent a roll-heavetwo-degree of freedom, system. (Eq. (86),  $j = 3,4$ ). The computer was run using a higher metacentric height (Scale, 8') and a smaller roll radius of gyration (Scale, 11') than the real ship because it was very impractical to adjust the measured model characteristics. At any rate, this made little difference in the predictions, because these changes impacted most heavily on roll response, and roll is always a small contributor to the second-order force calculated in (86).

Examination of the three graphs will show that the expected level of agreement is obtained for all wavelengths

\*see APPENDIX C.

FIGURE 4: MARINER MODEL,  $U=0$ ;  $\beta=90^\circ$

(20.5) (33.156)

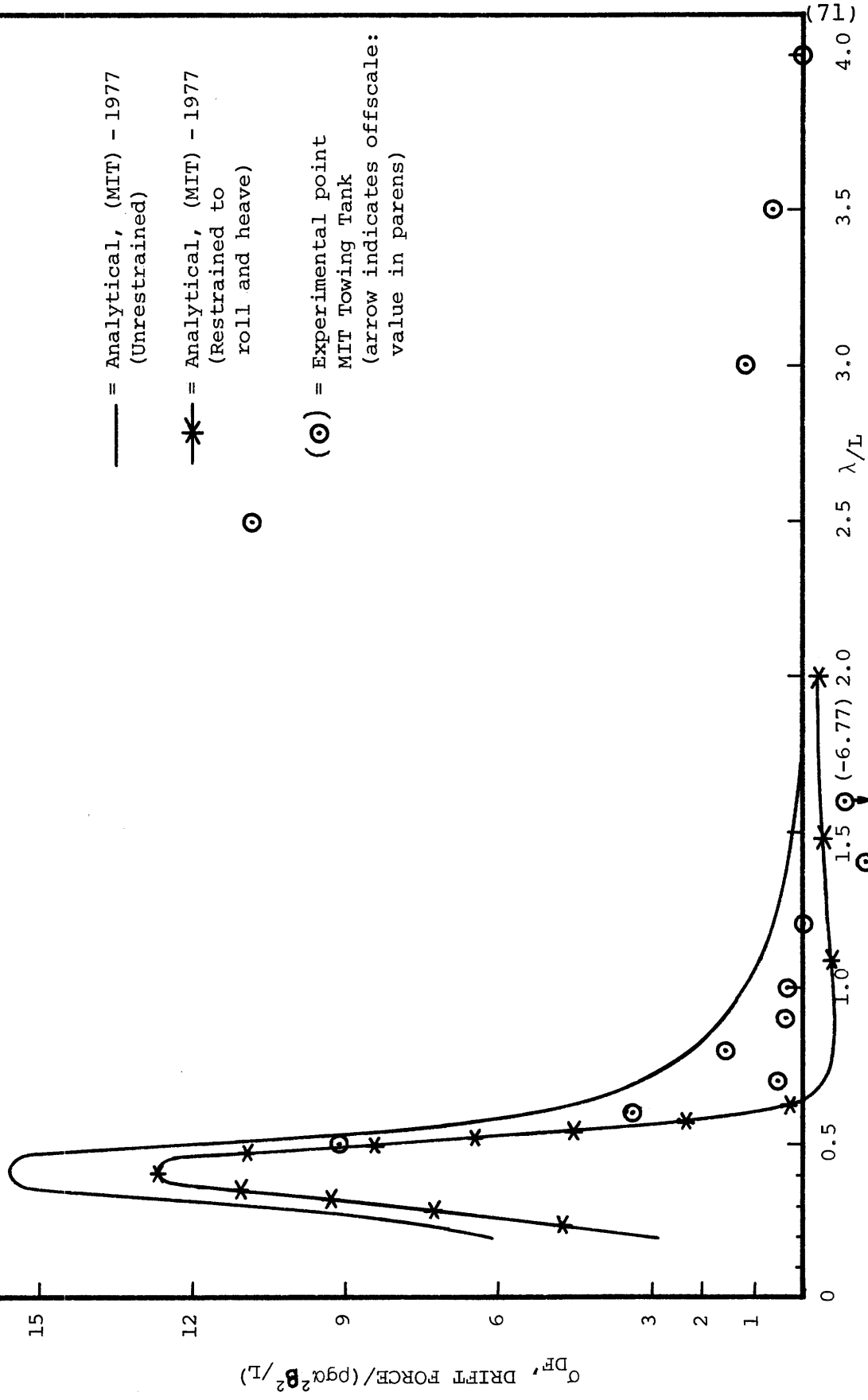


FIGURE 5: MARINER MODEL; U=0;  $\beta=105^\circ$

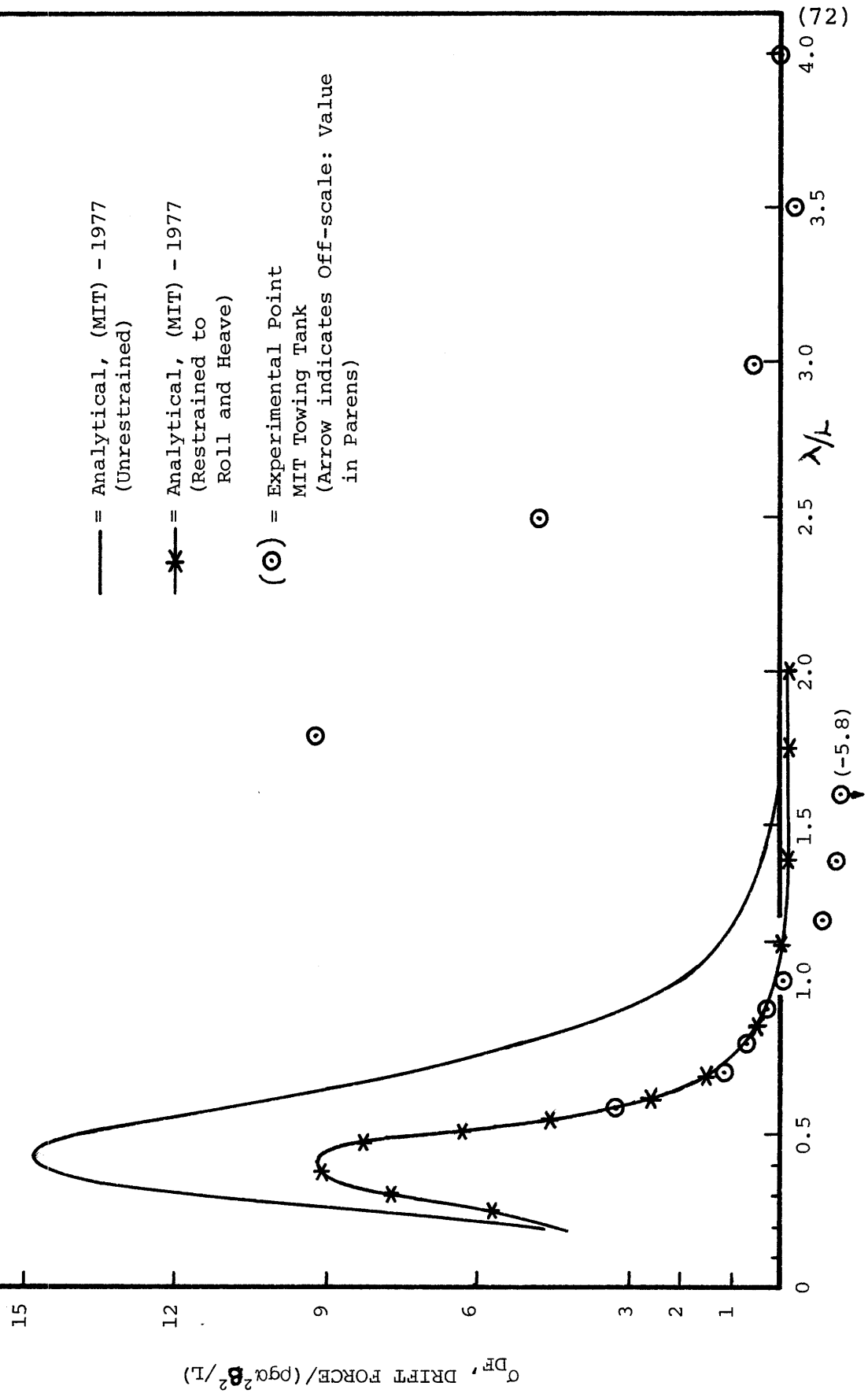
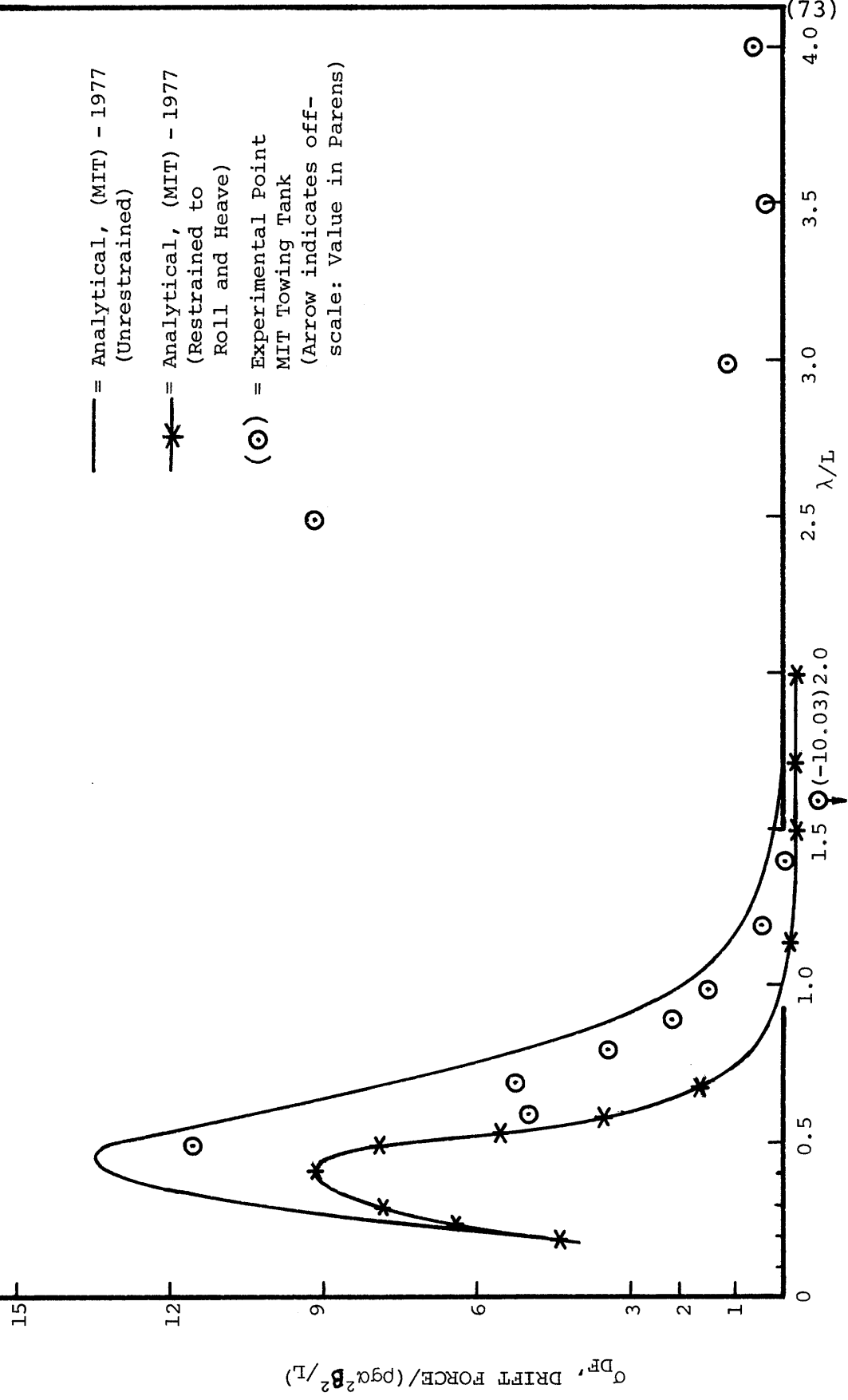




FIGURE 6: MARINER MODEL; U=0;  $\beta=75^\circ$

$\odot$  (17.25) (26.52)



between 0.5 and about 1.4 times the ship length. This is particularly true for the  $\beta = 105^\circ$  case (Figure 5), where the points fall nicely on the line predicted by the computer using the two-degree of freedom assumption. It can also be seen that for wavelengths greater than about 3.5 times the ship length, the mean forces go to zero as the computer predicts.

However, a serious surprise is contained in the data for the wavelengths between about 1.5 and 3.5 times the ship length. In this area on all three graphs, the computer predicts near zero mean force, but the measured results 'blow-up' as the wavelength increases. A solution or a full explanation for this theoretical discrepancy is, as yet, unavailable.

It can be noted that the model attains roll resonance in the area of  $\lambda/L = 1.7$  and sustains a very large roll angle (no less than plus or minus 15 degrees). Large roll amplitudes persist up to  $\lambda/L = 3.0$ . Furthermore, when the roll natural period of the ship was shifted by using outrigger weights, the location of the problem area shifted with it. Currently, it is felt that the observed behavior does not represent a problem with the measurement equipment. Rather, it is supposed that this represents a nonlinear interaction associated with the large roll angle. This would explain

the lack of correlation with any linear, small motion theory. An appreciation for the experimental difficulties involved in these measurements can be obtained, when it is realized that the measurements described above as 'blowing-up' represent a few tenths of a pound on model scale. In closing, it should be emphasized that good agreement was obtained over a sizable portion of the range where linear theory would be expected to apply.

#### B. Comparison With Other Theoretical Results

In the preceding portion of this chapter, Salvesen's second-order force was examined in some detail in order to gain insight into the behavior of its various components. Then it was compared with some existing and some new experimental results. The outcome was generally quite favorable in the area where linear theory would be expected to work, but some serious questions were also raised concerning applications in the area of roll resonance.

The next available step is to compare the results of the theory in the M.I.T. 5-D program with the results from other programs and linear theories. To date, the only second order force computational results published for oblique seas have been offered by Salvesen<sup>[28]</sup> and Loukakis (Ref. [16]).

Salvesen also programmed Equation (86), but he did so

within the framework of the Naval Ship Research and Development Center Ship Motion and Sea Load Program. This program uses a different scheme for creating the two-dimensional sectional potentials. It also incorporates several other differences in numerical techniques, so his results (called 'Salvesen' and labeled NAV) can be used to assess the impact of computational procedure on the theoretical predictions.

Loukakis presents results called 'Loukakis' and labeled (NTUA) which are based on a different theory. His method was briefly mentioned in Chapter II. It is based on the original work of Gerritsma and Beukelman, and it represents a totally different "radiated energy" formulation of the problem. However, this new theory was implemented on a version of the M.I.T. 5-D motions program, so the two theories can be compared without undue concern for the impact of numerical techniques. Admittedly, there will be discrepancies because Loukakis made his computation using only vertical motions in order to avoid a roll resonance problem. To summarize, it will be possible to make comparisons with the same theory in a different motions program (M.I.T.-NAV) and a different theory in the same motions program (M.I.T.-NTUA). The ship for these comparisons is the Mariner-type fast cargo vessel already described.

Figure 7 shows the predicted impact of forward speed on added resistance in head waves. Results are plotted for

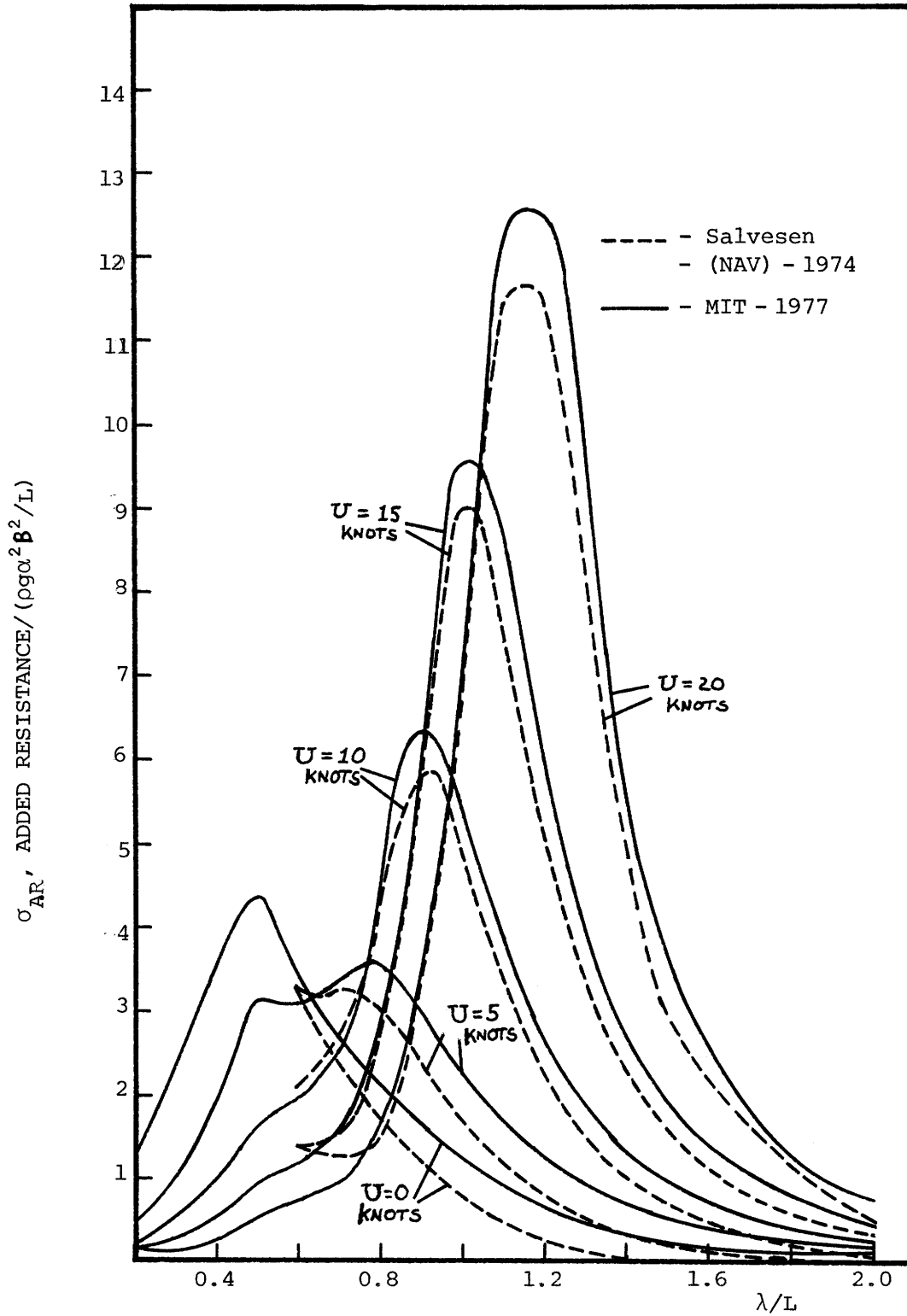


FIGURE 7: MARINER- ADDED RESISTANCE HEAD WAVES  
( $\beta = 180$  ) VARIOUS SPEEDS

both the M.I.T. program (MIT) and the Salvesen program (NAV). The magnitude of the peak appears to increase with the speed, except at speeds near zero. The higher speeds also tend to reach their associated peak values at longer wavelengths coinciding with the heave and pitch peaks. This is very important when the graph is considered as a response operator for use in the spectral analysis of irregular sea states because most of the ocean energy is in relatively long waves. The two computational methods compare well for the shorter wavelengths before the peaks; however, some discrepancies can be seen in the medium wavelength area beyond the peak. No explanation can be offered for this since the (NAV) program details are unavailable to the author. There is also some difference in the actual peak value predicted, but it is very difficult to obtain enough data points to truly characterize the peak. Of course, for long waves, all the results go to zero.

Figures 8 and 9 show the general effect of a heading change in bow waves on the added resistance component of the second order force. Figure 8 shows Salvesen and M.I.T. calculations, and Figure 9 gives Loukakis and M.I.T. Both Figures 8 and 9 were run at a speed of fifteen knots. The graphs show how the second order force peak comes in much shorter waves as Beta goes to ninety degrees, following

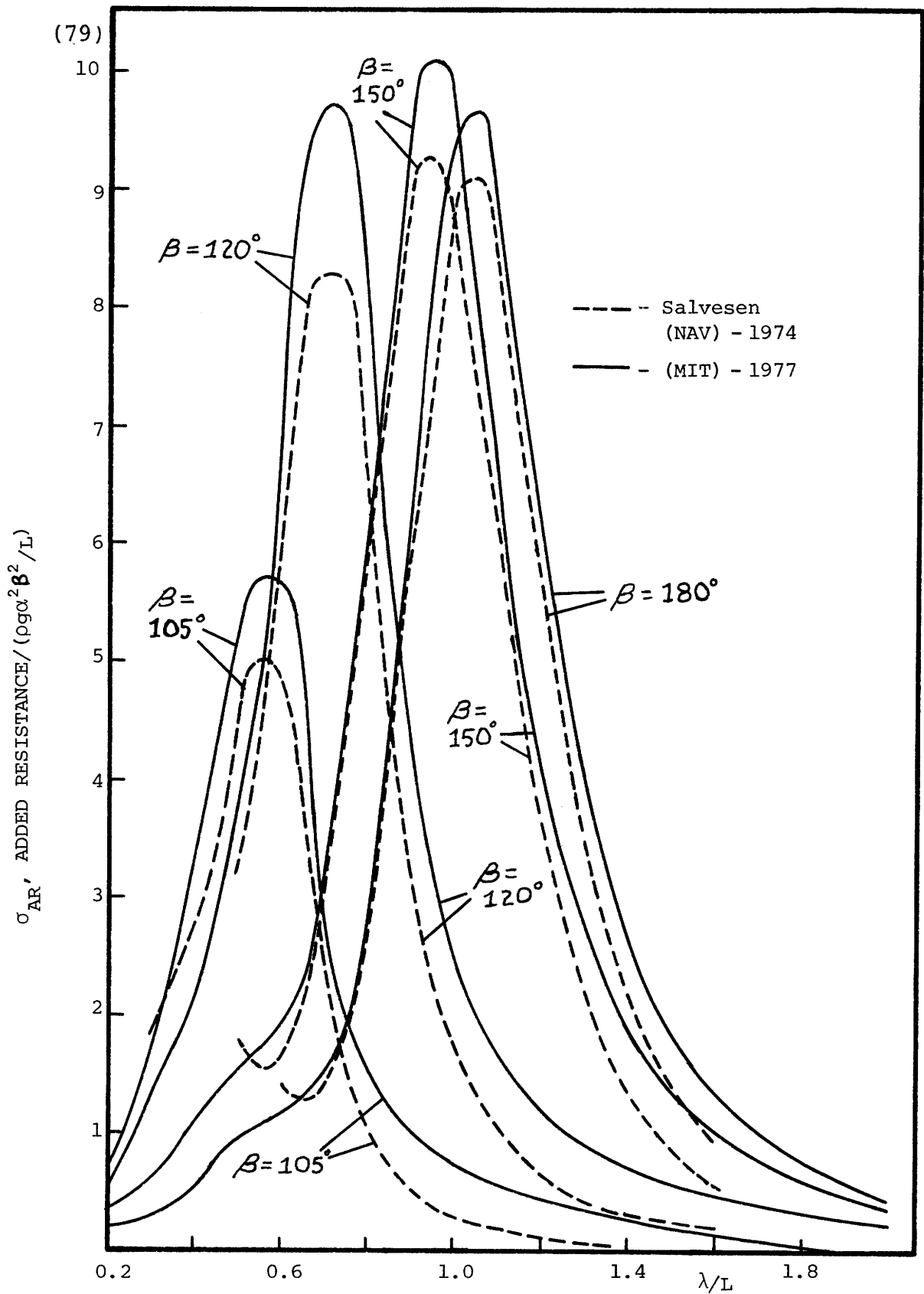


FIGURE 8: MARINER - ADDED RESISTANCE (SPEED - 15 knots)  
Various Headings

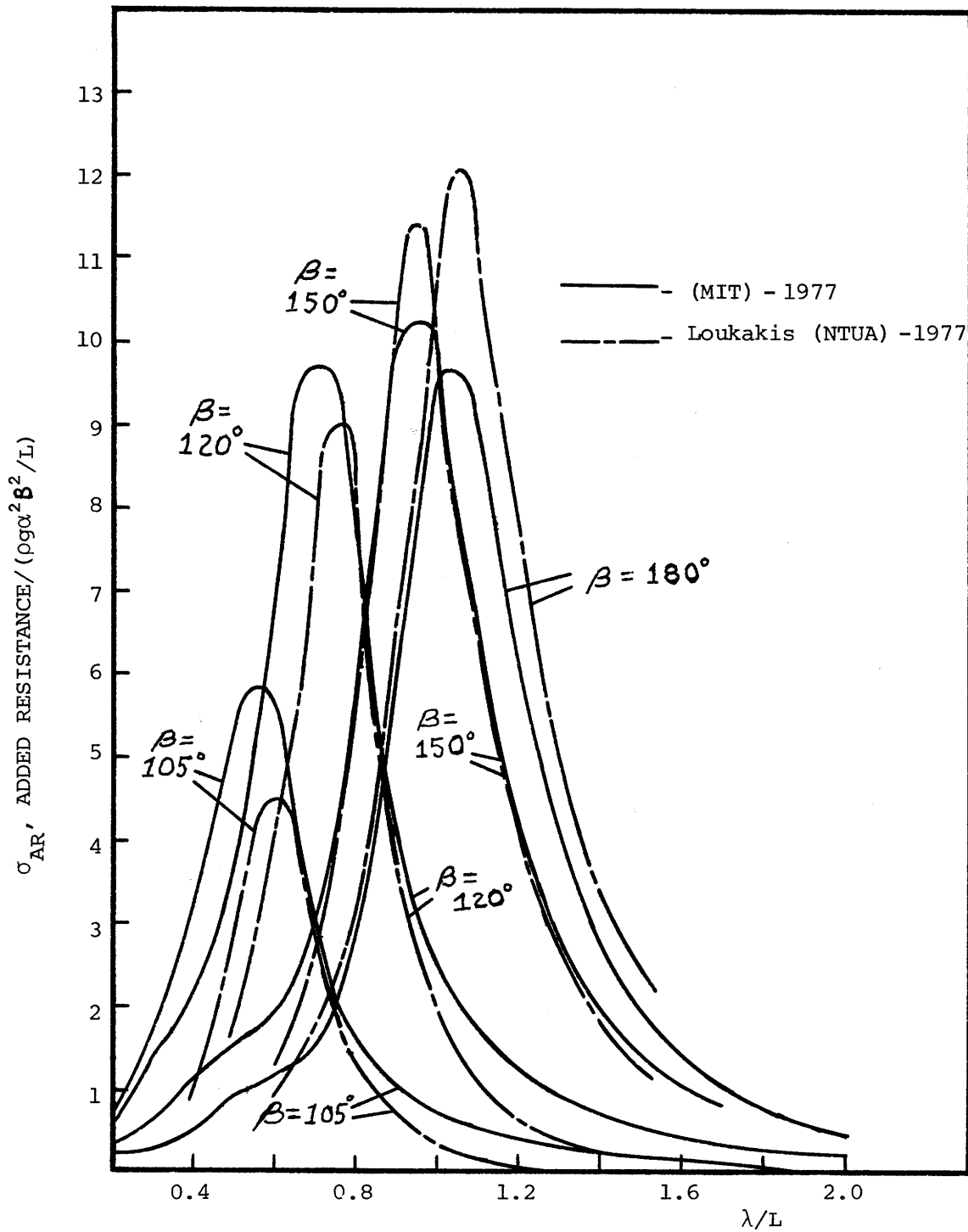


FIGURE 9: MARINER - ADDED RESISTANCE  
(SPEED - 15 knots); Various Headings



closely the movement of the heave motion peak. The M.I.T.-Salvesen correlation is much the same as in Figure 7: good correspondence for low wavelengths (except for  $\beta = 105^\circ$ ), peak magnitude differences and M.I.T. overpredicting NAV results for medium length waves. The Loukakis program predicts much higher peaks than the M.I.T. results for near head seas, but lower peaks for near beam seas. It also gives slightly different peak locations, and noticeable differences in the medium wavelength area. It is interesting to note that the character of the three solutions is generally the same, but they are by no means the same. Also, the M.I.T. program predicts more resistance at  $\beta = 150^\circ$  than in head waves (presumably due to contributions from the three extra degrees of freedom).

Figure 10 illustrates the effect of forward speed on drift force in oblique bow waves ( $\beta = 120^\circ$ ). Nondimensional drift force (defined by  $\sigma_{DF} = \text{drift force} / \rho g \alpha^2 B^2 / L$ ) is shown as a function of wavelength over ship length. Results are shown for the M.I.T. and Salvesen schemes. Higher forward speed again increases the peak drift force, as was observed for the added resistance in Figure 7. Increasing speed also shifts the peak value to longer wavelengths. Furthermore, (from the figures in Reference 28), there is an indication that the Salvesen curves turn sharply up in

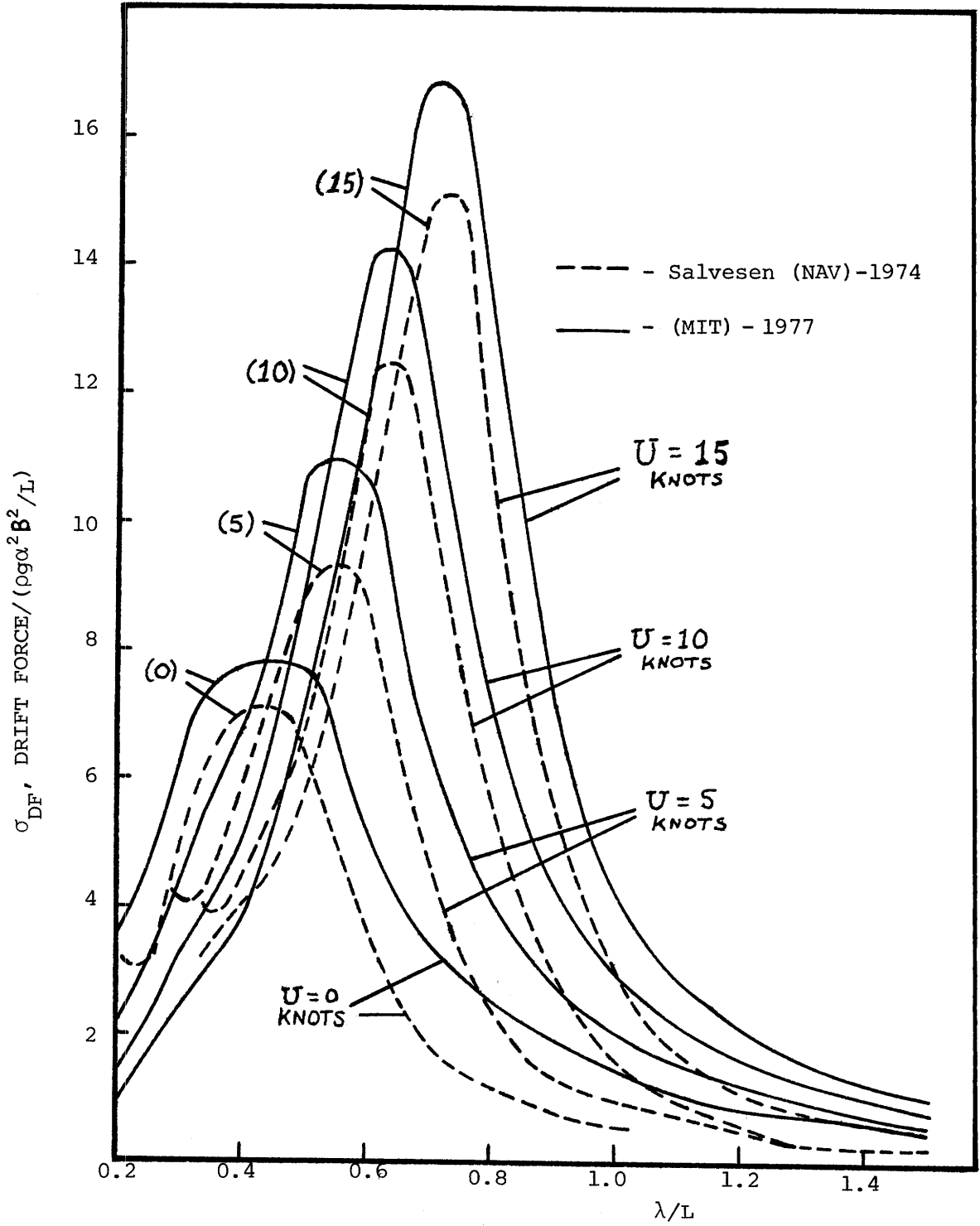


FIGURE 10: MARINER - DRIFT FORCE  
 $B = 120^\circ$ ; Various Speeds

the shorter waves; this does not occur in the M.I.T. calculation. The reason for this cannot be explained or justified. The usual differences between the two results in medium wavelengths show clearly. In general, it could be said that the correlation is improved by a speed increase.

It would perhaps be useful, at this point, to interject a quantitative idea concerning the real force magnitudes involved in these nondimensional numbers. For example, the peak added resistance at twenty knots (about '12' in Figure 7) in 5-foot amplitude waves, corresponds to a force of about 200,000 pounds on the real ship, a figure roughly on the order of the calm water resistance at the same speed. The peak drift force in Figure 10 at fifteen knots (about '17') would translate into almost 300,00 pounds in 5-foot amplitude waves. Of course, these numbers are for one particular highly tuned regular wave frequency. The spectral analysis to be outlined in Chapter V will lead to much lower mean values but the significance of the numbers involved can surely be appreciated.

Figures 11 and 12 present the impact on drift force of a heading angle change in bow waves at fifteen knots. The first of the two presents M.I.T. and Salvesen (NAV) results while the second gives M.I.T. and NTUA predictions. As expected from the added resistance curves of Figures 8

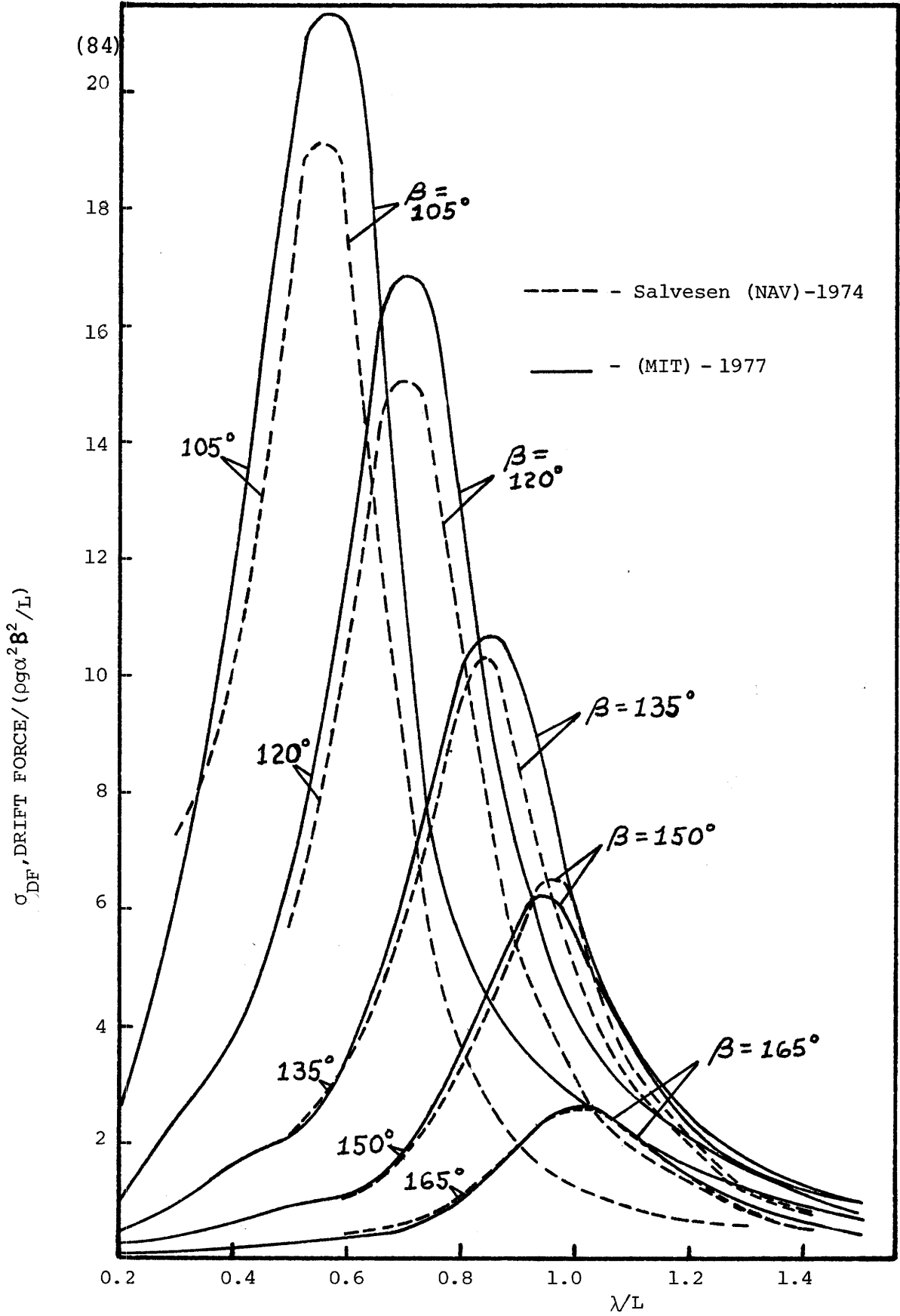


FIGURE 11: MARINER - DRIFT FORCE (SPEED - 15 knots) Various Headings

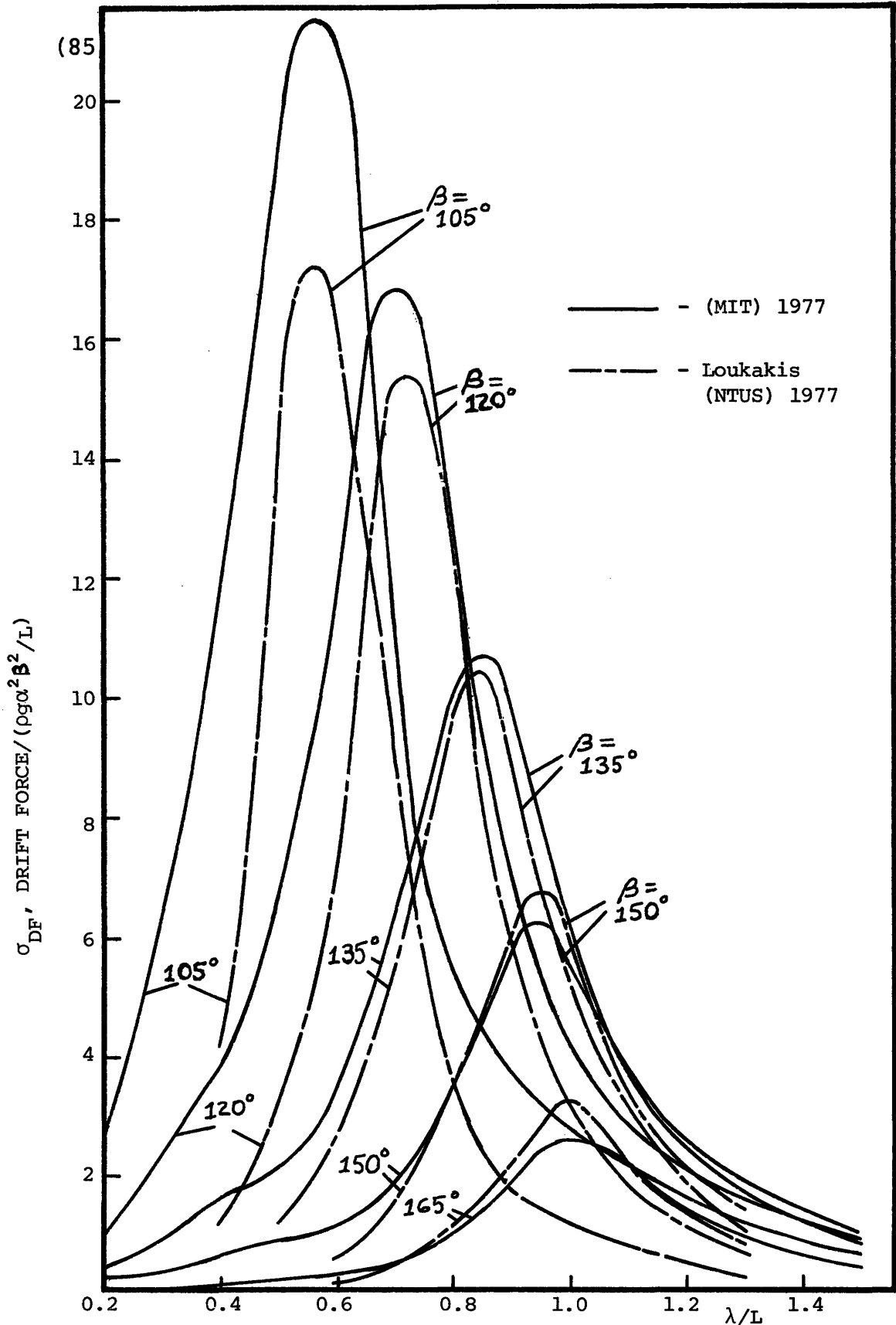


FIGURE 12: MARINER - DRIFT FORCE (SPEED-15 knots) Various Headings

and 9, the peak values occur at larger wavelengths and have decreasing magnitudes as the waves come on the bow. The M.I.T.-Salvesen comparison becomes better as the heading angle increases. The usual peak and medium wavelength differences appear except at  $\beta = 150^\circ$  where the Salvesen peak is higher. The NTUA results illustrate much the same tendencies, and generally come closer to the Salvesen computation than the M.I.T. one.

The final two graphs (Figures 13 and 14) delve into an area that is the subject of considerable controversy in ship motion theory -- following seas. Salvesen did not give any results for heading angles less than  $105^\circ$  in his 1974 paper, so the only available comparison is provided by Loukakis.

Figure 13 shows negative added resistance for a range of headings at fifteen knots. Both sets of results are fairly consistent in the longer wavelengths, showing a tendency to decrease the prediction with increasing heading angle. However, the M.I.T. results tend to wander around the axis for  $\beta = 75^\circ$  and  $\beta = 60^\circ$ . This can most likely be attributed to numerics. The peak magnitudes generated by the two methods differ considerably, but anyway, the existence of any peak, at all, has not as yet been established experimentally. The container ship experiments of Journee

FIGURE 13: MARINER - NEGATIVE ADDED RESISTANCE (Speed-15 knots) (87)  
Various Headings

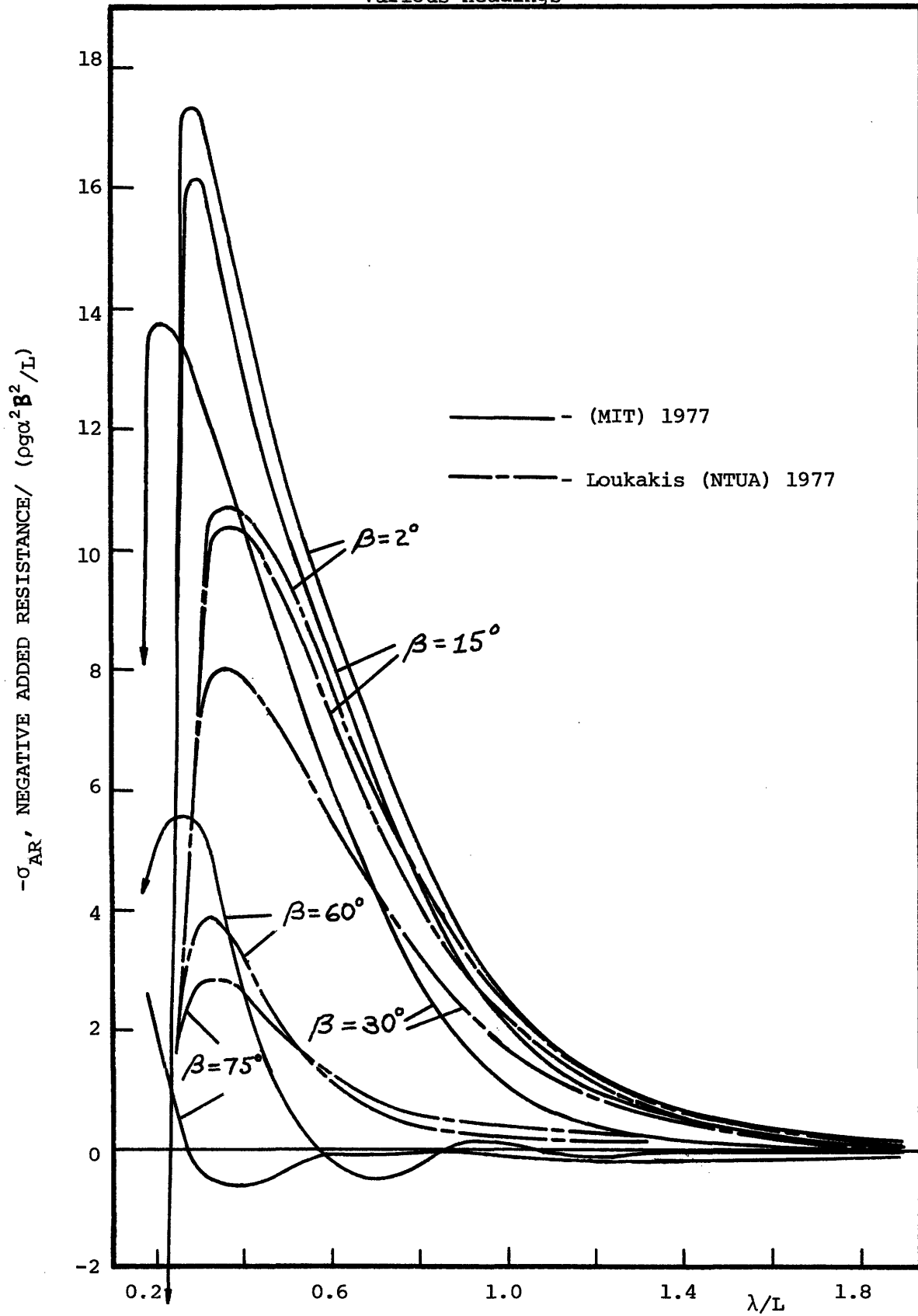
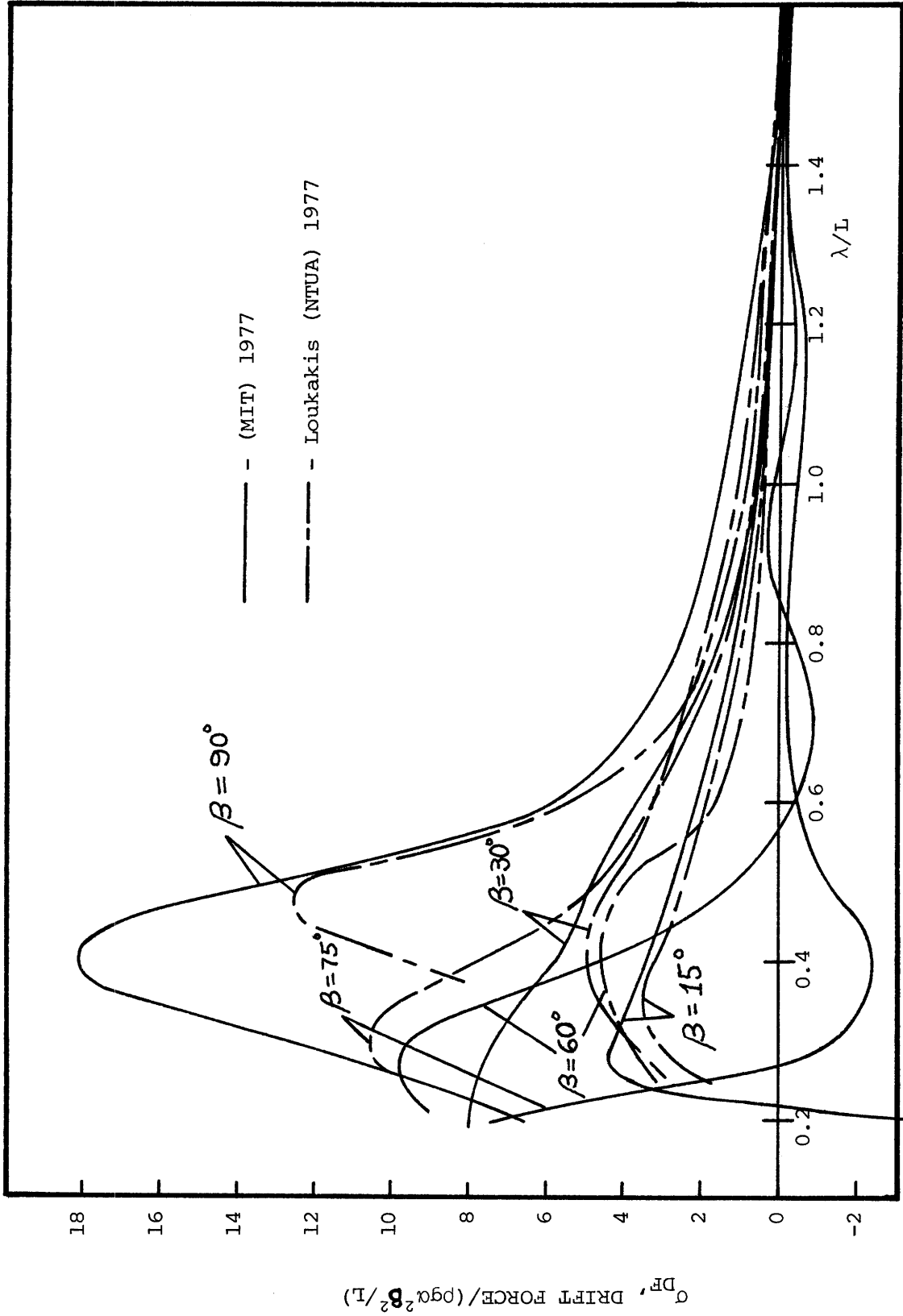


FIGURE 14: MARINER - DRIFT FORCE (SPEED - 15 knots) Various Headings





(Ref. 12) show this quite clearly since he obtained positive added resistance throughout the entire wave range in following seas ( $\beta = 0^\circ$ ). Loukakis attempted a computation based on the container ship and received results similar to those of Figure 13<sup>[16]</sup>. Further doubt can be placed on these peak predictions by virtue of the fact that they occur very near zero encounter frequency for the lower heading angles. As the ship passes into the negative encounter frequency region, the curves all take a large 'jump' to a positive added resistance. This jump does seem to occur in a somewhat more orderly fashion in Loukakis' work. Additional insight into the problem can be obtained by considering Figure 14 which shows positive drift force at fifteen knots for the same following seas cases and for beam seas. The results show a large amount of inconsistency in the magnitudes. There is no clear-cut decrease of force with decreasing heading angle for either set of data. All the same problems mentioned for Figure 13 are, of course, present for all the following sea headings. In addition, the beam seas case gives a rather disappointing comparison between the two theories. The M.I.T. and NTUA results do agree well in beam seas down to a wavelength/ship length ratio of 0.5; then they diverge rapidly. The experiments of Figure 4 might be used to illuminate this

matter, but unfortunately they could not be extended to smaller waves.

In summary, the three theories presented compare very well with each other over the full speed range of the Mariner for heading angles greater than  $105^\circ$  (bow waves). In most of these cases, the M.I.T. results show a larger second-order force in medium wavelengths than the other two methods. The head seas results of Figure 3 show experimental points that fall slightly above the M.I.T. predictions in the long wave range, so this may well be an asset in the M.I.T. version of the theory. However, experimental data for any oblique bow wave case is noticeably absent, and final conclusions cannot yet be drawn for this region.

Agreement between the theories becomes noticeably poorer in the beam seas regime. Loukakis' decision to ignore the lateral motions contribution may be a factor. Also, the 'weak-scatterer' potential assumption (See Eqs. (65) and (66)) incorporated in the Salvesen theory is expected to cause problems in this area, but, again, the lack of experimental work prevents a conclusion. The beam seas experimental work that was done (Figs. 4,5,6) raised serious questions concerning the validity of any linear theory in the presence of large roll amplitudes. The Salvesen theory, in particular, is quite insensitive to the roll mode of motion. This mode makes little contribution

to the second-order force, even when its predicted amplitude is large.

On the subject of numerical computation problems, the M.I.T. version of the Salvesen theory exhibits some oscillations at fifteen knots in quartering seas (Figs. 13,14). Some of the Salvesen (NAV) results indicate a sharp upward turn in the second-order force for short bow waves (e.g., Fig. 8 or 10). This is noticeably absent in the M.I.T. computation.

In following seas, both the NTUA and M.I.T. calculations exhibit difficulties. Neither shows any real consistency, and the agreement between either theory and experiment is poor. This problem is discussed in some detail by Loukakis (Ref. 16).

He shows how the total added mass and damping tend to zero, while some of the sectional coefficients go to infinity, as the encounter frequency decreases. This decay will take on one of several forms, depending on the order of magnitude relation between the encounter frequency and the incident wave frequency. All these tendencies are artificially introduced by the strip theory assumptions. Nevertheless, the equations of motion produce 'reasonable' (but not necessarily 'accurate') predictions. This may well be due to the hydrostatic terms dominating

the equations, making the damping and added mass insignificant. The linear second-order force predictions are a different matter, though. They are dependent to a large extent on the same sectional potentials that cause the problems in the motions computation.

Very near zero encounter frequency, it has been observed that several of the components of the Salvesen theory grow very large; and it is only the fact that they have opposite signs that keeps the prediction bounded. In conclusion, it is obvious that much work remains to be done on the following seas problem.

## V. DESIGN ANALYSIS

An ocean seaway represents a true random process. The wave patterns are continually changing in time and space, and their complexity defies any deterministic analysis. In view of this, the results of Chapter IV for regular sinusoidal waves must be considered as only a first step in a procedure that will lead ultimately to a statistical formulation of second order wave force in the real ocean.

Conceptually, the method to be used involves obtaining a Fourier integral representation of the ocean. The actual sea surface is represented by superimposing many infinite, in theory, regular waves of different periods, random phase and infinitesimal amplitude. The end result is an amplitude or energy spectrum for the sea, depicting the energy in the ocean as a function of frequency. For a linear system, the principle of superposition can be invoked so the response to a number of input regular waves is the sum of the responses to each, individually. Therefore, if the response of the system can be obtained as a function of frequency, then this can be combined with the sea spectrum to yield a response spectrum. Under certain other probabilistic assumptions, predictions regarding, for example, the highest likely response or the probability of an event, can

then be made using the response spectrum.

This theory of random excitations for linear systems has been used to good advantage to provide a design tool in the area of ship motions, and many good references on the technique are available<sup>[4]</sup>. However, it is not immediately obvious that this technique can be used for the second order force. Vassilopoulos<sup>[30]</sup> proved it rigorously using nonlinear system theory<sup>[30]</sup>, but Maruo first gave an intuitive derivation<sup>[7]</sup> that is repeated below.

If the sea can be described by a long-crested (unidirectional) energy spectrum,  $E(\omega)$ , the following will be true for each infinitesimal frequency component, where  $d\alpha$  is the infinitesimal wave amplitude.

$$E(\omega_s) d\omega_s \sim (d\alpha)^2 \quad (87)$$

Futhermore, if the second order force is purely proportional to wave amplitude squared for any frequency, as originally stated in the Introduction, then it follows that:

$$\Delta F / (d\alpha)^2 = f(\omega_s) \quad (88)$$

where  $F$  represents the second order force. (Note that  $f(\omega) / (\rho g B^2 / L)$  is the quantity plotted as a function of

wavelength (frequency) in all the results of Chapter IV.)  
Combining (87) and (88) for a frequency increment, gives:

$$\Delta F = f(\omega_s) E(\omega_s) d\omega_s \quad (89)$$

It follows from probability theory that the integral of the second order force spectral component (89) over all possible frequencies will represent the expected mean second order force for a long period of time in the long-crested seaway,

$$\bar{F} = \int_0^{\infty} f(\omega_s) E(\omega_s) d\omega_s \quad (90)$$

The result (90) was developed by Maruo using a spectrum  $E(\omega)$ , based on the full wave amplitude (See (87)). The spectrum definition which is most commonly used in practice is based on one-half the amplitude squared. Calling this spectrum  $\Phi_{ff}^+(\omega)$ , the formula (90) becomes,

$$\bar{F} = 2 \int_0^{\infty} f(\omega_s) \Phi_{ff}^+(\omega_s) d\omega_s \quad (91)$$

This is the formula given in Strom-Tejsen, et. al. [29].  
Should a more rigorous derivation be desired, Vassilopoulos

should be consulted. [30] If the long-crested unidirectional seas assumption (made before (87)) is relaxed, Maruo showed (and Newman [22] recently rederived rigorously) that the mean second order force in short-crested seas can be approximated in this manner,

$$\bar{F}(\theta) \cong \frac{2}{\pi} \int_{-\frac{\pi}{2}}^{\frac{\pi}{2}} \bar{F}(\beta) \cos^2 \mu d\mu \quad (92)$$

$(\mu \equiv \beta - \theta)$

In this expression,  $\theta$  is the principal wind direction or primary directional source of waves (defined the same as  $\beta$  in Chapter III.  $\bar{F}(\beta)$  is a mean force for a particular ship heading angle, developed from (91). The well-known 'cosine-squared' spreading function has been employed to distribute the effective energy in the sea placing it primarily in the waves coming from the principal wind direction. Equation (92) represents a double integral over frequency and propagation direction, but it is still, conceptually, a superposition of many small sine waves.

Returning, for now, to long-crested seas, (91) was found to be well suited to inclusion in the M.I.T. 5-D program (which already calculated many statistical quantities associated with ship motions). Response operators in the form of (88) were easily developed from the results of



regular wave calculations. Then these were combined with the various sea spectra and numerically integrated in subroutine STATIS according to (91).

A separate auxiliary program that performed motions calculations in short-crested seas was already in existence. This was modified so that it could receive the second order (long-crested) mean force output from the 5-D program (according to (91)). It then performs a calculation set forth in (92), yielding, finally, a predicted long-time mean added resistance and drift force in a short-crested, irregular seaway.

In order to test the feasibility of employing (91) and (92) in the design process, six wave spectra were chosen. The six are shown in Figure 15.

Spectra 1, 2, 3, and 6 are Peirson-Moskowitz fully-developed one-parameter representations from the formula:

$$\Phi_{ff}^+(\omega_s) = \frac{A}{\omega_s^5} e^{-\frac{B}{\omega_s^4}} \quad (93)$$

where  $A = .0081g^2$  and  $B = 33.56/\bar{h}_{1/3}^2$ . The quantity,  $\bar{h}_{1/3}$ , represents the significant wave height (the average height of the one-third highest observed waves). Spectra 4 and 5 were developed by use of the Bretschneider, two-parameter representation:

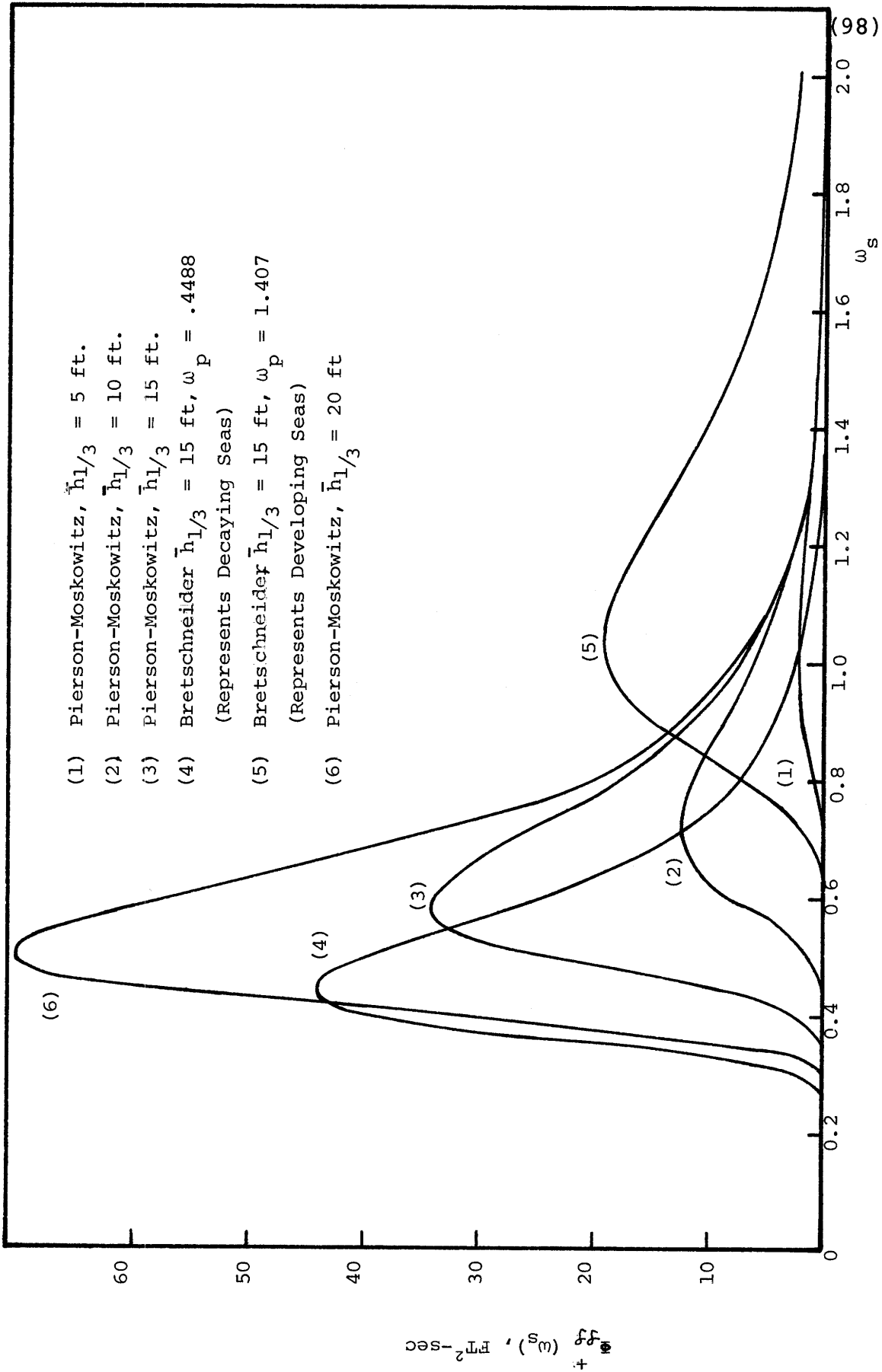


FIGURE 15: SEA SPECTRA

$$\Phi_{ff}^+(\omega_s) = \frac{5}{16} (\bar{h}_{1/3})^2 \frac{\omega_p^4}{\omega_s} e^{-\left(\frac{5}{4} \frac{\omega_p^4}{\omega_s}\right)} \quad (94)$$

where  $\omega_p$  is the desired location of the spectral peak. For spectrum 4, the peak was chosen at a much lower frequency than that generated by the Pierson-Moskowitz formula for the same  $\bar{h}_{1/3}$ . This corresponded to a decaying seaway, where the energy is found in longer waves. The peak for spectrum 5 was located at a much higher frequency, thereby simulating a developing sea, taking energy from the wind in the short wave region.

These six spectra were used in (91) in combination with response operators generated by the theory of Chapter III for regular waves. The operators were calculated for a full range of headings at the service speed of twenty knots. The resulting long-crested seas predictions were then used in (92) to provide information on second order forces in the corresponding short-crested seaway.

The results obtained from spectra 1, 2, 3, and 6 are shown in Figures 16 and 17 for added resistance and drift force, respectively. In these plots, the force is non-dimensionalized using significant wave height squared.

Figure 16 shows mean added resistance as a function of significant wave height for the Pierson-Moskowitz for-

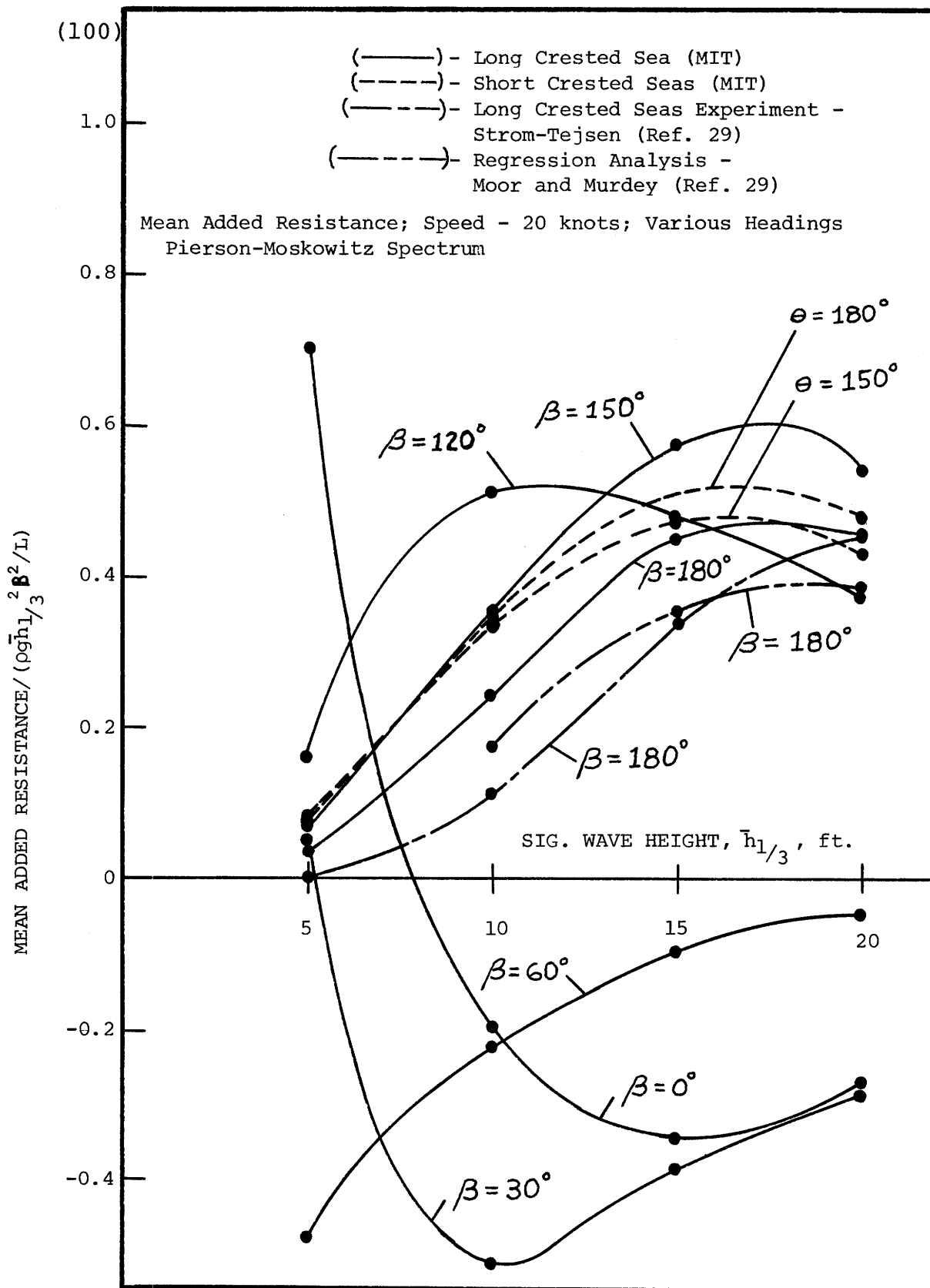


FIGURE 16: MARINER IRREGULAR SEAS RESULTS

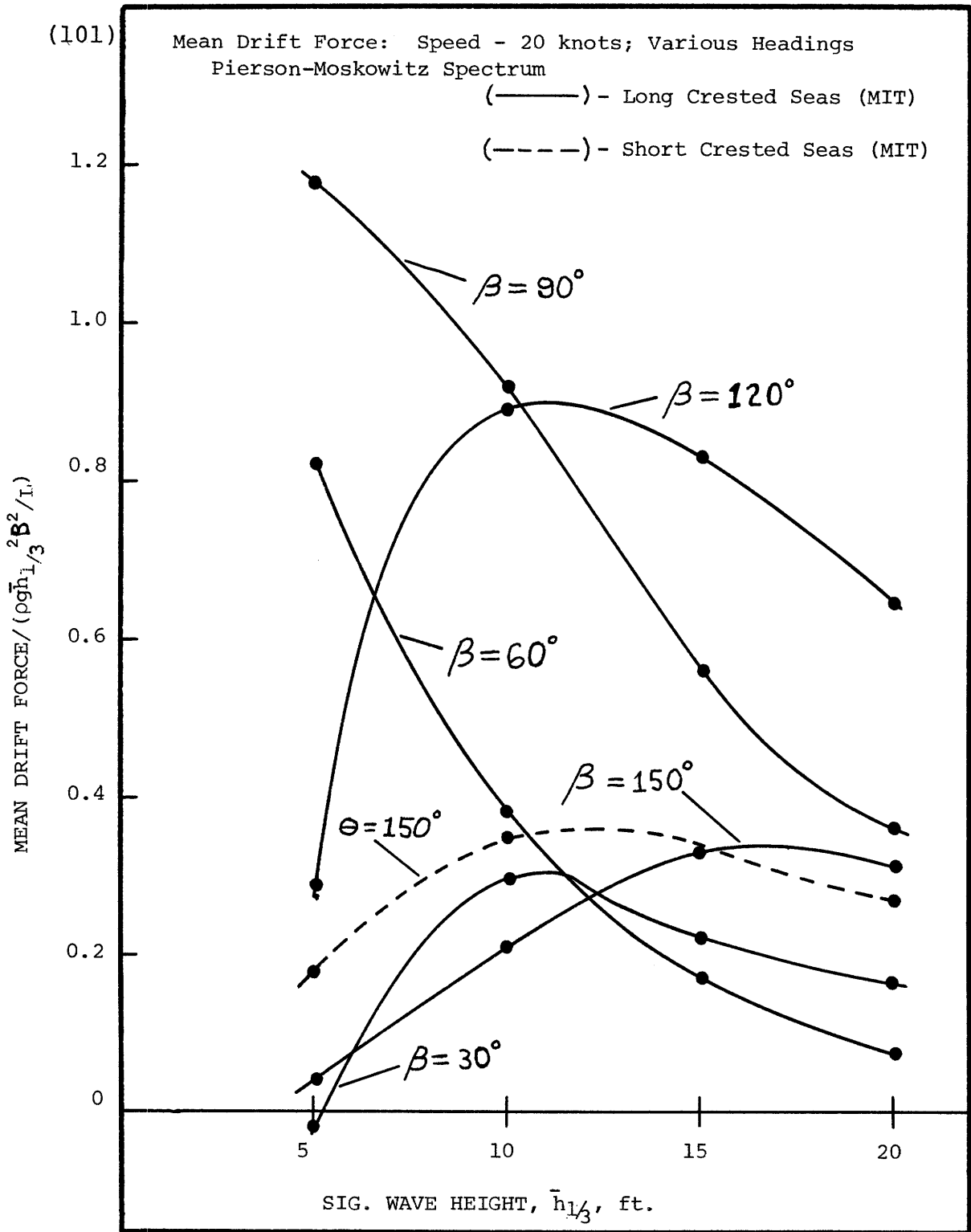


FIGURE 17: MARINER IRREGULAR SEAS RESULTS

mulation. The first important point revealed is that the added resistance in long-crested seas, for  $\beta = 150^\circ$  exceeds that of  $\beta = 180^\circ$  (head wave) throughout the entire wave height range. The reason for this must be found in the relative locations of the two response peaks and the spectral peak. In smaller waves, the  $\beta = 120^\circ$  curve outreaches both the higher beta angle predictions. The negative predictions for the following waves are created by the negative response operators (Shown in Fig. 13 for 15 knots). Since these negative response operators have not, as yet, been confirmed by experiment, any of these results for irregular following seas should be used very carefully. It should be noted that the plot for  $\beta = 180^\circ$  can be compared with the Series 60,  $C_B = 0.60$  experimental and regression analysis results for irregular head seas given by Strom-Tejsen<sup>[29]</sup>. The short-crested seas calculation (92) for the  $180^\circ$  'wind' direction tends to be greater than the  $180^\circ$  long-crested prediction. This is a result of extra energy being channeled into near head-sea headings which also have very large added resistance operators. The  $150^\circ$  'wind' direction curve falls considerably below the long-crested  $150^\circ$  plot because, in this case, the energy is being shifted to headings with lower added resistance responses.

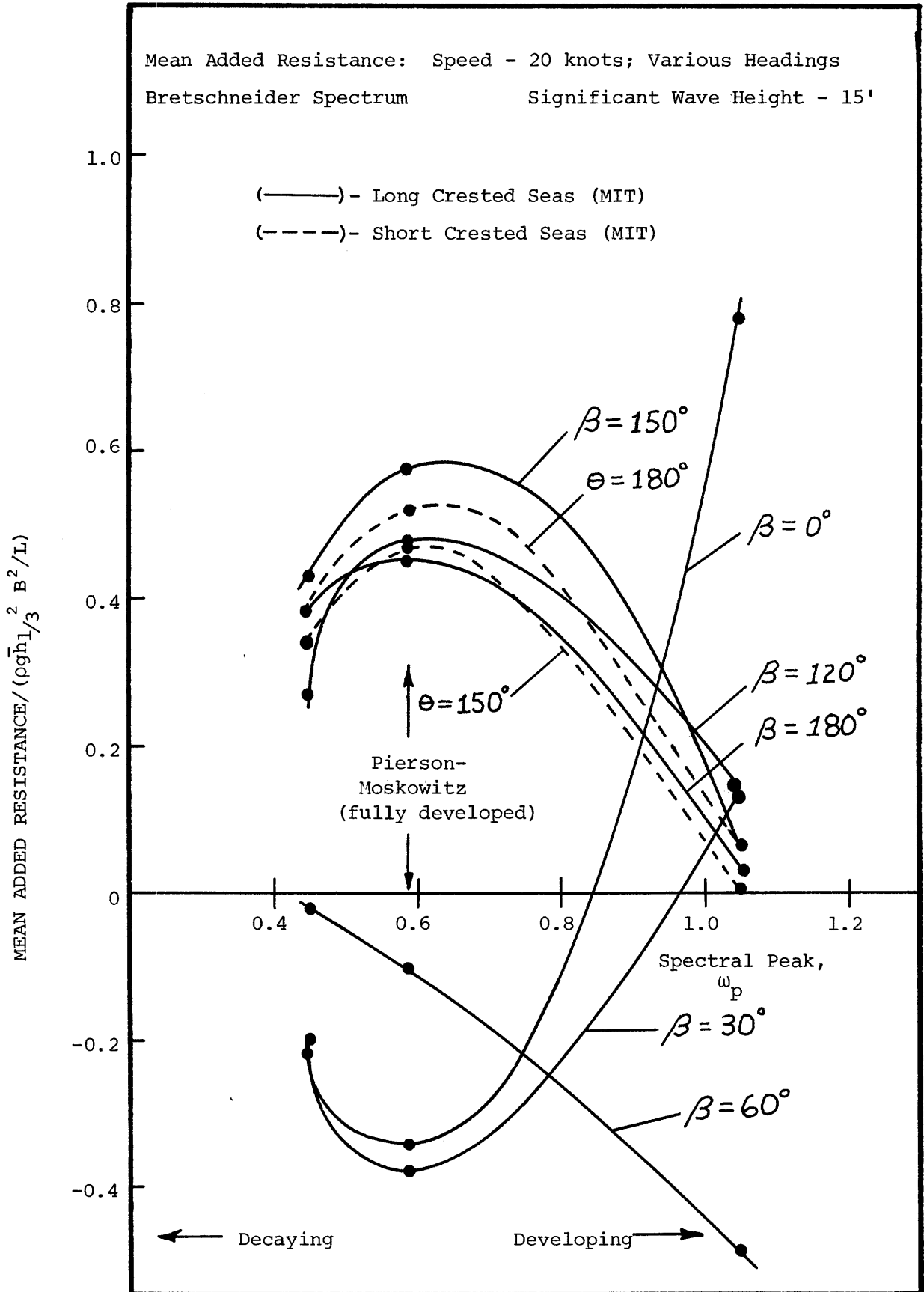
Figure 17 gives the mean drift force for the same

heading range. The beam seas case produces the biggest drift in smaller waves, but, again as a consequence of peak positions, the  $\beta = 120^\circ$  curve dominates in higher seas. The relative amount of drift produced at  $\bar{h}_{1/3} = 20'$  by the  $\beta = 150^\circ$  case is surprising since it almost matches the beam seas case. The short-crested seas calculation for a 'wind' direction of  $150^\circ$  overshadows its long-crested companion in smaller waves, then falls beneath in higher waves. This can be predicted from a line of reasoning similar to that given above.

In all these plots, the reader is cautioned to regard the results for beam and following seas with some suspicion in view of the results of Chapter IV. For example, the sharp dip and peak in the near beam seas experimental data (Figs. 4, 5, 6), was measured directly in the way of most of these spectral peaks. This underscores even more heavily the need for further research in this area.

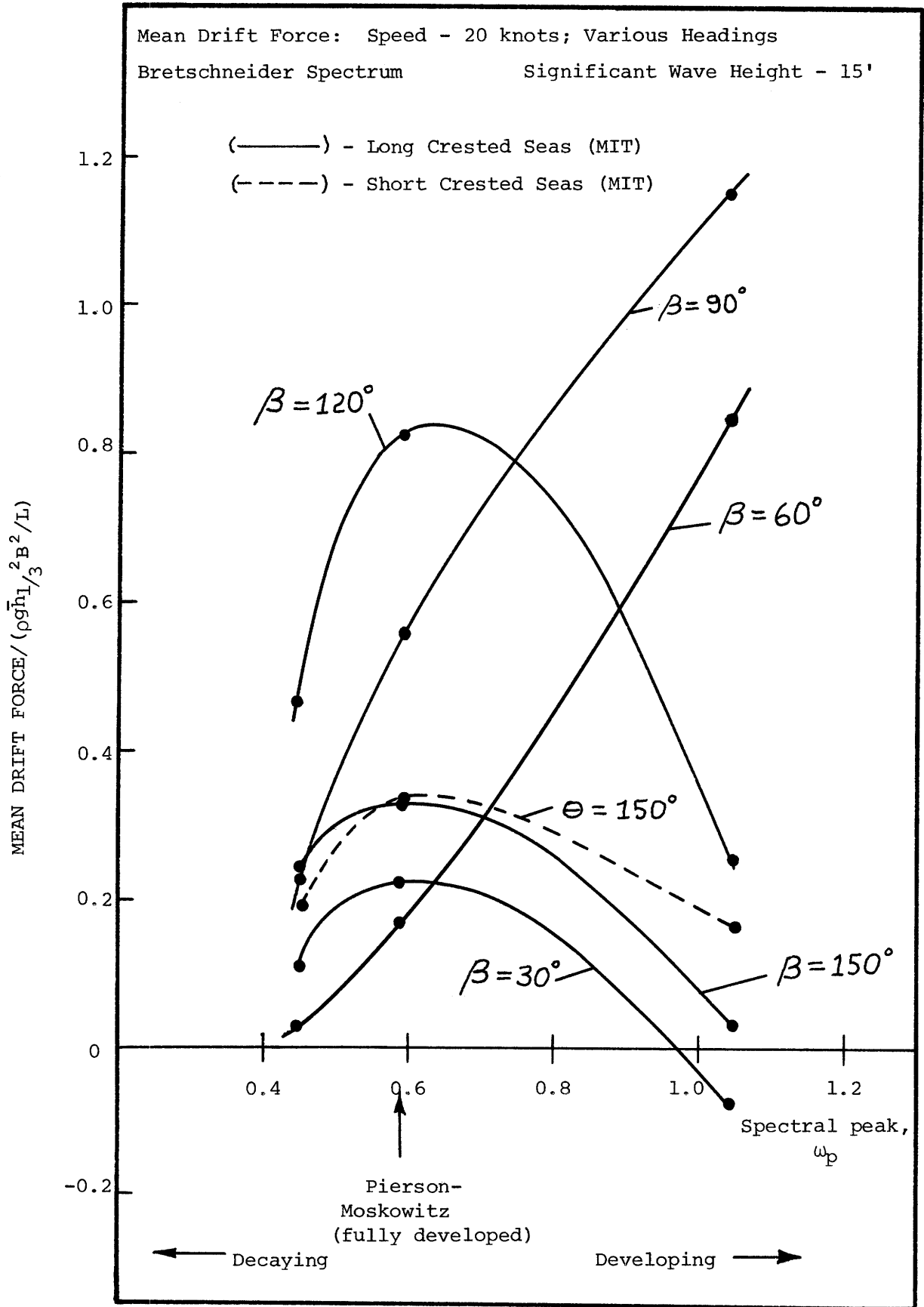
Finally, Figures 18 and 19 show the effect of spectral peak location on the added resistance and drift force. Spectra 3, 4, and 5 were used as being representative of fully developed, decaying, and developing seas. For the bow waves, the decaying and fully developed seas tend to produce the most drift force or added resistance. The  $\beta = 150^\circ$  and  $\beta = 120^\circ$  long-crested added resistance curves plot higher

(104) FIGURE 18: MARINER IRREGULAR SEAS RESULTS





(105) FIGURE 19: MARINER IRREGULAR SEAS RESULTS



than the head waves case through most of the range. The short-crested calculations have the same general character as their long-crested counterparts, but not the same magnitude. For the Mariner at service speed, the force maximum for bow waves seem to occur near the fully developed seas.

The drift force is dominated by the  $\beta = 120^\circ$  case for decaying and developed seas, but the beam seas case is very large in the developing sea. The short-crested seas calculation follows quite closely the comparable long-crested case.

To provide an assessment of the actual forces in the different sea states without dealing with the significant wave height, the predicted forces, in pounds, for all the points plotted in Figures 16 through 19 are given in Table I.

The maximum added resistance occurs at a heading of  $150^\circ$ , in 20-foot seas and its magnitude represents around three quarters of the calm water resistance (inferred from the Mariner shaft horsepower requirements<sup>[25]</sup> to be about 200,000 pounds). Before the requirements for service margins in ship propulsion are rewritten, it should be pointed out that these high waves put the linearity assumptions of the theory to a severe test. Also, there may be other factors (e.g. structural integrity, motions, etc.) that prevent operation of a 500-foot ship at service speed

(Long Crest)	Second-Order Wave Force*	Fully Developed			Decaying $h_{1/3} = 15'$	Developing $h_{1/3} = 15'$
		$h_{1/3} = 5'$	$h_{1/3} = 10'$	$h_{1/3} = 15'$		
$\beta = 0$	$\frac{AR}{DF}$	$\frac{12,290}{0}$	$\frac{-13,413}{0}$	$\frac{-53,443}{0}$	$\frac{-75,959}{0}$	$\frac{-34,498}{0}$
30	$\frac{AR}{DF}$	$\frac{871}{-503}$	$\frac{-35,583}{20,554}$	$\frac{-59,902}{-34,585}$	$\frac{-78,475}{45,308}$	$\frac{-30,904}{17,843}$
60	$\frac{AR}{DF}$	$\frac{-8,268}{14,321}$	$\frac{-15,227}{26,461}$	$\frac{-15,450}{26,761}$	$\frac{-12,418}{21,509}$	$\frac{-2,607}{4,516}$
90	$\frac{AR}{DF}$	$\frac{0}{20,476}$	$\frac{0}{63,924}$	$\frac{0}{87,856}$	$\frac{0}{99,102}$	$\frac{0}{35,016}$
120	$\frac{AR}{DF}$	$\frac{2,865}{4,961}$	$\frac{35,679}{61,797}$	$\frac{74,922}{129,769}$	$\frac{103,643}{179,515}$	$\frac{42,309}{73,282}$
150	$\frac{AR}{DF}$	$\frac{1,197}{691}$	$\frac{24,604}{14,205}$	$\frac{89,622}{51,744}$	$\frac{149,707}{86,433}$	$\frac{67,044}{38,708}$
180	$\frac{AR}{DF}$	$\frac{622}{0}$	$\frac{16,695}{0}$	$\frac{70,253}{0}$	$\frac{126,118}{0}$	$\frac{59,369}{0}$
(Short-Crest) $\theta = 150$	$\frac{AR}{DF}$	$\frac{1,370}{3,119}$	$\frac{23,345}{24,328}$	$\frac{73,636}{52,699}$	$\frac{119,818}{74,745}$	$\frac{53,354}{30,915}$
180	$\frac{AR}{DF}$	$\frac{1,283}{0}$	$\frac{23,813}{0}$	$\frac{80,715}{0}$	$\frac{134,166}{0}$	$\frac{60,363}{0}$

\*AR/DF = Added Resistance/Drift Forces in pounds (Arrangement of figures in columns to the left)

TABLE 1: ADDED RESISTANCE/DRIFT FORCE IN POUNDS FOR VARIOUS SEA STATES

in such a sea state. In a more modest sea (say  $\bar{h}_{1/3} = 10'$ ) the maximum added resistance occurs at a heading of  $120^\circ$  and it represents a more modest twenty percent of the calm water resistance. The drift force reaches its maximum in the developing beam seas. A similar value is obtained in a 20-foot fully developed sea state at a heading of  $120^\circ$ . However, the drift force at speeds near zero is more likely to be of interest to the naval architect.

It has been demonstrated in this section that the techniques of spectral analysis can be used in combination with a regular wave theory to gain quantitative insight into the second order force acting on ships at sea. On the basis of this brief study, it is already possible to conclude that the a priori assumption that irregular head seas will represent the worst case for added resistance is unjustified. It is encouraging for the simplicity of calculation that, at least for Mariner-like ships, fully developed seas appear to yield the maximum mean added resistance responses. The problems associated with regular following seas were seen to carry naturally into the spectral analysis. These difficulties and the doubts raised by the beam seas experimental work should make designers wary of the full application of the short-crested sea analysis (92). However, the author is optimistic that (92) will be very useful.

in connection with the Salvesen second order force theory if added resistance predictions are desired for primarily head winds ( $\theta \approx 180^\circ$ ). Finally, the extreme sensitivity of the calculated mean force to the input ocean spectrum can be easily seen.

VI. CONCLUSION AND RECOMMENDATIONS

This report represents an attempt to develop a design tool for use by the naval architect in calculating the second order wave force in a real seaway on a proposed vessel. This force impacts heavily on the design in that it is a major source of extra resistance and/or side slip that must be counteracted by the power plant in a seaway. The main thrust of the effort has been to develop a reliable computational method requiring only basic information about the ship (See Appendix) as an input. Second order force predictions were desired for any heading angle of the ship at any speed in regular waves of any frequency. The present study starts by introducing and defining the problem in the context of the general ship design process used by naval architects. Then the previous theoretical work on second order forces was outlined, and it was shown how several methods of prediction have been recently developed by hydrodynamicists for use in oblique seas. One of these theories, due to Salvesen, was derived in the context of modern strip theory of ship motions.

This theory was implemented within the M.I.T. 5-D ship motions program. Calculations were performed using the Mariner-type cargo ship in regular waves, and a brief

investigation of the character of the final equation was conducted. The next step involved comparison with existing regular head sea experimental data. Due to the lack of oblique seas experimental data, an experiment using a Mariner model for net drift force measurements in near beam seas was conducted in the M.I.T. Towing Tank. When this data was compared with the computer predictions, it was partially supportive, but it also raised some important linearity questions.

A theoretical comparison was then made using results from the same theory in a different motions program and a different theory in the same motions program. The results were encouraging for heading angles between  $180^\circ$  and  $90^\circ$ , but the predictions were shown to be subject to question in the following waves. Next, the theoretical extension of the regular wave computer results to an arbitrary long-crested or short-crested irregular seaway was outlined. This extension is crucial to the usefulness of the method as a design tool. The resulting spectral analysis technique was implemented in the M.I.T. 5-D program, and a brief design analysis of the Mariner was performed using six representative ocean spectra and a range of headings at the service speed.

The following important points can be presented as a

result of this study:

1. The linear estimate of second order force used in this study represents a very useful design tool in combination with the spectral analysis.
2. It is very important that a full range of bow wave headings be considered in the spectral analysis in order to define the true maximum added resistance.
3. Further experimental work in oblique bow waves is urgently needed to provide comparisons with the available theories.
4. The problems encountered in obtaining reasonable calculated results in following seas indicate the necessity for further theoretical developments in this area. Further experimental work would also be very helpful.
5. Every effort must be made to gain an understanding of the source of the phenomenon observed in regular beam wave experiments -- particularly in view of the fact that this second order force 'jump' occurs very near most spectral peaks.
6. As a result of point 4 above, the short-crested seaway equation would be most usefully applied, at this time, for waves propagating in a direction generally opposite to the ship (head winds).



7. The second order yaw moment, which can also be calculated in an extension of the theory presented (Ref. 28), should be developed for the M.I.T. 5-D program. This should not be a high priority effort, however, since there are very few theoretical or experimental comparisons to make.

REFERENCES

1. Ankudinov, V. K., "The Added Resistance of a Moving Ship in Waves," International Shipbuilding Progress, Vol. 19, 1972.
2. Beck, R. F., "The Added Resistance of Ships in Waves," Massachusetts Institute of Technology, Department of Naval Architecture and Marine Engineering, Report 67-9, 1967.
3. Chryssostomidis, C., Loukakis, T., Steen, A., "The Seakeeping Performance of a Ship in a Seaway," to be published by the U.S. Maritime Administration.
4. Comstock, J. P., Principles of Naval Architecture, Society of Naval Architects and Marine Engineers, 1967.
5. Gerritsma, J. and Beukelman, W., "Analysis of the Resistance Increase in Waves of a Fast Cargo Ship," International Shipbuilding Progress, Vol. 19, 1972.
6. Hanaoka, T., "Non-Uniform Wave Resistance," Journal of Zosen Kiokai, Vol. 94, 1954.
7. Hanaoka, T., et. al., "Researches on the Seakeeping Qualities of Ships in Japan", Chapter 5: Resistance in Waves, Society of Naval Architects of Japan, 60th Anniversary Series, Vol. 8, 1963.
8. Haskind, M. D., "Two Papers on the Hydrodynamic Theory of Heaving and Pitching of a Ship," S.N.A.M.E. Technical and Research Bulletin, 1-12.
9. Havelock, T. H., "The Drifting Force on a Ship Among Waves," Philosophical Magazine, Vol. 33, Series 7, 1942.
10. Hosoda, R., "The Added Resistance of Ships in Regular Oblique Waves," Selected Papers from the Journal of the Society of Naval Architects of Japan, Vol. 12, 1974.
11. Joosen, W. P. A., "Added Resistance of Ships in Waves", Proceedings of the 6th Symposium on Naval Hydrodynamics, Washington, D.C., 1966.

12. Journé, J. M. J., "Motions and Resistance of a Ship in Regular Following Waves," Laboratory for Ship Hydrodynamics, Delft, Report 440, 1976.
13. Korvin-Kroukovsky, B. V. and Jacobs, W. R., "Pitching and Heaving Motions of a Ship in Regular Waves," Transactions, S.N.A.M.E., Vol. 65, 1957.
14. Kreitner, J., "Heave, Pitch, and Resistance of Ships in a Seaway," Transactions of the Royal Institute of Naval Architects, London, Vol. 87, 1939.
15. Lee, C. M. and Newman, J. N., "The Vertical Mean Force and Moment of Submerged Bodies Under Waves," Journal of Ship Research, Vol. 15, 1971.
16. Loukakis, T. and Sclavounos, P., "Some Extensions of the Classical Approach to Strip Theory of Ship Motions Including the Mean Added Forces and Moments in Oblique Regular Waves," Submitted February 1977 to Journal of Ship Research.
17. Marou, H., "The Excess Resistance of a Ship in Rough Seas," International Shipbuilding Progress, Vol. 4, 1957.
18. Newman, J. N., "The Damping and Wave Resistance of a Pitching and Heaving Ship," Journal of Ship Research, Vol. 3, June 1959.
19. Newman, J. N., "The Exciting Forces on a Moving Body in Waves," David Taylor Model Basin, Washington, D.C., February 1965.
20. Newman, J. N., "The Drift Force and Moment on a Ship in Waves," Journal of Ship Research, Vol. 11, 1967.
21. Newman, J. N., "The Second Order Slowly Varying Force and Moment on a Submerged Slender Body Moving Beneath an Irregular Wave System," 1973, unpublished.
22. Newman, J. N., "Second Order Slowly Varying Forces on Vessels in Irregular Waves," International Symposium on the Dynamics of Marine Vehicles and Structures in Waves, London, April 1974.

23. Newman, J. N., Marine Hydrodynamics, Lecture Notes, Massachusetts Institute of Technology, Third Edition, 1974.
24. Price, W. G. and Bishop, R. E. D., Probabilistic Theory of Ship Dynamics, Wiley and Sons, New York, 1974.
25. Russo, V. L. and Sullivan, E. K., "Design of the Mariner-type Ship," Transactions, S.N.A.M.E., Vol. 61, 1953.
26. St. Denis, M. and Pierson, W. J., "On the Motions of Ships in Confused Seas," Transactions, S.N.A.M.E., Vol. 61, 1953.
27. Salvesen, N., Tuck, E. O., Faltinsen, O., "Ship Motions and Sea Loads," Transactions, S.N.A.M.E., Vol. 78, 1970.
28. Salvesen, N., "Second Order Steady State Forces and Moments on Surface Ships in Oblique Regular Waves," International Symposium on the Dynamics of Marine Vehicles and Structures in Waves, London, April 1974.
29. Strom-Tejsen, J., Yeh, H. Y. H., Moran, D. D., "Added Resistance in Waves," Transactions, S.N.A.M.E., Vol. 81 1973.
30. Vassilopoulos, L. A., "The Application of Statistical Theory of Non-linear Systems to Ship Performance in Random Seas," International Shipbuilding Progress, Vol. 14, February 1967.
31. Wang, S., "Experiments on Added Resistance of a Ship Among Waves," Massachusetts Institute of Technology, Department of Naval Architecture and Marine Engineering, Report 65-1, March 1965.

APPENDIX A

CHANGES TO M.I.T. 5-D SEAKEEPING  
PROGRAM USER'S MANUAL

The program is now capable of computing mean second order force (added resistance and drift force) for any ship heading, in addition to calculating ship motions, dynamic loadings, and events. The second order force is calculated using a theory published by Salvesen (1974). It includes forces arising from wave-ship motion interaction and wave reflection. The second order force routine given here operates properly only in English unit systems with length dimensions in feet. For example, it has been tested in a system describing the ship in tons and feet; for this case, it gives output in pounds force.

All the subroutines in the original MIT 5-D seakeeping program remain in existence, although some have been modified as noted in Appendix C. RESIST has been changed from a function subprogram to a subroutine.

The input format remains unchanged. However, there is a new option associated with the integer, NADR, of card set number four. If NADR=2, only the final totals of the added resistance and drift force are printed out in dimensional and non-dimensional form. IF NADR=1, all eleven components involved in the Salvesen computation (two for

each mode of motion and one for wave reflection) are printed out. Examples of each of these output forms are presented in Appendix B. If  $NADR = 0$ , no second order force computations are performed.

The short-crested seas auxiliary program has been modified to include a mean second order force calculation. In order to implement this change, one integer called  $NADR$  has been added to card set number one. It is written in column 40, following the standard I5 format used by the original program. If second order force data is to be read, this integer should be equal to one. The mean drift force and added resistance will be prepared for input by the 5-D (if requested) in the same way as the mean squares of the other responses, so card set #3 can still be included just as it is punched by the main program.

APPENDIX B

SAMPLE OUTPUT

B-1: Example of the short form of output for second order force in regular waves obtained by setting NADR = 2. This follows the print out of the motion amplitudes and phase angles. The totals shown represent the sum of all eleven terms of the second order force formula developed in the main text (See Eq. (86)). Added resistance is the component along the longitudinal ship axis (positive aft). Drift force is the component along the transverse ship axis (positive in the direction of wave propagation). The dimensional quantities are in pounds force provided XRHO is given in slugs/ft<sup>3</sup> and provided that the ship is described in English units with feet as the length dimension. As noted in Appendix A, if this restriction is not met then the second order force output will be meaningless. The nondimensional quantities have been divided by the factor:  $\rho g \alpha^2 B^2 / L$  where  $\rho$  is the mass density of the water,  $g$  is the gravitational acceleration,  $\alpha$  is the wave amplitude,  $B$  is the ship beam, and  $L$  is the ship length.

MEAN ADDED RESISTANCE/DRIFT FORCE CALCULATION

MODE	DIMENSIONAL		NON-DIMENSIONAL	
	DRIFT FORCE	ADDED RESIST.	DRIFT FORCE	ADDED RESIST.
SOURCE	8106.7079	4680.4102	11.6726	6.7392
TOTALS				



B-2: Example of the long form of output for second order force in regular waves obtained by setting NADR=1. This follows the print out of the motion amplitudes and phase angles. Dimensional and non-dimensional quantities are as defined in B-1. Here all eleven components that are summed to give the final Salvesen second order force are shown. There are two components for each mode of motion; FR-KRL which represents the Froude-Kriloff or Havelock portion of the motion interaction,  $\mathcal{F}_j^I$  (Eq. (75) of the text), WVDIFF which represents the diffraction potential contribution of the motion interaction,  $\mathcal{F}_j^D$  (Eqs. (78) and (79) of the text). The eleventh component is DIFFR.POT.CONT., which represents the wave reflection,  $\mathcal{F}_D$  (Eqs. (80) and (85) of the text). Numerous subtotals are also given, including the contribution of each mode of motion, the total of all the  $\mathcal{F}_j^I$ 's, the total of all the  $\mathcal{F}_j^D$ 's, and the total of the  $\mathcal{F}_j^D$ 's and the  $\mathcal{F}_j^I$ 's.

MEAN ADDED RESISTANCE/DRIFT FORCE CALCULATION

MODE	SOURCE	DIMENSIONAL DRIFT FORCE	ADDED RESIST.	DRIFT FORCE	ADDED RESIST.	NON-DIMENSIONAL DRIFT FORCE	ADDED RESIST.
SWAY	FR-KRL	-5.6201	-9.7342	-0.0081	-0.0140		
	WVDIFF	27.2093	47.1279	0.0392	0.0679		
	TOTALS	21.5892	37.3936	0.0311	0.0538		
HEAVE	FR-KRL	1276.6926	2211.2944	1.8383	3.1840		
	WVDIFF	-1076.8601	-1865.2090	-1.5506	-2.6857		
	TOTALS	199.8125	346.0854	0.2877	0.4983		
ROLL	FR-KRL	0.7873	1.3637	0.0011	0.0020		
	WVDIFF	-1.5898	-2.7535	-0.0023	-0.0040		
	TOTALS	-0.8024	-1.3899	-0.0012	-0.0020		

-122-

PITCH	FR-KRL	3994.1274	6918.0234	5.7510	9.9610		
	WVDIFF	-1139.3252	-1973.3669	-1.6405	-2.8414		
	TOTALS	2854.8022	4944.6562	4.1105	7.1196		
YAW	FR-KRL	3.0620	5.3035	0.0044	0.0076		
	WVDIFF	99.2581	171.9197	0.1429	0.2475		
	TOTALS	102.3200	177.2232	0.1473	0.2552		

SUM OF ALL THE MODES AND THE DIFFRACTION POTENTIAL CONTRIBUTION

ALL MODES	FR-KRI	5269.0430	9126.2461	7.5867	13.1406		
ALL MODES	WVDIFF	-2091.3271	-3622.2815	-3.0112	-5.2156		
TOTALS		3177.7158	5503.9609	4.5755	7.9250		
DIFFR. POT. CONT.		676.2947	1171.3755	0.9738	1.6866		
TOTALS		3854.0105	6675.3359	5.5493	9.6116		

Information Processing Center

Information Processing Center

B-3: Example of the long-crested irregular seas output giving the mean second order force in a long-crested seaway (Eq. (91)). This is given if both spectral calculations and second order force calculations are requested. The (LBS) notation shown here is only correct if the variable XRHO in the main program (See Input, Appendix D) is given in slugs per cubic foot and the ship is described in English units using feet as the length dimension. If these requirements are not met, the computation will be invalid.

The two components, ADD.RES.(x) and DRIFT(Y-AX) are always in the output. The spectral amplitudes and associated statistical quantities may be obtained (as shown here) if NSPC  $\neq$  0 (See Appendix D). The integer (zero) that appears at the end of the line, "Response spectrum for..." appears because the SPIN subroutine (Appendix C) is used for all the statistical calculations. The integer has meaning only in the bending moment calculations, where it transmits the station number.

The spectral amplitudes represent the value of the integrand in Eq. (91) in the text at each spectral frequency (input by the user or given in default by the program; See Appendix D). The only statistical quantity shown that has meaning for the second order force analysis is the zeroth moment, which is the value of the integral

in (91) (half the second order force). The second moment, fourth moment, and broadness factor are printed out because use is made of subroutine SPIN already in existence in the 5-D program. Of course, these additional statistical quantities are useful, when they are associated with a motion spectrum in another part of the output.

MAIN SECTN ORDER FORCE (LBS.)

RESPONSE SPECTRUM FOR COMPONENT OF ALL RES. (X) 0  
0TH MOMENT = 0.4481103E+05 2ND MOMENT = 0.4647184E+05 4TH MOMENT = 0.7848762E+05 BROADNESS FACTOR = 0.62126

SPECTRAL AMPLITUDE'S :  
-0.378027E+01 0.611304E+02 0.101371E+04 0.528430E+04 0.586294E+04 0.261472E+05 0.642269E+05 0.104773E+06  
0.282569E+06 0.274682E+06 0.297934E+06 0.311175E+06 0.316655E+06 0.311160E+06 0.297637E+06 0.262980E+06 0.137072E+06 0.369563E+05  
0.529523E+05 0.262669E+05 0.254747E+05 0.172924E+05 0.124658E+05 0.103724E+05 0.879109E+04 0.549533E+04 0.312272E+04 0.196768E+04  
0.126205E+04 0.892378E+03 0.719916E+03 0.580470E+03 0.470122E+03 0.379709E+03 0.305550E+03 0.244373E+03 0.193556E+03 0.154312E+03  
0.123293E+03 0.961033E+02

CONNECTION CY ALL RES. (X) 89622.0625

RESPONSE SPECTRUM FOR COMPONENT OF DRIFT (Y-AX) 0  
0TH MOMENT = 0.2587186E+05 2ND MOMENT = 0.2683072E+05 4TH MOMENT = 0.4531491E+05 BROADNESS FACTOR = 0.62126

SPECTRAL AMPLITUDE'S :  
-0.219250E+01 0.352822E+02 0.585269E+03 0.305668E+04 0.334498E+04 0.150966E+05 0.370815E+05 0.604909E+05  
0.140047E+06 0.156589E+06 0.172032E+06 0.179933E+06 0.182480E+06 0.179548E+06 0.171345E+06 0.151830E+06 0.791415E+05 0.571325E+05  
0.305720E+05 0.151652E+05 0.147078E+05 0.998375E+04 0.719711E+04 0.633493E+04 0.507550E+04 0.317278E+04 0.184306E+04 0.113048E+04  
0.728659E+03 0.515275E+03 0.415645E+03 0.335135E+03 0.271426E+03 0.219226E+03 0.176409E+03 0.141089E+03 0.111750E+03 0.890923E+02  
0.711830E+02 0.566400E+02

CONNECTION CY DRIFT (Y-AX) 51783.7109

B-4: Example of the output of auxiliary program Short-crest giving the mean second order force in a short-crested irregular seaway (Eq. (92)). An entire set of output including case identification, motions, and second order force is obtained by specifying NADR=1 in the short-crest input. There is no full component print out option like the one described for the main 5-D. Either NADR=0 (and no second order force output is generated) or NADR=1 and the output shown is generated. If NADR=1 in Shortcrest, then the user must be sure to run data on long crested seas from the main 5-D that includes second order force computations (i.e. NADR=1 or 2 in the corresponding main 5-D data generation run).

The (LBS) notation is correct if the variable XRHO in the main 5-D program (See Input, Appendix D) was given in slugs per cubic foot and the ship was described in English units using feet as the length dimension. If these requirements are not met, the computation will be invalid.

IRREGULAR WAVE RESULTS -- SHOPT CRFSTED MULTI-DIRECTIONAL SEAS SHIP SPEED : 33.7800

SIGNIFICANT WAVE HEIGHT 15.0000  
PEAK SPECTRAL FREQUENCY 0.5877  
PRINCIPLE WIND DIRECTION 150.0000

MOTIONS @ ORIGIN	RMS	H (1/3)	H (1/10)	H (1/1000)
HEAVE	3.6421	14.5682	18.5745	28.0438
PITCH	1.4433	5.7731	7.3607	11.1132
SWAY	1.0443	4.1771	5.3258	8.0409
ROLL	2.1777	8.7109	11.1064	16.7684
YAW	0.2250	0.8999	1.1473	1.7323

MEAN SECCND OBDEF FORCE (LPS.)

ADDED RESISTANCE COMPONENT 73636.3125

DRIFT FORCE CCMFCNENT 52699.4297

APPENDIX C

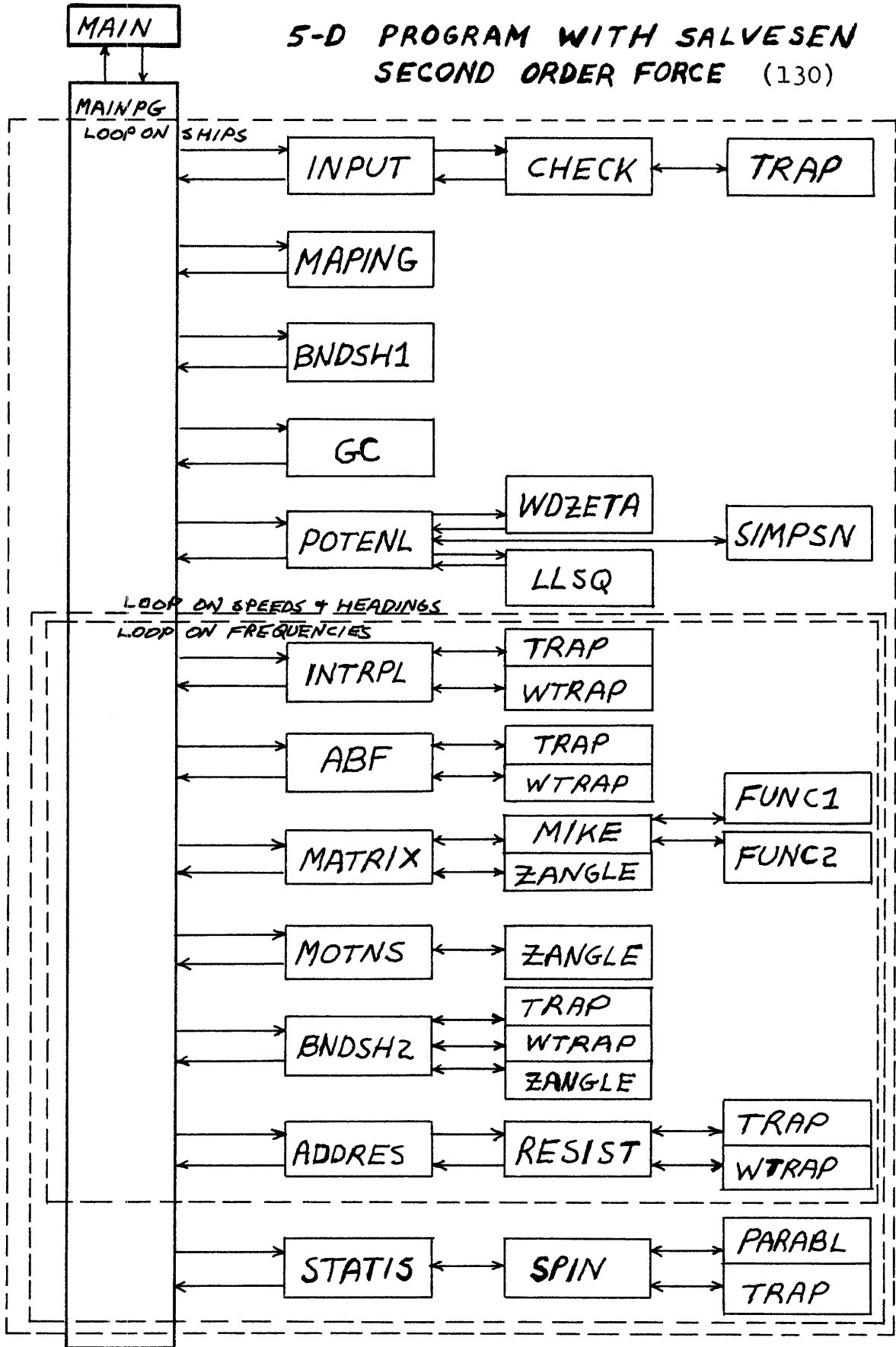
SUBROUTINES MODIFIED

The following briefly describes each subroutine modified in order to implement the Salvesen second order force computation in the MIT 5-D seakeeping program. A flow chart of this new version of the program is shown on the next page so that an understanding of the position and function of each routine is available. Further information on the routines not modified (and consequently not listed here) can be obtained from the 5-D Seakeeping Program User's Manual or Reference [3] of the main text.



NEW 5-D FLOW CHART

# 5-D PROGRAM WITH SALVESEN SECOND ORDER FORCE (130)



C-1: MAIN PG - This subroutine is the actual main program for the 5-D; it calls all the required routines, loops on frequencies, heading angles, and ship speeds. Several lines were added as part of the scheme for computing the sectional quantity  $\hat{h}_j(x)$  (Eq. (78d)). These new lines include numbers:

(14) A new common storage

(19) Some additional output data

(25-28) A zeroing routine

(100-102) Three new Write statements

A listing of the modified routine follows on pages 132-135.

MNFG0001  
 MNFG0002  
 MNFG0003  
 MNFG0004  
 MNFG0005  
 MNFG0006  
 MNFG0007  
 MNFG0008  
 MNFG0009  
 MNFG0010  
 MNFG0011  
 MNFG0012  
 MNFG0013  
 MNFG0014  
 MNFG0015  
 MNFG0016  
 MNFG0017  
 MNFG0018  
 MNFG0019  
 MNFG0020  
 MNFG0021  
 MNFG0022  
 MNFG0023  
 MNFG0024  
 MNFG0025  
 MNFG0026  
 MNFG0027  
 MNFG0028  
 MNFG0029  
 MNFG0030  
 MNFG0031  
 MNFG0032  
 MNFG0033  
 MNFG0034  
 MNFG0035  
 MNFG0036

```

SUBROUTINE MAINPG(AB,FF,PA)
  COMPLEX F2,F3,F4,H2,H3,H4,ETA,F,WS,WC,CMPLX,HHAT2,HHAT3,HHAT4
  COMMON /PAPA/ WS,WC,SB,OM,OM2,WN,RHO,GRAV,BETA,XI(32),DX(31)
  1,V,NSTA,NSE,MD,XLBE,ZETA,ALFA
  COMMON /ABFH/ F2(32),F3(32),F4(32),H2(32),H3(32),H4(32)
  1,A33(32),B33(32),A22(32),B22(32),A44(32),B44(32),A24(32),B24(32)
  COMMON /VISC/ R4$(32),B44V,TON,IAADR
  COMMON /MTN/ XMOT(10),YMOT(10),ZMOT(10),NMOT
  COMMON /SPECTRM/ AM(1200),BS(6400),RM(200),H13(10),OMP(10),NRCMS
  1,SPCTM(10,40),SPOMS(10,40),NSOMS,NWY,II,N1,N2,M1,NSEA,L,NS,NSEC,IO
  2,NADR,RST(80),NEVT,EVENT(3,3),NN1,NN2,NN3,VCR,REVNT(120),OMEGA(40)
  COMMON /COEFS/ ETA(6),F(6),G(6,6),A(6,6),B(6,6),C(6,6)
  COMMON /MOTHER/ UOB(16),BETA(16),OMEGA(40),NVL,NENC,NPCH,NFR,NFO
  COMMON /ERB/HHAT2(32),HHAT3(32),HHAT4(32)
  DIMENSION EFGABC(168),I(24),AB(1),PB(1),PA(1)
  EQUIVALENCE (EFGABC(1),ETA(1))
  DATA I/ETA,'G','A','B','C','F','A22','A33',
  *,A44,'A24','B22','B33','B44','B24','F2','F3',
  *,F4,'H2','H3','H4','B44*','HHT2','HHT3','HHT4'/
  PI=3.141593
  RAD=57.29578
  READ(5,1000) NCS
  CALL ERASE(EFGABC,168)
  DO 100 NCASE=1,NCS
  DO 5 IERB=1,32
  HHAT2(IERB)=(0.0,0.0)
  HHAT3(IERB)=(0.0,0.0)
  HHAT4(IERB)=(0.0,0.0)
  CALL TIMING(IPR)
  CALL INPUT
  CALL TIMING(ISR)
  TIN=(ISR-IPR)/100.
  CALL MAPING
  NRD=2/(N1+1)*N1
  IF(NMOT.NE.C.AND.IO.NE.C)
  1 WRITE(IO,2000) (XMOT(N),YMOT(N),ZMOT(N),NMOT),N=1,NMOT)

```

```

10 IF(N1.NE.0) CALL BNDSH1(N2,810,8100)
   WRITE(6,1002)
   CALL GC
   CALL TIMING(ISR)
   CALL POTEN1(AB,PR,PA)
   CALL TIMING(ISE)
   TPL=(ISE-ISR)/100.
   WRITE(6,2400) TIN,TPI
   DO 9C N=1,NVI
     V=UOB(N)
     IF(IC.NF.0) WRITE(10,2000) V
     DO 80 M=1,NFNC
       CALL ERASE(FEGABC,12)
       MD=2
       BETAA=BETA(M)
       IF(BETA.EQ.180..OF.BETA.EQ.C..OR.B44V.LT.C.) MD=1
       XI=3*MD
       M1=MD+1
       BET=BETAA/RAD
       SB=SIN(BET)
       CSB=COS(BET)
       IF(IC.NF.0) WRITE(10,2000) BETAA
       CALL TIMING(IPB)
       DO 70 I=1,NRCMS
         OMO=OMEGA(I)
         WN=OMC*OMC/GRV
         IF(ALFA.NF.0) ZETAA=ALFA/WN
         XI=2.*PI/WN/XLBF
         CK=-WN*CSB
         OM=OMC+V*CK
         OMFGE(I)=CM
         OM2=OM*OM
         WC=CMPIX(0.,CK)
         WS=CMPIX(0.,SB*WN)
         IF(NSEA.NE.1.AND.NBD.EQ.0) WRITE(5,1003)
         IF(NSEA.NE.1) WRITE(6,1001) NPD,V,BETAA,OMC,OM,XL,ZETAA

```

```

MNP60037
MNP60038
MNP60039
MNP60040
MNP60041
MNP60042
MNP60043
MNP60044
MNP60045
MNP60046
MNP60047
MNP60048
MNP60049
MNP60050
MNP60051
MNP60052
MNP60053
MNP60054
MNP60055
MNP60056
MNP60057
MNP60058
MNP60059
MNP60060
MNP60061
MNP60062
MNP60063
MNP60064
MNP60065
MNP60066
MNP60067
MNP60068
MNP60069
MNP60070
MNP60071
MNP60072

```

MNPGC073  
 MNPGC074  
 MNPGC075  
 MNPGC076  
 MNPGC077  
 MNPGC078  
 MNPGC079  
 MNPGC080  
 MNPGC081  
 MNPGC082  
 MNPGC083  
 MNPGC084  
 MNPGC085  
 MNPGC086  
 MNPGC087  
 MNPGC088  
 MNPGC089  
 MNPGC090  
 MNPGC091  
 MNPGC092  
 MNPGC093  
 MNPGC094  
 MNPGC095  
 MNPGC096  
 MNPGC097  
 MNPGC098  
 MNPGC099  
 MNPG100  
 MNPG101  
 MNPG102  
 MNPG103  
 MNPG104  
 MNPG105  
 MNPG106  
 MNPG107  
 MNPG108

```

CALL INTERPL(AB,PR,PA)
CALL ABF
CALL MATRIX
IF(NMOT+NEVT.NE.0) CALL MOTNS
IF(N1.NE.0) CALL BNDSH2
IF(NADR.NE.0) CALL ADDRES
IF(NPCH.LE.0) GO TO 65
WRITE(6,3000) T( 1),EIA
WRITE(6,3000) T( 2),G
WRITE(6,3000) T( 3),A
WRITE(6,3000) T( 4),B
WRITE(6,3000) T( 5),C
WRITE(6,3000) T( 6),F
WRITE(6,3001) T( 7), (A22(I), I=1, NSTA)
WRITE(6,3001) T( 8), (A33(I), I=1, NSTA)
WRITE(6,3001) T( 9), (A44(I), I=1, NSTA)
WRITE(6,3001) T(10), (A24(I), I=1, NSTA)
WRITE(6,3001) T(11), (B22(I), I=1, NSTA)
WRITE(6,3001) T(12), (B33(I), I=1, NSTA)
WRITE(6,3001) T(13), (B44(I), I=1, NSTA)
WRITE(6,3001) T(14), (R24(I), I=1, NSTA)
WRITE(6,3001) T(15), ( F2(I), I=1, NSTA)
WRITE(6,3001) T(16), ( F3(I), I=1, NSTA)
WRITE(6,3001) T(17), ( F4(I), I=1, NSTA)
WRITE(6,3001) T(18), ( H2(I), I=1, NSTA)
WRITE(6,3001) T(19), ( H3(I), I=1, NSTA)
WRITE(6,3001) T(20), ( H4(I), I=1, NSTA)
WRITE(6,3001) T(22), (HHAT2(I), I=1, NSTA)
WRITE(6,3001) T(23), (HHAT3(I), I=1, NSTA)
WRITE(6,3001) T(24), (HHAT4(I), I=1, NSTA)
IF(NPCH.NE.0)
  WRITE(6,3001) T(21), (B44(I), I=1, NSTA), B44V, B(4,4)
CONTINUE
IF(NSEA.NE.0) CALL STATIS
CALL TIMING(IPE)
THD=(IPE-IPB)/100.

```

65  
 \*  
 70

```

WRITE(6,2500) THD
IF(N1.NE.1) WRITE(6,1002)
CONTINUE
80 CONTINUE
90 CONTINUE
100 CONTINUE
RETURN
1000 FORMAT(I5)
1001 FORMAT(I1,'*** REGULAR WAVE RESULTS SHIP SPEED',F9.4,' HEADING
1 ANGLE DEG.',F10.4,' OMEGA',F8.4,' LAMRDA/XLBP',
2,F9.4,'OZETA =',F9.4)
1002 FORMAT('1')
1003 FORMAT('0',130(1H-))
2000 FORMAT(8F10.4)
2400 FORMAT('TIMING OF INPUT DATA :',F6.2,' SEC. '/
* 'TIMING OF POTENI CALC :',F6.2,' SEC. ')
2500 FORMAT('TIMING OF RESPONSES :',F5.2,' SEC. ')
3000 FORMAT('0',A4,6G14.6/(5X,6G14.6))
3001 FORMAT('0',A4,9G14.5/(5X,9G14.6))
END
MNEGC109
MNEGC110
MNEGC111
MNEGC112
MNEGC113
MNEGC114
MNEGC115
MNEGC116
MNEGC117
MNEGC118
MNEGC119
MNEGC120
MNEGC121
MNEGC122
MNEGC123
MNEGC124
MNEGC125
MNEGC126
MNEGC127

```

C-2:    INTRPL - This routine interpolates the hydrodynamic coefficients for the desired frequency and calculates Froude-Kriloff and sectional diffraction forces. Now it also computes the sectional quantity  $\hat{h}_j(x)$ , (Eq. (78d)) needed for the second order force calculation. The new lines include:

14, 15, 16, 26, 28, 30, 37, 42, 43, 44,  
69, 72, 82, 84, 86, 88, 90, 92, 94, 97,  
109, 110, 114, 118, 122, 125, 129.

A listing of the modified routine follows on pages 137-140.



INTL0001  
 INTL0002  
 INTL0003  
 INTL0004  
 INTL0005  
 INTL0006  
 INTL0007  
 INTL0008  
 INTL0009  
 INTL0010  
 INTL0011  
 INTL0012  
 INTL0013  
 INTL0014  
 INTL0015  
 INTL0016  
 INTL0017  
 INTL0018  
 INTL0019  
 INTL0020  
 INTL0021  
 INTL0022  
 INTL0023  
 INTL0024  
 INTL0025  
 INTL0026  
 INTL0027  
 INTL0028  
 INTL0029  
 INTL0030  
 INTL0031  
 INTL0032  
 INTL0033  
 INTL0034  
 INTL0035  
 INTL0036

```

SUBROUTINE INTERPL (AB, PR, PA)
IMPLICIT COMPLEX (C, F, H, W)
REAL WN
COMMON WPI (15), WH (15), FW (15), RDI (15), ADY (15), RDZ (15), ADZ (15)
1, AYZ (15), DT (14)
COMMON /ABFH/ F2 (32), F3 (32), F4 (32), H2 (32), H3 (32), H4 (32)
1, A33 (32), B33 (32), A22 (32), B22 (32), A44 (32), B44 (32), A24 (32), B24 (32)
COMMON /PAPA/ WS, WC, SB, CM, CM2, WN, PHO, GRAV, BETAA, XI (32), DX (31)
1, V, NSIA, NSP, MD, XLBP, ZETA, ALFA
COMMON /STA/ YM (32), ZM (32), SIGMA (32)
COMMON /MAE/ NC (32), NP, ME
COMMON /POT/ YN (32, 14), ZN (32, 14), DYN (32, 15), DZN (32, 14), DTB (32, 14)
COMMON /INTPOL/ DEITA (41)
COMMON /ERB/ HHAT2 (32), HHAT3 (32), HHAT4 (32)
DIMENSION FH (192), ADDA (256), AB (1), PR (1), PA (1), RDY (15), RDZ (15),
1ADYY (15), ADZZ (15), FWRE (15), WHEB (15)
FOURVALENCE (F2 (1), F3 (1)), (A33 (1), ADDA (1))
D (P, Q, R, S) = (P-R) * (P-S) / (R-Q) / (S-Q)
X (Y1, Y2, Y3) = D1 * Y1 + D2 * Y2 + D3 * Y3
NF1 = NF - 1
NN = 0
NEW = 41 * (3 * NP - 2)
OMA = ABS (OM)
SQ = SORT (OMA)
RDZ (NP) = 0.
RDZZ (NP) = 0. C
ADZ (NP) = 0.
ADZZ (NP) = 0. 0
ADY (NP) = 0.
ADYY (NP) = 0. 0
AYZ (NP) = 0.
DC 200 N=1, NSTA
NEO = NC (N)
IF (NEQ. GE. C) GO TO 30
IF (NFC. EQ. -2) GO TO 200
WX = CEXP (WC * CMPIX (-DX (N-1), 0.))

```

INTL0027  
 INTL0038  
 INTL0039  
 INTL0040  
 INTL0041  
 INTL0042  
 INTL0043  
 INTL0044  
 INTL0045  
 INTL0046  
 INTL0047  
 INTL0048  
 INTL0049  
 INTL0050  
 INTL0051  
 INTL0052  
 INTL0053  
 INTL0054  
 INTL0055  
 INTL0056  
 INTL0057  
 INTL0058  
 INTL0059  
 INTL0060  
 INTL0061  
 INTL0062  
 INTL0063  
 INTL0064  
 INTL0065  
 INTL0066  
 INTL0067  
 INTL0068  
 INTL0069  
 INTL0070  
 INTL0071  
 INTL0072

```

WBBY=CEXP(WC*CMPLX(DX(N-1),C.0))
  DC 10 I=N,256,32
  ADDA(I)=ADDA(I-1)
  DO 20 I=N,192,32
    FH(I)=WX*FH(I-1)
  HHAT2(N)=WBBY*HHAT2(N-1)
  HHAT3(N)=WBBY*HHAT3(N-1)
  HHAT4(N)=WBBY*HHAT4(N-1)
  GO TO 20C
30 NWPN=NN*NEW
  DL=OM2*ZM(N)/GRAV
  IF(DL.GT.5.) DI=5.
  DL1=DELTA(1)
  DL2=DELTA(2)
  DL3=DELTA(3)
  DO 40 J=4,42
    L=J
    IF(DL.LT..5*(DL2+DL3)) GO TO 50
    IF(J.EQ.42) GO TO 50
    DL1=DL2
    DL2=DL3
    DL3=DELTA(J)
  D1=D(DL,DL1,DL2,DL3)
  D2=D(DL,DL2,DL1,DL3)
  D3=D(DL,DL3,DL2,DL1)
  C=SQ
  NI=328*NN+L-3
  DO 60 I=N,256,32
    O=1./O
    ADDA(I)=X(AB(NI),AB(NI+1),AB(NI+2))* (O*SQ)
    NI=NI+41
  WX=CEXP(WC*CMPLX(XI(N),0.))
  WBBY=CEXE((-1.0,0.0)*WC*CMPLX(XI(N),0.0))
  WYG=WX*CMPLX(GRAV,0.)
  WXO=WX*CMPLX(OMC,0.)
  WXB=WBWBY*CMPLX(OMC,0.0)

```

INTL0073  
 INTL0074  
 INTL0075  
 INTL0076  
 INTL0077  
 INTL0078  
 INTL0079  
 INTL0080  
 INTL0081  
 INTL0082  
 INTL0083  
 INTL0084  
 INTL0085  
 INTL0086  
 INTL0087  
 INTL0088  
 INTL0089  
 INTL0090  
 INTL0091  
 INTL0092  
 INTL0093  
 INTL0094  
 INTL0095  
 INTL0096  
 INTL0097  
 INTL0098  
 INTL0099  
 INTL0100  
 INTL0101  
 INTL0102  
 INTL0103  
 INTL0104  
 INTL0105  
 INTL0106  
 INTL0107  
 INTL0108

```

DT(1)=DTB(N,1)
DO 70 I=1,NP1
  Y=YN(N,I)
  Z=ZN(N,I)
  DY=DYN(N,I)
  DZ=DZN(N,I)
  IF(NEQ.EQ.1) DT(I)=DTR(N,I)
  EX=EXP(-WN*Z)
  CX=CEXP(WS*CMPLX(Y,0.))
  CRBY=CEXP((-1.0,C.0)*WS*CMPLX(Y,0.0))
  RW=EX*REAL(CX)
  FWRB=EX*REAL(CRBY)
  AW=EX*AIMAG(CX)
  AWRB=EX*AIMAG(CRBY)
  ADY(I)=RW*DY
  EDY(I)=RWRB*DY
  ADY(I)=AW*DY
  ADY(I)=AWRB*DY
  RDZ(I)=RW*DZ
  FDZZ(I)=RWRB*DZ
  ADZ(I)=AW*DZ
  ADZZ(I)=AWRB*DZ
  70  AYZ(I)=AW*(Y*DY+Z*DZ)
      RDY(NP)=EXP(-WN*ZM(N))*DYN(N,NP)
      EDY(NP)=EXP(-WN*ZM(N))*DYN(N,NP)
      DO 160 NC=1,3
        NFP=NP-(NC/2)
        NWP=NWPN+(L-4)*NPP+((NC-1)*NP-(NC/3))*41
        DC 80 I=1,NFP
          NWI=NWP+I
          PGM=X(PR(NWI),PR(NWI+NPP),PR(NWI+2*NPP))*OMA
          PGM=X(PA(NWI),PA(NWI+NPP),PA(NWI+2*NPP))*OMA
          WEI(I)=CMPLX(PGR,PGM)
      GO TO (100,120,140),NC
      DO 110 I=1,NP
        FW(I)=CMPLX(-ADY(I)-SB*EDZ(I),0.)
  100

```

INTLO109  
 INTLO110  
 INTLO111  
 INTLO112  
 INTLO113  
 INTLO114  
 INTLO115  
 INTLO116  
 INTLO117  
 INTLO118  
 INTLO119  
 INTLO120  
 INTLO121  
 INTLO122  
 INTLO123  
 INTLO124  
 INTLO125  
 INTLO126  
 INTLO127  
 INTLO128  
 INTLO129  
 INTLO130  
 INTLO131  
 INTLO132  
 INTLO133  
 INTLO134

```

110  FWRB(I)=CMPLX(-ADYY(I)+SB*EDZZ(I),0.0)
      WRRB(I)=CMPLX(RDYY(I)+SB*ADZZ(I),0.0)*WPI(I)
      WH(I)=CMPLX(RDY(I)-SB*ADZ(I),0.0)*WPI(I)
      F3(N)=CMPLX(-2.*TRAP(DT,PDY,NP,NEQ),0.0)*WXG
      H3(N)=(0.,2.)*WTRAF(DI,WH,NE,NEQ)*WXO
      HHAT3(N)=(0.,2.)*WTRAE(DT,WRRB,NE,NEQ)*WXRB
      GO TO 160
120  WPI(NP)=(0.,0.)
      DO 130 I=1,NP
130  WRRB(I)=FWRB(I)*WPI(I)
      WH(I)=FW(I)*WPI(I)
      F2(N)=CMPLX(0.,-2.*TRAP(DT,ADZ,NP,NEQ))*WXG
      H2(N)=(-2.,0.)*WTRAF(DT,WH,NE,NEQ)*WXO
      HHAT2(N)=(2.,0.)*WTRAE(DT,WRRB,NE,NEQ)*WXRB
      GO TO 160
140  DO 150 I=1,NP
150  WRRB(I)=FWRB(I)*WPI(I)
      WH(I)=FW(I)*WPI(I)
      F4(N)=CMPLX(0.,-2.*TRAE(DI,AYZ,NE,NEQ))*WXG
      H4(N)=(2.,0.)*WTRAF(DT,WH,NE,NEQ)*WXO
      HHAT4(N)=(2.,0.)*WTRAE(DT,WRRB,NE,NEQ)*WXRB
      CONTINUE
      NN=NN+1
200  CONTINUE
      RETURN
      END

```

C-3:    ADDRES - This is a new routine which computes the second order mean force on a ship in a regular wave due to all five motion components and wave reflection. This is performed according to the 1974 theory of Salvesen. ADDRES is primarily intended to handle output computing various sub-totals and storing the response operators for the statistical routines.

A listing of this new routine follows on pages 142-144.

```

SUBROUTINE ADDRESS
IMPLICIT COMPLEX (F,H)
CCOMPLEX WS,WC,ETA
REAL*8 $ (6)
REAL H13
COMMON/EAPA/WS,WC,SB,CMO,OM,OM2,WN,RHO,GRAY,BETA,XI (32),DX (31),
1V,NSTA,NSP,MD,XLBP,ZETA,ALFA
COMMON/STAYM (32),ZM (32),SIGMA (32)
COMMON/ABFH/F2 (32),F3 (32),F4 (32),H2 (32),H3 (32),H4 (32),A33 (32),
1R33 (32),A22 (32),B22 (32),A44 (32),B44 (32),A24 (32),B24 (32)
COMMON/VISC/ B4$ (32),B44V,ION,TADE
COMMON/SPCTRM/ AM (1200),RS (6400),RM (200),H13 (10),OMP (10),NEOMS,
1SECTM (10,40),SPOMS (10,40),NSOMS,NWX,TI,N1,N2,M1,NSEA,L,NS,NSPC,ZO,
2NADR,EST (80),NEVT,EVENT (3,3),NN1,NN2,NN3,VCR,PEVNT (120),OMEGE (40)
COMMON/COFFS/FTA (6),F (6),G (6,6),A (6,6),B (6,6),C (6,6)
COMMON/FRB/HHAT2 (32),HHAT3 (32),HHAT4 (32)
COMMON/INTNL/DIM (4),TRIG (4),PACX,S2,PON
DIMENSION ADEPT (2,3,4)
DATA RAD/57.29578/
DATA $/' ',' SWAY ',' HEAVE ',' ROLL ',' PITCH '
1' YAW ' /
IRB=2
JRB=6
KRB=1
ICNT=1
DO 5 JKB=1,2
DO 5 JKP=1,3
DO 5 JKR=1,4
ADRST (JKJ,JKF,JKE)=0.0
Z2=ZETA*ZETA
CR=COS (BETA/RAD)
S2=SB*SE
FACX=(0.0,1.0)*V/CM
W2=OMC*CMO/CM
PON=Z2*WN*W2
DIM (1)=1.0

```

```

ADRS0001
ADRS0002
ADRS0003
ADRS0004
ADRS0005
ADRS0006
ADRS0007
ADRS0008
ADRS0009
ADRS0010
ADRS0011
ADRS0012
ADRS0013
ADRS0014
ADRS0015
ADRS0016
ADRS0017
ADRS0018
ADRS0019
ADRS0020
ADRS0021
ADRS0022
ADRS0023
ADRS0024
ADRS0025
ADRS0026
ADRS0027
ADRS0028
ADRS0029
ADRS0030
ADRS0031
ADRS0032
ADRS0033
ADRS0034
ADRS0035
ADRS0036

```

```

DIM(2)=1.0
DIM(3)=TADR*Z2
DIM(4)=DIM(3)
TRIG(1)=SB
IF(BETAA.EQ.180.0.OR.BETAA.EQ.0.0) TRIG(1)=0.0
TRIG(2)=-CF
IF(BETAA.EQ.90.0) TRIG(2)=0.0
TRIG(3)=TRIG(1)
TRIG(4)=TRIG(2)
IF(NADR.NE.2.AND.NSEA.NE.1) WRITE(6,999)
IF(NSEA.NE.1)
*WRITE(6,1000)
IF(MD.EQ.2) GO TO 10
IPB=3
JRP=5
KRE=2
DC 30 ICK=IPB,JRB,KRP
CALL RESIST (ICNT,IQK,ADEST)
IF(NADR.NE.2.AND.NSEA.NE.1)
*WRITE(6,1001) (ADRST(1,1,KQK),KQK=1,4)
IF(NADR.NE.2.AND.NSEA.NE.1)
*WRITE(6,1002) $(IQK),(ADRST(1,2,KQK),KQK=1,4)
DC 20 JQK=1,4
ADRST(2,3,JQK)=ADRST(1,1,JQK)+ADEST(1,2,JQK)
IF(NADR.NE.2.AND.NSEA.NE.1)
*WRITE(6,1003) (ADEST(2,3,KQK),KQK=1,4)
CONTINUE
IF(NADR.NE.2.AND.NSEA.NE.1)
*WRITE(6,1004) (ADEST(2,1,KQK),KQK=1,4)
IF(NADR.NE.2.AND.NSEA.NE.1)
*WRITE(6,1005) (ADEST(2,2,KQK),KQK=1,4)
DO 40 JQK=1,4
ADRST(2,3,JQK)=ADEST(2,1,JQK)+ADEST(2,2,JQK)
IF(NADR.NE.2.AND.NSEA.NE.1)
*WRITE(6,1006) (ADEST(2,3,KQK),KQK=1,4)
IF(NADR.NE.2.AND.NSEA.NE.1)

```

```

ADRSC0037
ADRSC0038
ADRSC0039
ADRSC0040
ADRSC0041
ADRSC0042
ADRSC0043
ADRSC0044
ADRSC0045
ADRSC0046
ADRSC0047
ADRSC0048
ADRSC0049
ADRSC0050
ADRSC0051
ADRSC0052
ADRSC0053
ADRSC0054
ADRSC0055
ADRSC0056
ADRSC0057
ADRSC0058
ADRSC0059
ADRSC0060
ADRSC0061
ADRSC0062
ADRSC0063
ADRSC0064
ADRSC0065
ADRSC0066
ADRSC0067
ADRSC0068
ADRSC0069
ADRSC0070
ADRSC0071
ADRSC0072

```

10

-143-

20

30

40

```

*WRITE (6,1007) (ADRST(1,3,KCK),KCK=1,4)
DC 50 JCK=1,4
ADRST(2,3,JCK)=ADRST(2,3,JCK)+ADRST(1,3,JCK)
IF(NSIA.NE.1)
*WRITE(6,1006) (ADRST(2,3,KCK),KCK=1,4)
IF(NADR.NE.2.AND.NSEA.NE.1)
*WRITE(6,1008)
IF(NSEA.EQ.C) RETURN
RST(L)=ADEST(2,3,2)/Z2
RST(L+NROMS)=ADRST(2,3,1)/Z2
RETURN
999 FORMAT('1')
1000 FORMAT('0',10X,'MEAN ADDED RESISTANCE/DRIFT FORCE CALCULATION',//,
*36X,'DIMENSIONAL',19X,'NON-DIMENSIONAL',//,7X,'MODE SOURCE',7X,
*'DRIFT FORCE ADDED RESIST.',5X,'DRIFT FORCE ADDED PERSIST.')
```

1001 FORMAT('0',14X,'FR-KEL',4(5X,F11.4))

1002 FORMAT('0',5X,A8,'WVDIFF',4(5X,F11.4))

1003 FORMAT('0',14X,'TOTALS',4(5X,F11.4),//,1X,90(1H-))

1004 FORMAT(1X,90(1H-),//,11X,'SUM OF ALL THE MODES AND THE DIFFRACTION  
\* POTENTIAL CONTRIBUTION',//,5X,'ALL MODES FR-KEL',4(5X,F11.4))

1005 FORMAT('0',4X,'ALL MODES WVDIFF',4(5X,F11.4))

1006 FORMAT(22X,4(5X,11(1H-)),//,15X,'TOTALS',4(5X,F11.4))

1007 FORMAT('0',4X,'DIFFR. POT. CONT.',4(5X,F11.4))

1008 FORMAT(1H1)

END

```

ADRS0073
ADRS0074
ADRS0075
ADRS0076
ADRS0077
ADRS0078
ADRS0079
ADRS0080
ADRS0081
ADRS0082
ADRS0083
ADRS0084
ADRS0085
ADRS0086
ADRS0087
ADRS0088
ADRS0089
ADRS0090
ADRS0091
ADRS0092
ADRS0093
ADRS0094
ADRS0095
ADRS0096
ADRS0097
```



C-4: RESIST - This is a new routine which is called by ADDRES. It performs the real calculation of the second order force outlined in the theory of Chapter III, and then returns the resulting values to ADDRES for manipulation.

A listing of this new routine follows on pages 146-147.

RSST0001  
 RSST0002  
 RSST0003  
 RSST0004  
 RSST0005  
 RSST0006  
 RSST0007  
 RSST0008  
 RSST0009  
 RSST0010  
 RSST0011  
 RSST0012  
 RSST0013  
 RSST0014  
 RSST0015  
 RSST0016  
 RSST0017  
 RSST0018  
 RSST0019  
 RSST0020  
 RSST0021  
 RSST0022  
 RSST0023  
 RSST0024  
 RSST0025  
 RSST0026  
 RSST0027  
 RSST0028  
 RSST0029  
 RSST0030  
 RSST0031  
 RSST0032  
 RSST0033  
 RSST0034  
 RSST0035  
 RSST0036

```

SUBROUTINE RESIST (ICNT,IQK,ADRST)
      DOFS NOT WORK IN METERS--- HAS A GLICH-----
      IMPLICIT COMPLEX (F,H)
      COMPLEX WS,WC,ETA,CMPLX,WTRAP,CONJG
      COMMON/PAFA/ WS,WC,SB,CMC,OM,CM2,WN,RHO,GRAV,BETAA,XI(32),DX(31),V
      1,NSTA,NSP,MD,XLBP,ZETA,ALFA
      COMMON/STA/ YM(32),ZM(32),SIGMA(32)
      COMMON/ABPH/F2(32),F3(32),F4(32),H2(32),H3(32),H4(32),A33(32),
      1B33(32),A22(32),B22(32),A44(32),B44(32),A24(32),B24(32)
      COMMON/VISC/ B45(32),B44V,TON,TADR
      COMMON/COEFS/FTA(6),F(6),G(6,6),A(6,6),B(6,6),C(6,6)
      COMMON/ERB/HHAT2(32),HHAT3(32),HHAT4(32)
      COMMON/INTNL/DIM(4),TRIG(4),FACY,S2,PQN
      DIMENSION YY(32),FYY(32),ADEST(2,3,4)
      FACT=(0.0,0.5)*WN*ETA(IQK)
      IF(ICNT.EQ.2) GO TO 10
      DO 8 ISK=1,NSTA
      F2= EXP(-2.0*WN*ZM(ISK)*SIGMA(ISK))
      YY(ISK)=F2*(B33(ISK)+(S2*B22(ISK)))
      CMPD=C.5*TRAP(DX,YY,NSTA,NSP)*FQN
      DO 9 ISK=1,4
      ADPST(1,3,ISK)=CMPD*TRIG(ISK)*TON/DIM(ISK)
      ICNT=2
      GO TO (11,12,13,14,15,16),IQK
      RETURN
      FRKR=RHO*ZETA*WTRAP(DX,F2,NSTA,NSP)
      FRKE=CONJG(FRKR)*FACT
      FDF=RHO*ZETA*WTRAP(DX,HHAT2,NSTA,NSP)*FACT
      GO TO 17
      FRKE=RHO*ZETA*WTRAP(DX,F3,NSTA,NSP)
      FRKE=CCNJG(FRKE)*FACT
      FDF=RHO*ZETA*WTRAP(DX,HHAT3,NSTA,NSP)*FACT
      GC TO 17
      FRKR=RHO*ZETA*WTRAP(DX,F4,NSTA,NSP)

```

C  
 C  
 C

-146-

8  
 9  
 10  
 11  
 12  
 13  
 14

RSST0037  
 RSST0038  
 RSST0039  
 RSST0040  
 RSST0041  
 RSST0042  
 RSST0043  
 RSST0044  
 RSST0045  
 RSST0046  
 RSST0047  
 RSST0048  
 RSST0049  
 RSST0050  
 RSST0051  
 RSST0052  
 RSST0053  
 RSST0054  
 RSST0055  
 RSST0056  
 RSST0057  
 RSST0058  
 RSST0059  
 RSST0060  
 RSST0061

```

FRKR=CONJG(FRKR)*FACT
FDF=RHO*ZETA*WTRAP(DX,HHAT4,NSTA,NSP)*FACT
GC TO 17
DC 25 ISK=1,NSTA
FYY(ISK)=XI(ISK)*F3(ISK)
FRKR=-1.0*RHO*ZETA*WTRAP(DX,FYY,NSTA,NSP)
FRKR=CONJG(FRKR)*FACT
DC 35 ISK=1,NSTA
FYY(ISK)=(CMPLX(XI(ISK),0.0)+FACX)*HHAT3(ISK)
FDF=-1.0*RHO*ZETA*WTRAP(DX,FYY,NSTA,NSP)*FACT
GC TO 17
DC 26 ISK=1,NSTA
FYY(ISK)=XI(ISK)*F2(ISK)
FRKR=EHO*ZETA*WTRAP(DX,FYY,NSTA,NSP)
FRKR=CONJG(FRKR)*FACT
DC 36 ISK=1,NSTA
FYY(ISK)=(CMPLX(XI(ISK),0.0)+FACX)*HHAT2(ISK)
FDF=RHO*ZETA*WTRAP(DX,FYY,NSTA,NSP)*FACT
DC 18 KD=1,4
ADRST(1,1,KD)=REAL(FRKR)*TRIG(KD)*TON/DIM(KD)
ADRST(1,2,KD)=REAL(FDF)*TRIG(KD)*TON/DIM(KD)
ADRST(2,1,KD)=ADRST(2,1,KD)+ADRST(1,1,KD)
ADRST(2,2,KD)=ADRST(2,2,KD)+ADRST(1,2,KD)
RETURN
END

```

C-5: STATIS AND SPIN - These routines perform the statistical calculations necessary for long-crested irregular seaway response predictions. They have been modified to include the calculations of a mean second order force. The new lines in STATIS include:

22, 115-126, 135, 150.

The new lines in SPIN include:

26-31.\*

\*NOTE: These new lines in SPIN exist to take care of the problem of a negative value for the variable, SUM. This does not occur for motions which have R.A.O.'s which are always positive. However, it might occur for second order force (e.g. following seas where the waves will help to push the ship). Since it was desired to use SPIN for the second order force calculation (just as for all the other response calculations), it was necessary to provide a way to avoid taking the square root of a negative number and causing an error (See line 30). To summarize, these lines do not affect the positive motion R.A.O.'s and they exist only to avoid computer error messages when SPIN is called

-149-

for the second order force. The quantities S, S3, S10, S1000 are not meaningful for the second order force, and are not written out.

A listing of these two modified routines follows on pages 150-156.

STTSC001  
 STTSC002  
 STTSC003  
 STTSC004  
 STTSC005  
 STTSC006  
 STTSC007  
 STTSC008  
 STTSC009  
 STTSC010  
 STTSC011  
 STTSC012  
 STTSC013  
 STTSC014  
 STTSC015  
 STTSC016  
 STTSC017  
 STTSC018  
 STTSC019  
 STTSC020  
 STTSC021  
 STTSC022  
 STTSC023  
 STTSC024  
 STTSC025  
 STTSC026  
 STTSC027  
 STTSC028  
 STTSC029  
 STTSC030  
 STTSC031  
 STTSC032  
 STTSC033  
 STTSC034  
 STTSC035  
 STTSC036

SUBROUTINE STATIS  
 IMPLICIT REAL\*8 (\$)  
 LOGICAL IS  
 COMPLEX WS,WC  
 COMMON SPC(40), SPC(40), DOM(39), VGB, SM(40), SM2(40), SM4(40), AJMV(2)  
 1, S(32), S3(32), S10(32), S1000(32), OMOT(5), VMOT(7,10), BNDS(5,32), ZZ  
 COMMON /PAPA/ WS,WC,SB,OMC,OM,OM2,WN,ZHO,GRAV,BETA, XI(32), DX(31)  
 1, V, NSIA, NSP, MD, XLBE, ZETAA, ALFA  
 COMMON /MTN/ XMOT(10), YMOT(10), ZMOT(10), NMOT  
 COMMON /SECTRM/ AM(1200), BS(6400), RM(200), H13(10), OMP(10), NRCMS  
 1, SPCRM(10,40), SPOMS(10,40), NSOMS, NWX, JI, N1, N2, M1, NSEA, L, NS, NSPC, IO  
 2, NADR, RST(80), NEVT, EVENT(3,3), NN1, NN2, NN3, VCR, REVNT(120), OMEGE(40)  
 COMMON /MOTHER/ UCB(16), BETA(16), OMEGA(40), NVL, NENC, NECH, NFR, NFO  
 DIMENSION \$(41), R(40), I1(7), I2(7), I3(7), I4(7), OVB(235)  
 EQUIVALENCE (CMOT(1), OVB(1))  
 DATA \$/  
 1, 'HEAVE', 'PITCH', 'SWAY', 'ROLL'  
 2, 'YAW', 'ABSOLUTE', 'L MOTION', 'VELOCITY', 'ACCE'  
 3, 'L ERATICN', 'RELATIVE', 'TRANSVPR', 'SE ACCE', 'LONGITUD'  
 4, 'INAL SHE', 'AR STA', 'LONGITUD', 'INAL B.', 'M. STA.'  
 5, 'LAT', 'ERAL SHE', 'AE STA', 'TORSI', 'ONAL B.'  
 6, 'M. STA', 'LAT', 'ERAL B.', 'M. STA', 'VERTICA'  
 7, 'COMPONEN', 'T OF ADD', 'T OF DEF', 'RES.(X)', 'FT(Y-AX)'  
 8, 'DECK', 'PROFELLE', 'WETNESS', 'R RACING'  
 'SLAMMING'  
 DATA I1/7,1,1,12,1,1,13/, I2/30,1,10,30,1,10,14/, I3/8,9,11,8,9,11  
 1, I1/0,2,4,0,2,4,0/  
 LS=.TRUE.  
 IF (IO.EQ.0) IS=.FALSE.  
 IF ((LS).AND.II.EQ.3) CALL EFASE(CVB,235)  
 EAD=57.29578  
 VGB=V/GRAV\*COS(BETA/RAD)  
 DO 200 NW=1, NWX  
 ZZ=1.  
 WRITE(6,1000) V, BETA  
 WRITE(6,1001) H13(NW), OMP(NW)  
 SPO(1)=SPOMS(NW,1)



C  
C  
C

```

C      SHEAR & PENDING MOMENTS
C
C      K=0
C      WRITE(6,1006)
C      DO 100 N=2,II
C      J1=3*N+9
C      J2=J1+2
C      DC 90 I=N1,N2
C      DO 80 I=1,NRCMS
C      K=K+1
C      R(I)=BS(K)
C      80   BNDS(N-1,I)=SPIN$(J1),$(J1+1),$(J2),E,I,I
C      90   WRITE(6,1003) $(J),J=J1,J2
C      100  WRITE(6,1007) (I,S(I),S3(I),S10(I),S100(I),I=N1,N2)
C      110  IF(NEVT.EQ.0) GO TO 150
C
C      EVENTS : DECK WEINNESS, PROPELLER RACING, AND SLAMMING
C
C      WRITE(6,1009)
C      DO 140 I=NN1,NN2,NN3
C      DO 130 K=1,2
C      DO 120 L=1,NRCMS
C      120  R(L)=REVT(L+NRCMS*(I-1))*OMEGA(L)**LI(K)
C      J=K+3
C      130  AJMV(K)=SPIN$(I1(J)),$(I2(J)),$(I3(J)),E,K,0)
C      WRITE(6,1005) (EVENT(I,J),J=1,3)
C      WRITE(6,1003) $(12),$(32),$(8),S(1),S3(1),S10(1),S100(1)
C      WRITE(6,1003) $( 1),$( 1),$( 1),S(2),S3(2),S10(2),S100(2)
C      VV=0.
C      IF(I.EQ.3) VV=VCR**2
C      FJ=EVENT(I,3)**2
C      PP=.5*(FJ/AJMV(1)+VV/AJMV(2))
C      PROB=0.
C      IF(PP.LT.175.) PROB=EXP(-PP)
C      PP=10.*RAD*PROB*SQRI(AJMV(2)/AJMV(1))

```

C  
C  
C  
-152-

STTS0073  
STTS0074  
STTS0075  
STTS0076  
STTS0077  
STTS0078  
STTS0079  
STTS0080  
STTS0081  
STTS0082  
STTS0083  
STTS0084  
STTS0085  
STTS0086  
STTS0087  
STTS0088  
STTS0089  
STTS0090  
STTS0091  
STTS0092  
STTS0093  
STTS0094  
STTS0095  
STTS0096  
STTS0097  
STTS0098  
STTS0099  
STTS0100  
STTS0101  
STTS0102  
STTS0103  
STTS0104  
STTS0105  
STTS0106  
STTS0107  
STTS0108



STTS0109  
 STTS0110  
 STTS0111  
 STTS0112  
 STTS0113  
 STTS0114  
 STTS0115  
 STTS0116  
 STTS0117  
 STTS0118  
 STTS0119  
 STTS0120  
 STTS0121  
 STTS0122  
 STTS0123  
 STTS0124  
 STTS0125  
 STTS0126  
 STTS0127  
 STTS0128  
 STTS0129  
 STTS0130  
 STTS0131  
 STTS0132  
 STTS0133  
 STTS0134  
 STTS0135  
 STTS0136  
 STTS0137  
 STTS0138  
 STTS0139  
 STTS0140  
 STTS0141  
 STTS0142  
 STTS0143  
 STTS0144

```

140 WRITE(6,1010) $(I+35),$(I+38),EP
150 IF(NADR.EQ.0) GO TO 190
C
C MEAN ADDED RESISTANCE
C
ZZ=0.
WRITE(6,1011)
K=0
DO 170 I=1,2
DO 160 L=1,NROMS
K=K+1
R(L)=RST(K)
J=31+I
M=33+I
ADRST=2.*SPIN$(31),$(J),$(M),R,I,0)
IF(I.EQ.1) ADRST=ADRST
IF(I.EQ.2) DRIFT=ADRST
170 WRITE(6,1003) $(31),$(J),$(M),ADRST
190 IF(.NOT.IS) GO TO 200
C
C IO OF MEAN SQUARES FOR SHORT CRESTED SEA PREDICTIONS
C
WRITE(IO,2000) H13(NW),CME(NW)
WRITE(IO,2000) (CMOT(I),I=1,5)
IF(NMOT.NE.0) WRITE(IO,2000) ((VMOT(I,J),I=1,7),J=1,NMOT)
IF(N1.NE.0) WRITE(IO,2000) ((RNDS(I,J),I=1,5),J=N1,N2)
IF(NADR.NE.0) WRITE(IO,2000) ADRST,DRIFT
200 CONTINUE
RETURN
1000 FORMAT('IRREGULAR WAVE RESULTS -- LONG CRESTED UNIDIRECTIONAL SEA
1S'/'SHIP SPEED : ',F10.4,9X,'HEADING ANGLE : ',F10.4)
1001 FORMAT('SIGNIFICANT WAVE HEIGHT ',F10.4/' PEAK SPECTRAL FREQUENCY
1 ',F10.4/'0.',T58,'RMS',T71,'H(1/3)',T85,'H(1/10)',T99,'H(1/1000)')
1002 FORMAT(' MOTIONS @ ORIGIN')
1003 FORMAT('7X,3A8.5X,4F15.4)
1004 FORMAT('MOTIONS @ SPECIFIED PTS.')
```

```
1005 FORMAT('OX=',F10.4,', Y=',F9.4,', Z=',F9.4/)
1006 FORMAT('DYNAMIC LOADINGS')
1007 FORMAT(38Y,I2.6X,4F15.4)
1009 FORMAT('STATISTICS OF EVENTS')
1010 FORMAT('O',24X,2A8,F8.2,' OCCURANCES PFR HR.')
1011 FORMAT('O MEAN SECOND ORDER FORCE (LBS.)')
2000 FORMAT(6F13.6)
      END
```

```
STTSO145
STTSO146
STTSO147
STTSO148
STTSO149
STTSO150
STTSO151
STTSO152
```

```

FUNCTION SEIN($1,$2,$3,$4,$5,$6,$7,$8,$9,$10,$11,$12,$13,$14,$15,$16,$17,$18,$19,$20,$21,$22,$23,$24,$25,$26,$27,$28,$29,$30,$31,$32,$33,$34,$35,$36)
REAL*8 $1,$2,$3
COMMON SPC(40),SFO(40),DCM(39),VGB,SM(40),SM2(40),SM4(40),AJMV(2)
1,S(32),S3(32),S10(32),S100(32),OMOT(5),VMOT(7,10),BNDS(5,32),Z7
COMMON /SPECTRM/ AM(1200),RS(6400),EM(200),H13(10),OMP(10),NRCMS
1,SPCIM(10,40),SPOMS(10,40),NSOMS,NWX,II,N1,N2,M1,NSWA,I,NS,NSPC,IO
2,NADR,EST(80),NEVT,EVENT(3,3),NN1,NN2,NN3,VCB,REVNT(120),OMEGE(40)
COMMON /MOTHER/ UCR(16),BPTA(16),OMEGA(40),NVL,NENC,NECH,NFR,NFO
DIMENSION R(1)
L=2
OM1=OMEGA(1)
OM2=OMEGA(2)
OM3=OMEGA(3)
DO 20 J=1,NSCMS
OM=SPC(J)
IF(OM.LE..5*(OM2+OM3)) GO TO 20
IF(I+1.EO.NRCMS) GO TO 20
I=L+1
OM1=OM2
OM2=OM3
OM3=OMEGA(I+1)
GO TO 10
SM(J)=PARABL(OM,CM1,CM2,CM3,F(L-1),R(L),R(L+1),ZZ)*SPC(J)
SUM=TEAP(DCM,SM,NSCMS,1)
SEIN=SUM
SYGN=1.0
IF(SUM.EC.C.0) GO TO 25
SYGN=SIGN(1.C,SUM)
SUM=ABS(SUM)
S(I)=SORT(SUM)*SYGN
SUM=SUM*SYGN
S3(I)=4.0*S(I)
S10(I)=5.1*S(I)
S100(I)=7.7*S(I)
IF(NSFC.EC.0) RETURN
DC 30 J=1,NSCMS

```

```

SPINC001
SPINC002
SPINC003
SPINC004
SPINC005
SPINC006
SPINC007
SPINC008
SPINC009
SPINC010
SPINC011
SPINC012
SPINC013
SPINC014
SPINC015
SPINC016
SPINC017
SPINC018
SPINC019
SPINC020
SPINC021
SPINC022
SPINC023
SPINC024
SPINC025
SPINC026
SPINC027
SPINC028
SPINC029
SPINC030
SPINC031
SPINC032
SPINC033
SPINC034
SPINC035
SPINC036

```

10

-155-

20

25

SPIN0037  
 SPIN0038  
 SPIN0039  
 SPIN0040  
 SPIN0041  
 SPIN0042  
 SPIN0043  
 SPIN0044  
 SPIN0045  
 SPIN0046  
 SPIN0047  
 SPIN0048  
 SPIN0049  
 SPIN0050  
 SPIN0051  
 SPIN0052  
 SPIN0053

```

OM=SPO(J)*(1.-SPO(J)*VGR)
SM2(J)=SM(J)*OM**2
30 SM4(J)=SM(J)*CM**4
SUM2=TRAP(DOM,SM2,NSOMS,1)
SUM4=TRAP(DOM,SM4,NSOMS,1)
IF(SUM.EQ.0.0.OR.SUM4.EQ.0.0) GO TO 35
S24=SUM2*SUM2/SUM/SUM4
IF(S24.GT.1.) S24=1.
EPSILN=SQRT(1.-S24)
GO TO 39
35 EPSILN=99.
39 WRITE(6,1000) $1,$2,$3,M,SUM,SUM2,SUM4,EPSILN,(SM(J),J=1,NSOMS)
RETURN
1000 FORMAT('ORESEONSE SPECTRUM FOR ',3A8,I3,' CTH MOMENT =',E15.7
1,' 2ND MOMENT =',E15.7,' 4TH MOMENT =',E15.7,' BROADNESS FACTOR
2 =',F8.5,'CSPECTRAL AMPLITUDE'S :',4X,8E13.6/(1X,10B13.6))
END

```

C-6: AUXILIARY PROGRAM SHORTCREST

This program uses input prepared by the main 5-D program (subroutine STATIS) to calculate the mean responses in short-crested random seas according to Eq. (92) of the text. The conventional cosine-squared spreading function is used. This program has been modified to include a calculation of mean second order force as well as motion responses. The new lines include:

5, 6, 17, 58, 59, 71, 93, 148-161, 180, 181, 182.

A listing of the modified program follows on pages 158-163.

```

COMMON /SHCREST/ OMOT(13,10,5), VMOT(13,10,10,7), BNDS(13,10,32,5)
1, XMOT(10), YMOT(10), ZMOT(10), BETA(16), V, NENC, NWX, N1, N2, NMOT, NWIND
2, H13(10), SE(34), DB(33), R(32), LM(32), THETA(36)
3, S(32), S3(32), S1C(32), S1000(32), CMP(10), N, I
4, ADRES(13,10), DRIFT(13,10), SGNDF(32), NADR
READ(5,1000) NENC, NWX, N1, N2, NMOT, NWIND, K, NADR
READ(5,1001) (THETA(N), N=1, NWIND)
IF(NMOT.NE.0) READ(K,1001) (XMOT(N), YMOT(N), ZMOT(N), N=1, NMOT)
READ(K,1001) V
DO 10 M=1, NENC
READ(K,1001) BETA(M)
DO 10 NW=1, NWX
READ(K,1002) H13(NW), CMP(NW)
READ(K,1002) (CMOT(M, NW, I), I=1, 5)
IF(NMOT.NE.0) READ(K,1002) ((VMOT(M, NW, J, I), I=1, 7), J=1, NMOT)
IF(N1.NE.0) READ(K,1002) ((RNDS(M, NW, J, I), I=1, 5), J=N1, N2)
IF(NADR.NE.0) READ(K,1002) ADRES(M, NW), DRIFT(M, NW)
CONTINUE
10
WRITE(6,1001) (THETA(N), N=1, NWIND)
WRITE(6,1001) (BETA(N), N=1, NENC)
CALL SHORTC
20 CONTINUE
STOP
1000 FORMAT(16I5)
1001 FORMAT(8F10.4)
1002 FORMAT(6E13.6)
END
SUBROUTINE SHORTC
IMPLICIT REAL*8 ($)
COMMON /SHCREST/ OMOT(13,10,5), VMOT(13,10,10,7), BNDS(13,10,32,5)
1, XMOT(10), YMOT(10), ZMOT(10), BETA(16), V, NENC, NWX, N1, N2, NMOT, NWIND
2, H13(10), SE(34), DB(33), E(32), LM(32), THETA(36)
3, S(32), S3(32), S1C(32), S1000(32), CMP(10), N, I
4, ADRES(13,10), DRIFT(13,10), SGNDF(32), NADR
DIMENSION $(30), I1(7), I2(7), I3(7)
DATA $/
, , HFAVE, , PITCH, , SWAY, , ROLL,

```

```

SCRS0001
SCRS0002
SCRS0003
SCRS0004
SCRS0005
SCRS0006
SCRS0007
SCRS0008
SCRS0009
SCRS0010
SCRS0011
SCRS0012
SCRS0013
SCRS0014
SCRS0015
SCRS0016
SCRS0017
SCRS0018
SCRS0019
SCRS0020
SCRS0021
SCRS0022
SCRS0023
SCRS0024
SCRS0025
SCRS0026
SCRS0027
SCRS0028
SCRS0029
SCRS0030
SCRS0031
SCRS0032
SCRS0033
SCRS0034
SCRS0035
SCRS0036

```

SCRS0037  
 SCRS0038  
 SCRS0039  
 SCRS0040  
 SCRS0041  
 SCRS0042  
 SCRS0043  
 SCRS0044  
 SCRS0045  
 SCRS0046  
 SCRS0047  
 SCRS0048  
 SCRS0049  
 SCRS0050  
 SCRS0051  
 SCRS0052  
 SCRS0053  
 SCRS0054  
 SCRS0055  
 SCRS0056  
 SCRS0057  
 SCRS0058  
 SCRS0059  
 SCRS0060  
 SCRS0061  
 SCRS0062  
 SCRS0063  
 SCRS0064  
 SCRS0065  
 SCRS0066  
 SCRS0067  
 SCRS0068  
 SCRS0069  
 SCRS0070  
 SCRS0071  
 SCRS0072

```

1  ' YAW', 'ABSOLUTE', 'I MOTION', 'VELOCITY', ' ACCE',
2  ' LERATION', 'RELATIVE', 'TRANSVER', 'SE ACCE', 'LONGITUD',
3  ' INAL SHE', 'AR STA', 'LONGITUD', 'INAL B', 'M. STA.',
4  ' ' LAT', 'ERAL SHF', 'AR STA', ' TORSI', 'ONAL R.',
5  ' M. STA', ' LAT', 'ERAL R.', 'M. STA', ' VERTICA' /
  DATA I1/7,1,1,12,1,1,13/, I2/30,1,10,30,1,10,14/, I3/8,9,11,8,9,11
  1,11/
  SPREDF(B)=COS((T-B)/RAD)**2
  RAD=57.29578

```

C  
 C SEARCH FOR HEADING ANGLES WITHIN + OR -90. DEGREES  
 C

```

DO 200 K=1,NWIND
T=THETA(K)
T1=T-89.999
T2=T+89.999
R(1)=0.
SP(1)=0.
I=1
R1=T-90.
I1=1
DO 99 IERB=1,32
SGNDF(IEFB)=1.0
IF(T1.GT.0.) GO TO 20
IF(BETA(1).EQ.0.) L1=2
MM=NEVC+L1
DO 10 M=L1,NFNC
R2=-BETA(MM-M)
IF(B2.LT.I1) GO TO 10
DR(L)=B2-B1
L=L+1
IM(L)=MM-M
SP(L)=SPREDF(R2)
B1=B2
SGNDF(L)=-1.0
CONTINUE

```

SCRS0073  
 SCRS0074  
 SCRS0075  
 SCRS0076  
 SCRS0077  
 SCRS0078  
 SCRS0079  
 SCRS0080  
 SCRS0081  
 SCRS0082  
 SCRS0083  
 SCRS0084  
 SCRS0085  
 SCRS0086  
 SCRS0087  
 SCRS0088  
 SCRS0089  
 SCRS0090  
 SCRS0091  
 SCRS0092  
 SCRS0093  
 SCRS0094  
 SCRS0095  
 SCRS0096  
 SCRS0097  
 SCRS0098  
 SCRS0099  
 SCRS0100  
 SCRS0101  
 SCRS0102  
 SCRS0103  
 SCRS0104  
 SCRS0105  
 SCRS0106  
 SCRS0107  
 SCRS0108

```

20 DO 30 M=1,NENC
    B2=BETA(M)
    IF (B2.LT.I1) GO TO 30
    IF (R2.GT.T2) GO TO 60
    DR(L)=B2-R1
    L=L+1
    LM(L)=M
    SP(L)=SPREFD(P2)
    R1=B2
    CONTINUE
30 B1=B2-360.
    MM=NENC+1
    IF (BETA(NENC).EQ.180.) MM=NENC
    DC 40 M=1,NENC
    R2=-BPTA(MM-M)
    IF (R2+360..GT.T2) GO TO 50
    DR(L)=B2-R1
    L=L+1
    LM(L)=MM-M
    B1=B2
    SGNDP(L)=-1.0
    SP(L)=SPREFD(R2)
40 B1=R1+360.
50 DR(L)=T+90.-B1
60 M=L
    N=L+1
    R(N)=0.
    SP(N)=0.
    UNITY=SQRT(TEMPZD(DB,SP,N)/90.)
    WRITE(6,1010) UNITY
    WRITE(6,6000) (DB(L),L=1,M)
    WRITE(6,7000) (LM(L),L=2,M)
    WRITE(6,5000) (SP(L),L=1,N)
    SPA STATE CALCULATIONS
C
C
C
  
```



```

DC 200 NW=1, NWX
WRITE(6,1000) V
WRITE(6,1001) H13(NW),OMP(NW),T
C
C
C
MOTIONS @ CRIGIN
WRITE(6,1002)
DO 120 I=1,5
DC 110 I=2,M
R(I)=SP(I)*OMOT(LM(L),NW,I)
CALL SPIN
WRITE(6,1003) $(1),$(1+1),S(I),S3(I),S10(I),S100(I),I=1,5)
IF(NMOT.EC.C) GO TO 160
C
C
C
MOTIONS @ SPECIFIED PTS.
WRITE(6,1004)
DC 150 J=1,NMOT
DO 140 I=1,7
DO 130 L=2,M
R(I)=SE(L)*VMOT(LM(L),NW,J,I)
CALL SPIN
WRITE(6,1005) YMOT(J),ZMOT(J)
WRITE(6,1003) $(I1(I)),$(I2(I)),$(I3(I)),S(I),S3(I),S10(I)
1, S100(I),I=1,7)
160 IF(N1.EO.C) GO TO 195
C
C
C
SHEAR & BENDING MOMENTS
WRITE(6,1006)
DO 190 J=1,5
J1=3*J+12
J2=J1+2
DO 180 I=N1,N2
DO 170 L=2,M
R(L)=SE(L)*BNDS(LM(L),NW,I,J)
170

```

```

180          CALL SPIN
          WRITE(6,1003) ($I),I=J1,J2)
190          WRITE(6,1007) (I,S(I),S3(I),S10(I),S1000(I),I=N1,N2)
195          IF(NADR.EQ.0) GO TO 200
C
C SECOND ORDER FORCE
C
          WRITE(6,7500)
          DO 196 L=2,M
196          R(L)=SP(L)*ADRES(LM(L),NW)
          SUM=TRAPZD(DE,R,N)/90.
          WRITE(6,8000) SUM
          DO 197 L=2,M
197          R(L)=SP(L)*DRIFT(LM(L),NW)*SGNDF(L)
          SUM=TRAPZD(DB,R,N)/90.
          IF(T.EQ.0.0.CR.T.EQ.180.0) SUM=0.0
          WRITE(6,9000) SUM
200          CONTINUE
          RETURN
1000 FORMAT('1 IRREGULAR WAVE RESULTS -- SHORT CRESTED MULTI-DIRECTIONAL
1 SEAS SHIP SPEED : ',F10.4)
1001 FORMAT('0 SIGNIFICANT WAVE HEIGHT ',F10.4/' PFAK SPECTRAL PEROUENCY
1 ',F10.4/' PRINCIPLE WIND DIRECTION',F10.4/'0',T58,'RMS',T71,'H(1/
23)',T85,'H(1/10)',T99,'H(1/100)')
1002 FORMAT(' MOTIONS @ ORIGIN')
1003 FORMAT('17X,3A8,5X,4F15.4)
1004 FORMAT('0 MOTIONS @ ETS. CF INTEREST')
1005 FORMAT('0X=',F10.4,' Y=',F9.4,' Z=',F9.4/)
1006 FORMAT('0 DYNAMIC LOADINGS')
1007 FORMAT('38X,I2,5X,4F15.4)
1010 FORMAT('1 THE SPREADING FUNCTION WITH THE INPUT HEADING ANGLES IN DEG
*ATED TO ',F10.6)
5000 FORMAT('0 SE : ',5X,12F10.6/(' ',13F10.6))
6000 FORMAT('0 DE : ',5X,12F10.6/(' ',13F10.6))
7000 FORMAT('11X,12I10/(' ',13I10))
7500 FORMAT('0 MEAN SECOND ORDER FORCE (LBS.)')

```

```

SCRS0145
SCRS0146
SCRS0147
SCRS0148
SCRS0149
SCRS0150
SCRS0151
SCRS0152
SCRS0153
SCRS0154
SCRS0155
SCRS0156
SCRS0157
SCRS0158
SCRS0159
SCRS0160
SCRS0161
SCRS0162
SCRS0163
SCRS0164
SCRS0165
SCRS0166
SCRS0167
SCRS0168
SCRS0169
SCRS0170
SCRS0171
SCRS0172
SCRS0173
SCRS0174
SCRS0175
SCRS0176
SCRS0177
SCRS0178
SCRS0179
SCRS0180

```

```

8000 FCRMAT('G   ADDED RESISTANCE COMPONENT ',F15.4)
9000 FCRMAT('G   DRIFT FORCE COMPONENT ',F15.4)
      END
      SUBROUTINE SPIN
      COMMON /SHCRSI/ OMOT(13,10,5), VMOT(13,10,10,7), BMDS(13,10,32,5)
1, XMOT(10), YMOT(10), ZMOT(10), BEIA(16), V, NENC, NFX, N1, N2, NMOI, NWIND
2, H13(10), SE(34), DE(33), R(32), LM(32), THETA(36)
3, S(32), S3(32), S10(32), S1000(32), GME(10), N, I
4, ADRES(13,10), DRIFT(13,10), SGNDF(32), NADR
      S(I)=SQRT(TEAPZD(DB,R,N)/90.)
      S3(I)=4.0*S(I)
      S10(I)=5.1*S(I)
      S1000(I)=7.7*S(I)
      RETURN
      END
      FUNCTION TEAPZD(DX,Y,N)
      DIMENSION DX(1),Y(1)
      TEAPZD=0.
      N1=N-1
      IF(N.LE.1) RETURN
      DO 10 I=1,N1
      TEAPZD=TEAPZD+DX(I)* (Y(I)+Y(I+1))
      TEAPZD=.5*TEAPZD
      RETURN
      END

```

```

SCRS0181
SCRS0182
SCPS0183
SCRS0184
SCRS0185
SCRS0186
SCRS0187
SCRS0188
SCPS0189
SCRS0190
SCRS0191
SCRS0192
SCRS0193
SCPS0194
SCPS0195
SCRS0196
SCPS0197
SCRS0198
SCPS0199
SCPS0200
SCRS0201
SCRS0202
SCPS0203
SCRS0204
SCPS0205

```

C-7: MATRIX - In Chapter IV-A of the main text, it was noted that, to obtain some of the computer results shown in Figures 4, 5, and 6, the 5-D program was restrained to roll and heave (a 2-D system). This was done by making a few changes in subroutine MATRIX. The concept behind the changes can best be illustrated by letting  $D_{jk}$  represent the term in brackets in Eq. (24); and letting the terms indicated become zero:

$$\begin{bmatrix}
 0 & 0 & 0 & 0 & 0 & 0 \\
 0 & D_{22} & 0 & \cancel{D_{24}} & 0 & \cancel{D_{26}} \\
 0 & 0 & D_{33} & 0 & \cancel{D_{35}} & 0 \\
 0 & \cancel{D_{42}} & 0 & D_{44} & 0 & \cancel{D_{46}} \\
 0 & 0 & \cancel{D_{53}} & 0 & D_{55} & 0 \\
 0 & \cancel{D_{62}} & 0 & \cancel{D_{64}} & 0 & D_{66}
 \end{bmatrix}
 \begin{bmatrix}
 0 \\
 f_2 \\
 f_3 \\
 f_4 \\
 f_5 \\
 f_6
 \end{bmatrix}
 =
 \begin{bmatrix}
 0 \\
 \cancel{F_2} \\
 F_3 \\
 F_4 \\
 \cancel{F_5} \\
 \cancel{F_6}
 \end{bmatrix}$$

Giving  $D_{22}f_2 = 0$ ,  $D_{33}f_3 = F_3$ ,  $D_{44}f_4 = F_4$ ,  $D_{55}f_5 = 0$ ,  $D_{66}f_6 = 0$  which represent the equations for a decoupled two-degree of freedom system. Of course, this can be done for any mode or modes of motion desired.

-165-

The necessary changes to subroutine MATRIX are given next. The new lines include: 26, 27, 29, 41, 42, 44, 45.

A listing of the routine modified for a 2-D system follows on pages 166-168.

MTRX0001  
MTRX0002  
MTRX0003  
MTRX0004  
MTRX0005  
MTRX0006  
MTRX0007  
MTRX0008  
MTRX0009  
MTRX0010  
MTRX0011  
MTRX0012  
MTRX0013  
MTRX0014  
MTRX0015  
MTRX0016  
MTRX0017  
MTRX0018  
MTRX0019  
MTRX0020  
MTRX0021  
MTRX0022  
MTRX0023  
MTRX0024  
MTRX0025  
MTRX0026  
MTRX0027  
MTRX0028  
MTRX0029  
MTRX0030  
MTRX0031  
MTRX0032  
MTRX0033  
MTRX0034  
MTRX0035  
MTRX0036

```

SUBROUTINE MATRIX
IMPLICIT COMPLEX (C,D,E,F,W)
REAL C,DX,EM,ET,ETM,MIKE,WN,EVENT,CABS
COMPLEX ZANGLF
COMMON D(6,6),Z(6),EM(6)
COMMON /PAPA/ WS,WC,SB,OM,OM2,WN,BHO,GRAV,BETA,XI(32),DX(31)
1,V,NSTA,NSE,MD,XLRE,ZETA,ALFA
COMMON /VISC/ B4$(32),B44V,TON,TAADR
COMMON /SECTRM/ AM(1200),BS(6400),RM(200),H13(10),OMP(10),NEOMS
1,SPCTM(10,40),SPOMS(10,40),NSOMS,NWX,II,N1,N2,M1,NSEA,L,NS,NSEC,IO
2,NADR,RST(80),NEVT,EVENT(3,3),NN1,NN2,NN3,VCR,REVT(120),OMFGE(40)
COMMON /COEFS/ FTA(6),F(6),G(6,6),A(6,6),B(6,6),C(6,6)
DIMENSION ET(2,6),ETM(18),P(2),Z(2),MJ(6)
EQUIVALENCE (E(1),ET(1,1),ETM(1)),(F2,F(2)),(F4,F(4)),(F6,F(6))
DATA P/,',NON-'/,Z/,',',P,',HAST'/,MJ/,-1,2,0,3,1,4/
DNV(D1,D2,D3,D4,D5,D6)=(F2*(D1*D2-D3*D4)+F4*(D4*D5-D2*D6)
+ F6*(D3*D6-D1*D5))/DET
1 M=5-M1
N=M-1
I=0
LONGITUDINAL MOTIONS
DO 10 J=3,5,2
DO 10 K=3,5,2
D(J,K)=CMPLX(-CM2*(G(J,K)+A(J,K))+C(J,K),OM*B(J,K))
IF(J.NE.K) D(J,K)=CMPLX(C.O,C.O)
CONTINUE
F(5)=CMPLX(C.O,C.O)
DET=D(3,3)*D(5,5)-D(3,5)*D(5,3)
FTA(3)=(F(3)*D(5,5)-F(5)*D(3,5))/DET
FIA(5)=(F(5)*D(3,3)-F(3)*D(5,3))/DET
IF(M1.NE.2) GC IC 15
CALL ERASE(ETM,18)
GC TO 60

```

C  
C  
C  
10  
C

```

C      TRANSVERSE MOTIONS
C
15      DO 20 J=2,6,2
        DO 20 K=2,6,2
          D(J,K)=CMPLX(-OM2*(G(J,K)+A(J,K))+C(J,K),OM*B(J,K))
        IF(J.NE.K) D(J,K)=CMPLX(C.O,C.O)
        CCNTINUE
        F2=CMPLX(C.O,C.O)
        F6=CMPLX(C.O,C.O)
        R44I=B(4,4)
        B44=D(4,4)
        DT1=D(2,4)*(D(4,5)*D(6,2)-D(4,2)*D(6,6))
        1  +D(6,4)*(D(4,2)*D(2,6)-D(2,2)*D(4,6))
        DT2= D(2,2)*D(6,6)-D(2,6)*D(6,2)
        DIT=DT1+DT2*D(4,4)
        FTA(2)=DNV(D(4,4),D(6,6),D(4,6),D(6,4),D(2,6),D(2,4))
        ETA(4)=DNV(D(4,6),D(6,2),D(4,2),D(6,6),D(2,2),D(2,6))
        FTA(6)=DNV(D(4,2),D(6,4),D(4,4),D(6,2),D(2,4),D(2,2))
        FTA(4)=ETA(4)*DIT
        GO TO 60
    30 N=N+2
C
C      ITERATE TO ACCOUNT FOR VISCOUS ROLL DAMPING
C
        FOLL1=CABS(ETA(4))
        DO 40 J=1,40
          I=I+1
          B44V=MIKE(RCILL1,OM)
          D(4,4)=D44+CMPLX(C.,CM*B44V)
          DET=DT1+DT2*D(4,4)
          ETA(4)=ETA/DIT
          ROLL2=CABS(FTA(4))
          IF(ABS((FOLL1-ROLL2)/FOLL1).LT..001) GO TO 50
          ROLL1=.1*ROLL1+.9*ROLL2
    40 FTA(2)=DNV(D(4,4),D(6,6),D(4,6),D(6,4),D(2,6),D(2,4))
    50 FTA(6)=DNV(D(4,2),D(6,4),D(4,4),D(6,2),D(2,4),D(2,2))

```

```

MTRX0037
MTRX0038
MTRX0039
MTRX0040
MTRX0041
MTRX0042
MTRX0043
MTRX0044
MTRX0045
MTRX0046
MTRX0047
MTRX0048
MTRX0049
MTRX0050
MTRX0051
MTRX0052
MTRX0053
MTRX0054
MTRX0055
MTRX0056
MTRX0057
MTRX0058
MTRX0059
MTRX0060
MTRX0061
MTRX0062
MTRX0063
MTRX0064
MTRX0065
MTRX0066
MTRX0067
MTRX0068
MTRX0069
MTRX0070
MTRX0071
MTRX0072

```

```

60 DO 70 J=M,6,N
    Y=J/4
    Y=1.+Y*56.29578
    Y=(Y*WN+(1.-Y))*ZETA
    E(J)=ZANGLE(FIA(J))
    EM(J)=ET(1,J)/Y
    E(J)=CMPLX(FT(1,J)*X,FT(2,J))
    RM(L+MJ(J)*NFCMS)=(ET(1,J)/ZETA)**2
70 IF(NSEA.E0.1) GO TO 80
    IF(I.E0.0) WRITE(6,1000) Z,Z,Z,Z,Z,Z
    WRITE(6,1001) P(N/M+1),(E(J),J=2,6),(FM(J),J=2,6)
80 IF(M1.E0.2) RETURN
    IF(I.E0.0) GO TO 30
    IF(NSEA.N3.1) WRITE(6,1002) I
    RETURN
1000 FORMAT('0',T37,'SWAY',3X,2A4,T57,'HEAVY',2X,2A4,T77,'FOLL',3X,2A4
1,T97,'PITCH',2X,2A4,T118,'YAW',3X,2A4)
1001 FORMAT(' ',A4,'LINEAR MOTIONS',I32,10F10.4/' NON-DIMENSIONALIZED'
1,T22,5F20.4/)
1002 FORMAT(' VISCIOUS ROLL DAMPING ATTAINED AFTER',I3,' ITERATIONS')
END

```

```

MTRX0073
MTRX0074
MTRX0075
MTRX0076
MTRX0077
MTRX0078
MTRX0079
MTRX0080
MTRX0081
MTRX0082
MTRX0083
MTRX0084
MTRX0085
MTRX0086
MTRX0087
MTRX0088
MTRX0089
MTRX0090
MTRX0091
MTRX0092
MTRX0093

```



APPENDIX D

LISTING OF MARINER EXAMPLE DATA

This section contains listings of data used in the MIT 5-D program to create the various graphs presented in the text. Two data decks are given. The first is based on 21 stations, and it represents the data used to make the comparisons in all the graphs except Figures 4, 5, and 6. These three graphs (for the beam seas experiment) were created using the second data deck based on 11 stations. The "towing tank" data cards have a different density, metacentric height, roll and pitch radius of gyration, and a different number of stations. These changes were made to more accurately represent the model and tank characteristics as measured. The station number was lowered to minimize expense.

An explanation of the meaning of each number is provided by reproducing the portion of the 5-D output that gives the input data (See D-3). The input shown includes a sample selection of regular wave frequencies, ship speeds, and ship heading angles. Spectral information may be added if desired as shown in D-3. Further details may be obtained from the 5-D User's Manual already mentioned. This manual should be consulted before any runs are attempted.

D-1: Data used for all graphs and calculations except Figures 4, 5, and 6 (the beam seas experiments).

MARINER - BETA RANGE AT 15 KNOIS												
21	25	12	1	0	0	10	6	1	1	0	0	0001
0.62028	528.	75.684	29.75	29.75	29.75	32.17	-14.4859	64.0839	-9.6425	-2.97	4.63496	0002
128.6340	22.9729	128.6000	0.0001023	0.0008900	1.9899998	0.0001280	52919.0	0003	0004	0005	0006	0007
264.	0	-9.6425	1.0	0	0	0	0	0	0	0	0	0008
237.5	9.2522	29.75	29.75	29.75	29.75	29.75	29.75	29.75	29.75	29.75	29.75	0009
211.2	20.6762	29.75	29.75	29.75	29.75	29.75	29.75	29.75	29.75	29.75	29.75	0010
184.8	33.6770	29.75	29.75	29.75	29.75	29.75	29.75	29.75	29.75	29.75	29.75	0011
158.4	46.6480	29.75	29.75	29.75	29.75	29.75	29.75	29.75	29.75	29.75	29.75	0012
132.0	58.0422	29.75	29.75	29.75	29.75	29.75	29.75	29.75	29.75	29.75	29.75	0013
105.6	66.9672	29.75	29.75	29.75	29.75	29.75	29.75	29.75	29.75	29.75	29.75	0014
79.2	72.6496	29.75	29.75	29.75	29.75	29.75	29.75	29.75	29.75	29.75	29.75	0015
52.8	75.2080	29.75	29.75	29.75	29.75	29.75	29.75	29.75	29.75	29.75	29.75	0016
26.4	75.6840	29.75	29.75	29.75	29.75	29.75	29.75	29.75	29.75	29.75	29.75	0017
	75.6840	29.75	29.75	29.75	29.75	29.75	29.75	29.75	29.75	29.75	29.75	0018
-26.4	75.6840	29.75	29.75	29.75	29.75	29.75	29.75	29.75	29.75	29.75	29.75	0019
-52.8	75.6840	29.75	29.75	29.75	29.75	29.75	29.75	29.75	29.75	29.75	29.75	0020
-79.2	75.6840	29.75	29.75	29.75	29.75	29.75	29.75	29.75	29.75	29.75	29.75	0021
-105.6	75.6246	29.75	29.75	29.75	29.75	29.75	29.75	29.75	29.75	29.75	29.75	0022
-132.0	73.7800	29.75	29.75	29.75	29.75	29.75	29.75	29.75	29.75	29.75	29.75	0023
-158.4	69.0796	29.75	29.75	29.75	29.75	29.75	29.75	29.75	29.75	29.75	29.75	0024
-184.8	60.1842	29.75	29.75	29.75	29.75	29.75	29.75	29.75	29.75	29.75	29.75	0025
-211.2	46.4512	29.75	29.75	29.75	29.75	29.75	29.75	29.75	29.75	29.75	29.75	0026
-237.6	30.6722	29.75	29.75	29.75	29.75	29.75	29.75	29.75	29.75	29.75	29.75	0027
-264.0												0028
												0029
												0030
												0031
												0032
												0033
												0034
												0035
												0036

1 1 1 4 4 4 4 0 39.80 15.19 24.0 1.5 0.2708 0.17458 23.496

7	40.25	10.48	24.0	1.5	0.2708	0.17458	26.4	0037
7	40.50	9.52	24.0	1.5	0.2708	0.17458	26.4	0038
7	40.50	9.52	24.0	1.5	0.2708	0.17458	26.4	0039
7	40.00	13.68	24.0	1.5	0.2708	0.17458	26.4	0040
8	38.25	14.00	24.0	1.5	0.2708	0.17458	7.592	0041
3								0042
3								0043
3								0044
3								0045
3								0046
3								0047
								0048
								0049
25.335								0050
2.	15.	30.	60.	75.	90.	105.	120.	0051
135.	150.	165.	180.					0052
.1	.15	.2	.25	.3	.35	.4	.45	0053
.4375	.4612	.4891	.5052	.5229	.5427	.5648	.5899	0054
.6187	.6522	.6918	.7395	.7988	.8750	.9783	1.1295	0055
1.3835								

D-2: Data used for preparing comparisons with beam seas experiments (Figures 4, 5, and 6).

MARINER 10 STA FUN TOW TANK

	11	16	3	1	8	6	1	1	1	1	1	0
0.62028	528.	75.684	29.75	32.17	-9.6425	-2.97	8.00					0001
106.0000	11.0000	106.0000	.00001023	.0008675	1.9396954	.00001280	52919.0					0002
	0	-9.6425	1.0									0003
264.												0004
211.2	20.6762	29.75	0.771227	-13.2134	68.2646		10.0					0005
158.4	46.6480	29.75	0.781804	-12.9773	84.6208							0006
105.6	66.9672	29.75	0.857838	-13.4392	105.014							0007
52.8	75.2080	29.75	0.942307	-14.1595	120.632							0008
	75.6940	29.75	0.982668	-14.5472	126.495							0009
-52.8	75.6840	29.75	0.970319	-14.3198	123.866							0010
-105.6	75.6246	29.75	0.870373	-13.4339	112.903							0011
-158.4	69.0796	29.75	0.695764	-12.1463	96.7346							0012
-211.2	46.4512	29.75	0.499875	-10.8540	78.3807							0013
-264.0												0014
												0015
												0016
												0017
												0018
												0019
												0020
												0021
												0022
												0023
												0024
												0025
												0026
												0027
												0028
												0029
												0030
												0031
												0032

1  
4  
4  
9  
7  
7  
3  
3  
3

D-3: SAMPLE OUTPUT OF 5-D USED FOR CHECKING INPUT DATA

The variables can be described as follows:

Card 1	(not shown)	Number of cases (ships)
Card 2	NAME	Description of case run
Card 3	NSTA	Number of ship stations
	NROMS	Number of regular wave frequencies
	NENC	Number of headings
	NVL	Number of speeds
	NMOT	Number of points where motions are calculated
	NSP	Even spacing of ship stations? 0 = yes; 1 = no
	NP	Number of points used on each ship station
	MP	Number of multipoles used in hydrodynamic potential
	NTURB	Ship with bilge keels? 1 = yes; 0 = no
	HASBK	Vertical motions only or full 5-D
	NB	Station where bending moments computed
	NBEND	Are bending moment calculations desired?
	NWT	Number of weight ordinates
	NPCH	Controls printout of various matrices
	NFQ	Conveys form of regular wave frequency input data
	NFR	Conveys form of ship speed input data

Card 4 Set	NSEA	Regular wave calculations only?
	NWX	Number of sea states
	NSOMS	Number of spectral frequencies?
	NS	Default set of spectral frequencies?
	NSPC	Controls printout of various statistical quantities
	IO	Specifies output device for input to Shortcrest
	NADR	Controls added resistance calculations
	NEVT	Controls calculation of event probabilities
Card 5 Set	CB	Block coefficient
	XLBP	Length between perpendiculars
	BEAM	Midship beam
	DRAFT	Midship draft
	GRAV	Gravitational acceleration
	XCG	Longitudinal center of gravity measured from <del>X</del>
	VCG	Vertical center of gravity measured from the waterline
Card 6 Set	GM	Metacentric height
	RYY	Radius of gyration (Y-AX)
	RXX	Radius of gyration (X-AX)
	RZZ	Radius of gyration (Z-AX)
	XZI	Product of inertia (X-ZAX)
	RHO	Mass density in ship units
XRHO	Mass density in slugs/ft <sup>3</sup>	



	NU	Kinematic viscosity
	WSURFA	Wetted surface area
Card 7 Set	UNIT	Input units: English = 0; Metric = 1
	ORIGIN	Desired origin for motions calculation
	ZETAA	Wave amplitude
	ALFA	Maximum wave slope
Card 8 Set	XI	Distance to ship station from <del>0</del>
	YM	Sectional waterline beam
	ZM	Sectional draft
	SIGMA	Sectional area coefficient
	ZCB	Vertical sectional center of buoyancy
	GIRTH	Girth of section
	RIFLR	Rise of floor of section
	ALPH	Angle between ship side and vertical at section
Card 9 Set	IWBK	Determines type of viscous roll damping
	BKRAD	Geometric property of bilge keel
	BILRAD	Geometric property of bilge
	BKGIR	Geometric property of bilge
	BKWID	Geometric property of bilge keel
	PHI	Geometric property of bilge
	PSI	Geometric property of bilge
	LIWO	Length of bilge keel

- NOTES: 1) All of card set 9 are employed in the viscous roll damping (quasi-linear) calculation of  $B_{44}^*$ .
- 2) If structural bending moment or motions calculations are being performed, Card sets Number 10 and 11 must be included here as described in the User's Manual.

Card 12 Set	UOB	Ship speeds, units defined by NFR
Card 13 Set	BETA	Heading angles in degrees, ascending order
Card 14 Set	OMEGA	Wave frequencies, units defined by NFQ
Card 15 Set	H13	The 1/3 highest wave heights for which sea state calculations are desired
Card 16 Set	OMP	Peak spectral frequencies for the corresponding wave heights above. If blank, fully developed seas will be used.
Card 17 Set	SPOMS	Spectral frequencies of each sea state specified ( $\omega_s$ ). These values can be given as input ( $NS \neq 0$ ) or the program will supply a default set ( $NS = 0$ ) (as was done here).
Card 18 Set	SPCTM	Spectral amplitudes for the chosen sea spectrum. This card set may be omitted, and the program will calculate Bretschneider amplitudes that correspond to the frequencies in Card Set 17. Otherwise, NS may be set equal to two and spectral amplitudes may be read in for any type of spectrum the user may require. In this case the default Bretschneider spectrum was chosen.

NOTES: 1) Card Set 19 should follow here as described in the User's Manual if the probabilities of the various events detailed there are desired.

MARINER SPECTRAL ANALYSIS

MARINER SPECTRAL ANALYSIS															
NSIA	NROMS	MFNC	NVL	NMOT	NSP	NP	MP	NTURB	HASBK	NE	NBLND	NWT	NPCH	NFO	NPR
21	21	7	1	0	0	10	6	1	1	0	0	0	0	0	0
NSEA	NWX	NSCKS	NS	NSPC	IO	NADR	NEVT								
1	6	0	0	1	7	2	0								
CB	XIBP	BEAM	DEAPT	GRAV	XCG	VCG	GM								
0.6203	528.0000	75.6840	29.7500	32.1700	-9.6425	-2.9700	4.6341								
RYY	PXX	RZ7	XLT	RPO	XRHO	NU	MSURPA								
123.6340	22.9725	128.6000	0.0000	0.0008300	1.9899398	0.0700128	52919.00								
UNIT	ORIGIN	ZPTAA	PLPA												
0	-9.6425	1.0000	0.0												
STATION I	XI(I)	YM(I)	ZK(I)	SIGMA(I)	ZCD(I)	GIFTH(I)	RIFLP(I)	ALPH(I)							
1	264.0000	0.0	0.0	0.0	0.0	0.0	0.0	0.0							
2	237.6000	9.2522	29.7500	0.0049	-14.4859	64.0839	0.0	0.0							
3	211.2000	20.0762	29.7500	0.7713	-13.2134	68.2646	0.0	10.0000							
4	184.8000	33.6770	29.7500	0.7564	-12.8616	75.2049	0.0	15.0000							
5	158.4000	46.6480	29.7500	0.7814	-12.9773	84.6265	0.0	0.0							
6	132.0000	59.0422	29.7500	0.8150	-13.1334	94.9312	0.0	0.0							
7	105.6000	66.9572	29.7500	0.8576	-13.4332	105.0140	0.0	0.0							
8	79.2000	72.6496	29.7500	0.9018	-13.8361	113.8770	0.0	0.0							
9	52.8000	75.2080	29.7500	0.9423	-14.1595	120.6320	0.0	0.0							
10	26.4000	75.6840	29.7500	0.9757	-14.4466	125.1080	0.0	0.0							
11	0.0	75.6840	29.7500	0.9827	-14.5472	126.4950	0.0	0.0							
12	-26.4000	75.6840	29.7500	0.9769	-14.5055	126.2900	0.0	0.0							
13	-52.8000	75.6840	29.7500	0.9703	-14.3198	123.6560	0.0	0.0							
14	-79.2000	75.6840	29.7500	0.9423	-13.8668	119.2890	0.0	0.0							
15	-105.6000	75.6246	29.7500	0.8704	-13.4339	112.9030	0.0	0.0							
16	-132.0000	73.7800	29.7500	0.7310	-12.8558	105.3040	0.0	0.0							
17	-158.4000	69.0796	29.7500	0.6968	-12.1463	96.7346	0.0	0.0							
18	-184.8000	60.1642	29.7500	0.6011	-11.4443	87.2348	0.0	0.0							
19	-211.2000	46.4512	29.7500	0.4999	-10.8540	78.3807	0.0	0.0							
20	-237.6000	30.6722	29.7500	0.3540	-9.9263	70.3269	0.0	0.0							
21	-264.0000	0.0	0.0	0.0	0.0	0.0	0.0	0.0							
STATION I	IWBK(I)	RFAD(I)	HILAD(I)	NRGIR(I)	NRVID(I)	PH(I)	PSI(I)	LIWO(I)							
1	0	0.0	0.0	0.0	0.0	0.0	0.0	0.0							
2	1	0.0	0.0	0.0	0.0	0.0	0.0	0.0							
3	1	0.0	0.0	0.0	0.0	0.0	0.0	0.0							
4	1	0.0	0.0	0.0	0.0	0.0	0.0	0.0							
5	4	0.0	0.0	0.0	0.0	0.0	0.0	0.0							
6	4	0.0	0.0	0.0	0.0	0.0	0.0	0.0							
7	4	0.0	0.0	0.0	0.0	0.0	0.0	0.0							
8	4	0.0	0.0	0.0	0.0	0.0	0.0	0.0							
9	9	39.8000	15.1900	24.0000	1.5000	0.2708	0.1746	23.4960							
10	7	40.2500	10.4800	24.0000	1.5000	0.2708	0.1746	26.4000							
11	7	40.5000	9.5200	24.0000	1.5000	0.2708	0.1746	25.4000							
12	7	40.5000	9.5200	24.0000	1.5000	0.2708	0.1746	23.4000							
13	7	40.0000	13.6800	24.0000	1.5000	0.2708	0.1746	26.4000							
14	6	38.2500	14.0000	24.0000	1.5000	0.2708	0.1746	7.3920							
15	3	0.0	0.0	0.0	0.0	0.0	0.0	0.0							
16	3	0.0	0.0	0.0	0.0	0.0	0.0	0.0							
17	3	0.0	0.0	0.0	0.0	0.0	0.0	0.0							
18	3	0.0	0.0	0.0	0.0	0.0	0.0	0.0							
19	3	0.0	0.0	0.0	0.0	0.0	0.0	0.0							
20	3	0.0	0.0	0.0	0.0	0.0	0.0	0.0							
21	0	0.0	0.0	0.0	0.0	0.0	0.0	0.0							
DOE(N)	: 33.7800														
BETA(M)	: 0.0	30.0000	60.0000	90.0000	120.0000	150.0000	180.0000								
OMEGA(L)	: 0.2000	0.3000	0.4000	0.5000	0.6000	0.7000	0.8000	0.8700							
	: 1.0200	1.1700	1.2400	1.3000	1.4000	1.5000	1.6000	1.7000							
	: 1.8000	2.0000	2.2500	2.5000	3.0000										
H13(NW)	: 5.0000	10.0000	15.0000	15.0000	15.0000	20.0000									
OHF(NW)	: 0.0	0.0	0.0	0.4489	1.0472	0.0									

Information Processing Center

Information Processing Center

